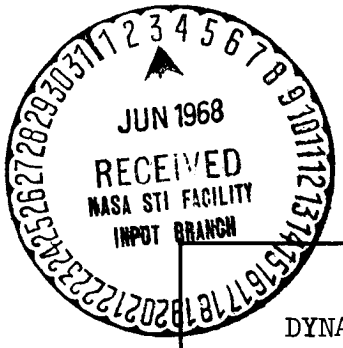

DYNAMICS OF SELECTIVE MOLECULAR EXCITATION: LASER PHOTOCATALYSIS OF BROMINE REACTIONS

by

William B. Tiffany

M. L. Report No. 1538

May 1967

SPECTROSCOPY AND QUANTUM ELECTRONICS GROUP
VARIAN LABORATORY OF PHYSICS

AND

MICROWAVE LABORATORY
W. W. HANSEN LABORATORIES OF PHYSICS

STANFORD UNIVERSITY
STANFORD, CALIFORNIA

DYNAMICS OF SELECTIVE MOLECULAR EXCITATION: LASER PHOTOCATALYSIS OF BROMINE REACTIONS

by

William B. Tiffany

M. L. Report No. 1538

May 1967

Internal Memorandum

NASA Grant NsG-331

Spectroscopy and Quantum Electronics Group

Varian Laboratory of Physics

and

Microwave Laboratory

W. W. Hansen Laboratories of Physics

Stanford University

Stanford, California

ERRATA SHEET

for

DYNAMICS OF SELECTIVE MOLECULAR EXCITATION:

LASER PHOTOCATALYSIS OF BROMINE REACTIONS

by

William B. Tiffany

M. L. Report No. 1538

May 1967

Page

iv Line 20, change "now" to read "not"

9 Line 1, add "apart" at end of line

35 Figure 2.13 - the Variac diagram is incorrect and should be

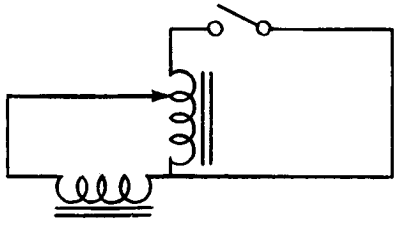

87 Eq. (7) should read $Br^* + Br_2 \rightarrow Br^*Br + Br$

97 Line 2, change "as"to read "at"

130 Line 25, change "to way" to read "the way".

ABSTRACT

A frequency-tuned, high repetition rate ruby laser was designed and used as a light source for the selective photocatalysis of gas-phase reactions between bromine and certain unsaturated fluorocarbons. The purpose was to demonstrate for the first time the usefulness of highly monochromatic, tunable laser light for selective molecular excitation.

In the 14,400 cm^{-1} region of the ruby laser, bromine absorption occurs in individual lines belonging to the $^3\Pi_1 \leftarrow {}^1\Sigma_g^+$ band system. In this study, certain lines were identified as belonging to particular isotopic species of bromine molecules. It was not known if weak continuous absorption, indicative of direct dissociation, also occurs in the same spectral region.

Absorption of the laser light by the bromine caused it to react with the fluorocarbon. Either perfluorobutene or heptafluorochlorobutene was used, and they gave essentially the same results. This was the first reported photochemical reaction of bromine in the 14,400 cm^{-1} region. When the laser frequency was tuned to coincide with individual absorption lines, the reaction rate was considerably enhanced. This showed that the primary photochemical process was the formation of stable excited bromine molecules with energies 500 to 800 cm^{-1} below the dissociation level. All previous photochemical activity in bromine was attributed to direct dissociation into atoms upon absorption of light in the continuum. Thus the use of monochromatic, tunable laser light provided the first evidence of a photochemical reaction of bromine in which excited molecules, not atoms, were formed in the primary process. However, when specific isotopes were selectively excited, no isotopic enrichment was detected in the product. The reaction kinetics and inhibition by nitric oxide gave evidence for a free radical chain mechanism, which required dissociated atoms. The dependence on laser

light intensity was linear. The photochemical quantum yield was about 100 times less in laser light than in light which produced direct dissociation of bromine, although the kinetic behavior was the same. The reaction products with both types of light were identified using gas chromatography and mass spectrometry, and were found to be the same.

To interpret these results, the theory of dynamic molecular processes was reformulated to take into account the pulsed laser excitation. The principal conclusions of the investigation were the following: Bromine added to the double bonds of the unsaturated fluorocarbons by means of a slow free-radical chain mechanism. The bromine atoms needed to initiate the reaction were furnished by collisional dissociation of the laser-activated $^3\Pi_{1,u}$ bromine molecules, which was estimated to require on the average only 20 or so gas-kinetic collisions. The only process competing appreciably with dissociation was collisional relaxation of the $^3\Pi_{1,u}$ molecules to the ground electronic state. This had to occur even slightly more rapidly than the gas-kinetic collision frequency to produce the observed decrease in quantum yield.

Knowledge of electronic energy transfer rates in gas collisions is, in general, fragmentary. The rate for $^3\Pi_1$ bromine molecules was previously now known, but believed to be high because of the failure to observe fluorescence. The present result provided the first quantitative estimate of this rate, which in turn was comparable with known rates for other molecules. It was also concluded that the continuous absorption of bromine at 14,400 cm^{-1} is at least 10^3 times weaker than the peak absorption of the strong individual lines in the same spectral region, at pressures of about 200 torr.

Selective excitation by means of a tunable laser was thus demonstrated to be a useful technique for investigating dynamic molecular processes, with important future applications in studies of photochemistry and energy transfer.

ACKNOWLEDGEMENTS

It is a pleasure to acknowledge the contributions made by many people during the course of this research.

Professor A. L. Schawlow first suggested this work, and supervised and encouraged its progress. I am grateful for his guidance and helpful suggestions. I wish to thank Professor H. W. Moos for substantial contributions during the initial phases of the research, and for his continuing interest.

I have benefitted from many stimulating and helpful discussions with Professor J. I. Brauman, Dr. H. W. Brewer, and Dr. M. J. Weber. I also acknowledge frequent assistance from my associates in the Spectroscopy and Quantum Electronics group, particularly J. L. Emmett, whose advice in the design of the ruby laser was most valuable.

I wish to thank Frank Peters and his staff for building much of the specialized glass apparatus, G. Bicker for the machining of many essential components, and K. H. Sherwin, J. Garrett, and F. P. Alkemade for their expert technical assistance. J. Mishory, J. C. Nickerson, and M. Riconosciuto helped with preparing the equipment and making measurements.

I would like to thank Professor R. M. White and Professor S. S. Hanna for reading the manuscript. I am grateful to Dr. A. S. Braun for his editorial assistance. It is a pleasure to acknowledge the cheerful and efficient preparation of the draft and of the final report by Iona Williams, Betty Dutton, Pauline Brady, and Suzanne Wise, and the expert and patient preparation of the figures by A. Vacek and N. Bettini.

I particularly appreciate the helpfulness and friendliness of Mrs. Fred-a Jurian and Mrs. Beverly Harper.

I wish to acknowledge the encouragement of Dr. B. J. McMurtry and other members of the Advanced Technology Laboratory of Sylvania Electronic Systems, and partial financial support from Sylvania.

Finally, I would like to acknowledge the guidance of my parents, the patient understanding and helpfulness of my wife, and the happy enthusiasm of my daughter, Sherryl, which have greatly enriched my life.

TABLE OF CONTENTS

LIST OF FIGURES

LIST OF TABLES

I. INTRODUCTION

Much of experimental physics is concerned with the measurement of static phenomena, such as the positions of energy levels and energy bands, Fermi surfaces, force constants, and interatomic distances. However, the real world is far from static, and the descriptions of the dynamic properties of matter present some of the most interesting and challenging problems to the modern physicist. The measurement of dynamic phenomena is inherently more difficult than that of static characteristics, because it generally requires knowledge of several processes which are occurring simultaneously. In most cases there are complicated interactions within a system which lead to a number of competing processes. Successful experimentation then must utilize techniques allowing a restricted number of processes to be studied, while permitting a great many others to be ignored.

The selective excitation of a physical system is a very useful method for facilitating the study of its dynamic properties. As an example, if a molecule can be excited to only a single prescribed energy state out of the many which are possible, one may more easily sort out the various radiative and nonradiative relaxation processes, as well as chemical interactions, which subsequently occur. The laser with its intense and highly monochromatic light is clearly a powerful tool for the study of dynamic phenomena through selective excitation. In the present investigation a pulsed, tunable ruby laser was used for the selective excitation of complicated systems containing bromine molecules. The subsequent behavior of the systems, which involved chemical reaction of the bromine with other gases, provided information about their dynamic properties.

Photochemistry using conventional light sources has been the subject of much interest and study in recent years.[1,2] The growth of this field has been stimulated, on the one hand, by developments in quantum theory and its applications and, on the other hand, by the emergence of advanced experimental techniques such as flash photolysis[3,4] and isotopic labeling.[5]

Similarly, the advent of the laser, providing a source of light whose properties differ from those of ordinary light,[6] suggests the possibility of new techniques which can stimulate additional growth and result in an increased understanding of photochemical processes. The purpose of the present investigation is to explore some of these possibilities by using light from a pulsed, tunable ruby laser to catalyze gas phase reactions between bromine and suitable organic compounds. Before discussing the details of this work it is appropriate to review some general qualitative aspects of photochemistry, and then to place this study in perspective by relating it to other previous and current investigations.

For a molecule to react chemically, it is usually necessary for it to have a certain amount of energy, known as activation energy.[7] This is illustrated in Fig. 1.1. The activation energy is supplied in most reactions by thermal collisions with other molecules, in which some of the molecules, in accordance with Boltzmann statistics, always possess the required energy at thermal equilibrium. In a photochemical reaction, however, activation energy is supplied to the molecules by light.(1) Clearly, only the light energy which is absorbed is capable of influencing the reaction. It is convenient to divide the overall photochemical process into two consecutive phases. The first phase, or primary photochemical process, begins with the absorption of a photon by a molecule and ends with the disappearance of that molecule by its reaction, dissociation, or ionization, or with its return to the deactivated equilibrium state. In the latter case deactivation may occur via transfer of the activation energy to a different molecule, which subsequently reacts, in a photosensitized reaction. Secondary processes include all subsequent reactions, and are no different from the types of elementary chemical processes which would occur if the activation had been supplied thermally. Thus in photochemistry we are concerned with activation of molecules by light absorption, the subsequent reactions whether or not they involve the initially activated molecule, and deactivation and energy transfer processes even if no net chemical reaction results.

---

(1) In this discussion and in following sections, use has been made of treatments of photochemistry by Herzberg,[8] Kondrat'ev,[9] and Pitts, et al.[10]

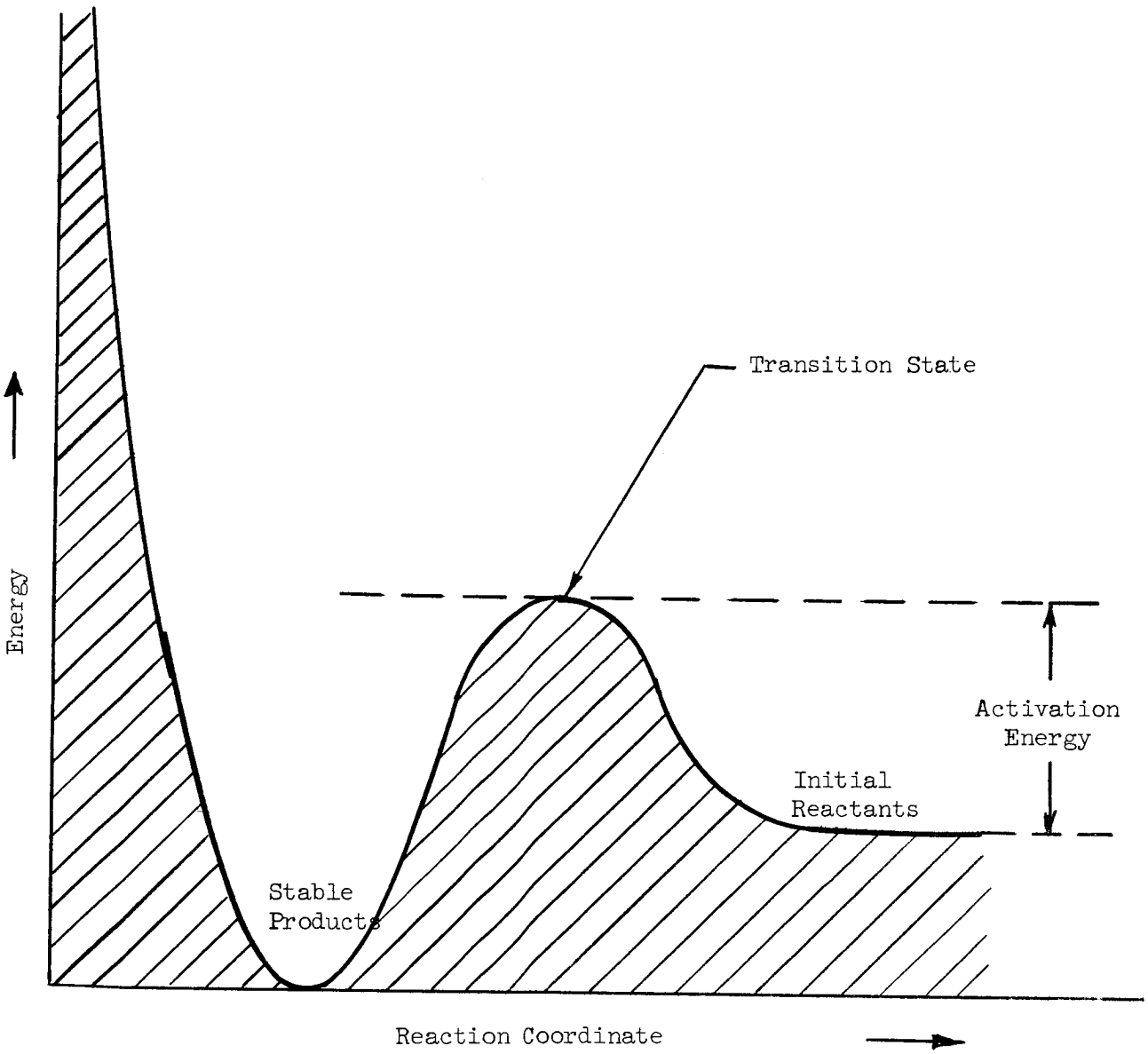

FIG. 1.1--Schematic illustration of activation energy in chemical reactions. The reactants require additional energy to pass through the "transition state," even though their energy is already greater than that of the final products.

Two observations are relevant at this point, First, the primary photochemical process is intimately related to the absorption spectrum of the molecule which is activated. In fact, the nature of the primary process can be established solely from the structure of the absorption spectrum in many cases. Second, and related to this, is that photochemical activation can be a more highly efficient and selective process than thermal activation. Light sources can be chosen such that their wavelengths are absorbed primarily only by specific molecules or parts of molecules in any given system, and such that even large amounts of activation energy can be delivered to these molecules in one step, rather than in many collisions which might also produce unwanted side reactions.

The use of lasers to influence chemical reactions was first suggested[11] at the time of their earliest development. Laser light differs from ordinary light in several features which might be exploited for photochemistry.[6] First, it is highly monochromatic, permitting the possibility of exciting an individual absorption line of a molecule, even when it lies very near to other absorption lines in the same molecule or in other molecules mixed with it. Thus, laser light could be used for extremely selective photochemical reaction of one type of molecule from a sample of several closely related species, such as isotopes, which have slightly different absorption spectra. The light from a frequency-tunable laser could also be used to probe the dependence of photochemical processes on individual absorption lines of a given molecular band system. Second, laser light can be highly intense and spatially coherent, which permits it to be focused to achieve very high radiation densities in small volumes. This can initiate chemical reactions by means of multiple photon absorption,[12,13] electric field effects,[14] or intense local heating of a sample.[15] Finally, the extremely short duration light pulses available from some lasers[16,17] are useful for the flash photolysis study of short-lived transient species in photochemical reactions.[18]

The idea of using monochromatic light for selective photochemistry did not originate with lasers, and there are a number of examples in earlier literature. In 1930 Badger and Urmston[19] reported the use of light of 5461 Å wavelength from a low-pressure mercury arc to react the

of a laser. In fact, none of the previously reported laser-activated photochemical reactions have fully exploited the monochromatic character of laser light.

The photochemistry of bromine in the 6940 Å wavelength region of the ruby laser provided an opportunity and a challenge for the monochromatic capabilities of the laser. First, photochemical activity produced by this wavelength had not previously been reported in bromine, although numerous studies had been made at shorter wavelengths.[32-38] Second, at the ruby laser wavelength, the absorption spectrum of bromine consists chiefly of many closely spaced but individual lines[39] which could be probed for chemical reactivity only with extremely monochromatic light. In contrast to this, the spectrum at the previously studied shorter wavelengths is dominated by a strong and very broad continuum.[40] Finally, the bromine atom has two natural isotopes of atomic weights 79 and 81,[41] and thus forms three isotopic species of diatomic molecules, which have slightly different absorption spectra. If a suitable reaction could be found, it might be possible to react only one isotope by exciting it selectively with the laser, thereby obtaining isotope separation.[42] Moreover, since the bromine isotopes are nearly equally abundant,[41] it would be impossible to separate them by the selective filtering technique proposed by Hartley, et al.,[23] necessitating the use of a monochromatic source such as a laser.

The present investigation resulted in the first reported observation of photochemical activation of bromine in the 6940 Å wavelength region, and the discovery that this activation depends upon the individual bromine absorption lines.[43] This showed that stable excited molecules were formed in the primary photochemical process, in contrast with previous investigations, in which the primary process consisted entirely of direct dissociation into bromine atoms upon absorption of light in the continuum.[32] The experimental results helped to elucidate the mechanism of the overall reaction and associated energy transfer processes. For the purpose of this study, a high repetition rate pulsed, tunable ruby laser was designed, developed, and operated, utilizing special techniques for control of spectral width and stability. This was the first known application of a

"ortho" nuclear spin species of iodine with hexene, in preference to the "para" species. The 2537 Å resonance lines of pure isotopic mercury lamps have been used to react the corresponding mercury isotopes preferentially from samples of ordinary mercury.[5,20] This technique was proposed by Mrozowski[21] and first demonstrated by Zuber.[22] It has been found valuable in the study of the mechanism of mercury-photosensitized reactions. These experiments have been reviewed recently by Gunning and Strausz.[5]

In 1922, Hartley, et al.,[23] attempted without success to react chlorine-37 preferentially with H_2 by exciting it with white light prefiltered by Cl_2 to remove the wavelengths absorbed by the more abundant isotopic molecules. In 1932 Kuhn and Martin[24] obtained a small enrichment of ^{35}Cl by using light at 2816.179 Å filtered from the emission spectrum of an aluminum-electrode arc to excite the phosgene isotopic molecule $CO^{35}Cl^{35}Cl$, which then decomposed due to subsequent collisions. Luiti, Dondes, and Harteck[25] recently produced C_3O_2 isotopically enriched in ^{13}C by preferentially exciting ^{13}CO with the 2062 Å emission line of atomic iodine, and used the isotopic labeling to elucidate the reaction mechanism. Schultz[26] proposed the extension of monochromatic photochemical activation technique into far infrared and millimeter wavelengths. However, it has never been demonstrated that these long wavelengths are effective photochemically, and the first evidence of photocatalysis even at near infrared wavelengths was not obtained until much later.[27]

The first use of laser light for photochemistry was demonstrated by Buddenhagen, et al.[28] Red light at 6943 Å from a ruby laser was absorbed by a blue dye, which acted as a sensitizer for a polymerization reaction. Similar experiments have been reported by Wiley[29] and by Verdieck.[30] Olson[31] used a ruby laser to selectively excite a red-absorbing chlorophyll in living cells, as a means of studying energy transfer processes. Because the materials involved in these experiments absorb in the red, the ruby laser was a convenient source for excitation. However, since the absorption spectra in these materials consisted chiefly of broad continua, it was actually not essential for the source to have the high monochromaticity

device with this combination of features in the field of photochemistry. A number of previous uncertainities concerning the spectrum of bromine were also clarified during the course of the work.

In such an investigation, already interdisciplinary in nature, it was not feasible to study every facet in exhaustive detail. Nevertheless the principal objective of demonstrating the usefulness of the laser for selective photocatalysis was accomplished. This, in turn, suggested possibilities for more detailed photochemical studies in the future through the use of lasers.

Chapter II describes the apparatus and techniques which were employed in this investigation. Chapter III contains a review of previous work on the spectrum of bromine,[39-40,44-48] followed by a description of the spectroscopic results of the present study. The results of the photocatalysis experiments are presented in Chapter IV, and their interpretation is discussed in Chapter V. Possible extensions of this work, including applications of lasers in photochemical primary process and energy transfer studies, are suggested in Chapter VI. The general conclusions of the work are summarized in Chapter VII.

II. EXPERIMENTAL TECHNIQUES AND APPARATUS

2.1 INTRODUCTION

Considerable time and effort in this project was spent in designing and constructing the apparatus used for the experiments, and in learning or developing techniques appropriate for the work. This was necessary for a number of reasons. First, the principal purpose of the investigation was to explore a new technique in photochemistry, namely the use of the laser as a source of monochromatic light. At the beginning of the project (and even at present, to our best knowledge) a laser with all the necessary characteristics was not commercially available, and so it had to be built in the laboratory. Also, the handling and analysis of the chemical reactants and products required equipment and techniques not generally found in a physics laboratory. In this regard, the writer is deeply grateful to a number of individuals for their time and assistance.

In the following sections the important construction and performance features of the high repetition rate, tunable ruby laser will be presented. Then the other apparatus and the experimental procedure for carrying out the photochemical reactions in laser light will be discussed. Additional sections will deal respectively with the preparation and handling of chemicals, the analysis of the reactants and products, and spectroscopic techniques.

2.2 RUBY LASER DESIGN AND CONSTRUCTION

The primary consideration of the design of the laser was the requirement that it have both high monochromaticity and spectral stability. The tolerance placed upon these characteristics was in turn dictated by the spectral width and spacing of the absorption lines of bromine. As we

shall see, these lines were quite close together, typically no farther than $\sim 0.3\ cm^{-1}$, [1] and under the usual experimental conditions had widths of about $0.1\ cm^{-1}$. In addition to linewidth and stability requirements, it was necessary to have some means of shifting the frequency of the laser output to bring it into coincidence with a given absorption line. Finally, it was desirable to maintain a relatively high average power output over a period of time sufficient to perform the experiment. Preliminary studies indicated that the pulsed ruby laser[50] was potentially capable of fulfilling these requirements. Its wavelength of 6943 Å at room temperature could be shifted to approximately 6934 Å by cooling the ruby rod to liquid nitrogen temperature ($77^{\circ}K$). Intermediate temperatures would permit coverage of this 9 Å range ($\sim 20\ cm^{-1}$) within which were included many prominent bromine absorption lines. The technology of the ruby laser was also more advanced than other lasers at the beginning of the project. Actually, these facts had a strong influence on the selection of bromine as a subject for laser photocatalysis, because the ruby laser wavelength was in the region of individual bromine absorption lines. The purpose of this section will be to describe the methods used (1) to maintain a high pulse reptition rate over a long period of time in order to provide high average power, (2) to tune the frequency, and (3) to narrow and stabilize the spectral output.

---

[1] A reciprocal centimeter, or wavenumber as it is often called in spectroscopy, is the unit for measuring inverse wavelength of radiation.[49] Since wavelength λ and frequency f are related by $f\lambda = c$ where c is the speed of light (conventionally taken in vacuo), we have the relationship $\nu = 1/\lambda = f/c$ where ν is the symbol we shall use for reciprocal wavelength, or wavenumber, and ν, λ, and c are measured in vacuo. Since the frequency of visible light is in the range 10^{15} Hz, the wavenumber becomes a more convenient unit for numerical work. In addition, the inaccuracy introduced through the factor $\underline{c}$ in going from measured wavelength to calculated frequency is thereby eliminated. Since energy and frequency are related by $E = hf$ where h is Planck's constant, ν is also proportional to energy, and so can be used to measure atomic and molecular energies. Other units for expressing energy frequently encountered in molecular physics and chemistry are ergs/molecule, calories/mol (mol ≡ gram molecular weight of a substance), and electron-volts. Table 2.1 gives the conversion factors relating these units.

TABLE 2.1

CONVERSION FACTORS FOR ENERGY UNITS

Unit	cm^{-1}	ergs/molecule	cal/mol_{chem}	electron-volts
1 cm^{-1}	1	$1.9855_1 \times 10^{-16}$	2.8584_8	$1.23941_6 \times 10^{-4}$
1 erg/molecule	$5.0364_1 \times 10^{15}$	1	$1.43965_1 \times 10^{16}$	$6.2422_1 \times 10^{11}$
1 cal/mol_{chem}	0.34983_6	6.94612×10^{-17}	1	$4.3359_2 \times 10^{-5}$
1 electron-volt	8068.3_2	$1.60199_6 \times 10^{-12}$	23063.2	1

A photograph of the laser with some of its associated power supply and control equipment is shown in Fig. 2.1. An overall schematic diagram is given in Fig. 2.2. The sapphire-clad ruby rod and the flash lamp for pumping it were located at the foci of a hollow elliptical cylinder, which was highly polished and aluminized on the inside for efficient coupling of pump energy into the rod. The laser end reflectors consisted of a totally reflecting Brewster-angle input roof prism and a partially reflecting uncoated sapphire optical flat, the ends of the rod itself being anti-reflection coated. These elements were fastened to an optical bench on adjustable mounts. The entire apparatus was purged with nitrogen gas to eliminate dust and moisture condensation from the optical surfaces. The principal components of the laser are described under separate headings in the following paragraphs.

2.2.1 Energy Discharge and Control Circuits

The high repetition rate was achieved mainly by using a water-cooled flash lamp (Model XE14-C-3, PEK Labs, Sunnyvale, Calif.). It had a three-inch arc length, the same as the length of the rod and the elliptic cylinder, and was fitted with a water jacket obtained from the same manufacturer. It had a maximum rated input energy per pulse of 1000 J. At the more conservative input energy of 600 J, some of these lamps survived more than 70,000 pulses without failure or noticeable deterioration. The lamp was pulsed by the discharge of two 240 μF, 5 kV capacitors in parallel through a 175 μH inductor in series with the lamp. Initial ionization of the lamp to trigger the discharge was accomplished by a faster, higher voltage pulse directly through the lamp. This was introduced by winding part of the main discharge circuit as the secondary of a trigger transformer and discharging a 1 μF capacitor at 2 kV through two xenon thyratrons (C3J-A) in series with the primary. The thyratrons in turn were activated by applying a positive pulse to the grid of one of them, either with a manual button or with a voltage-sensitive relay in a variable divider circuit which was designed to close when the capacitor voltage reached a predetermined value. This latter method permitted the laser to be fired repetitively at a rate which could be chosen by varying the rate at which the power supply charged

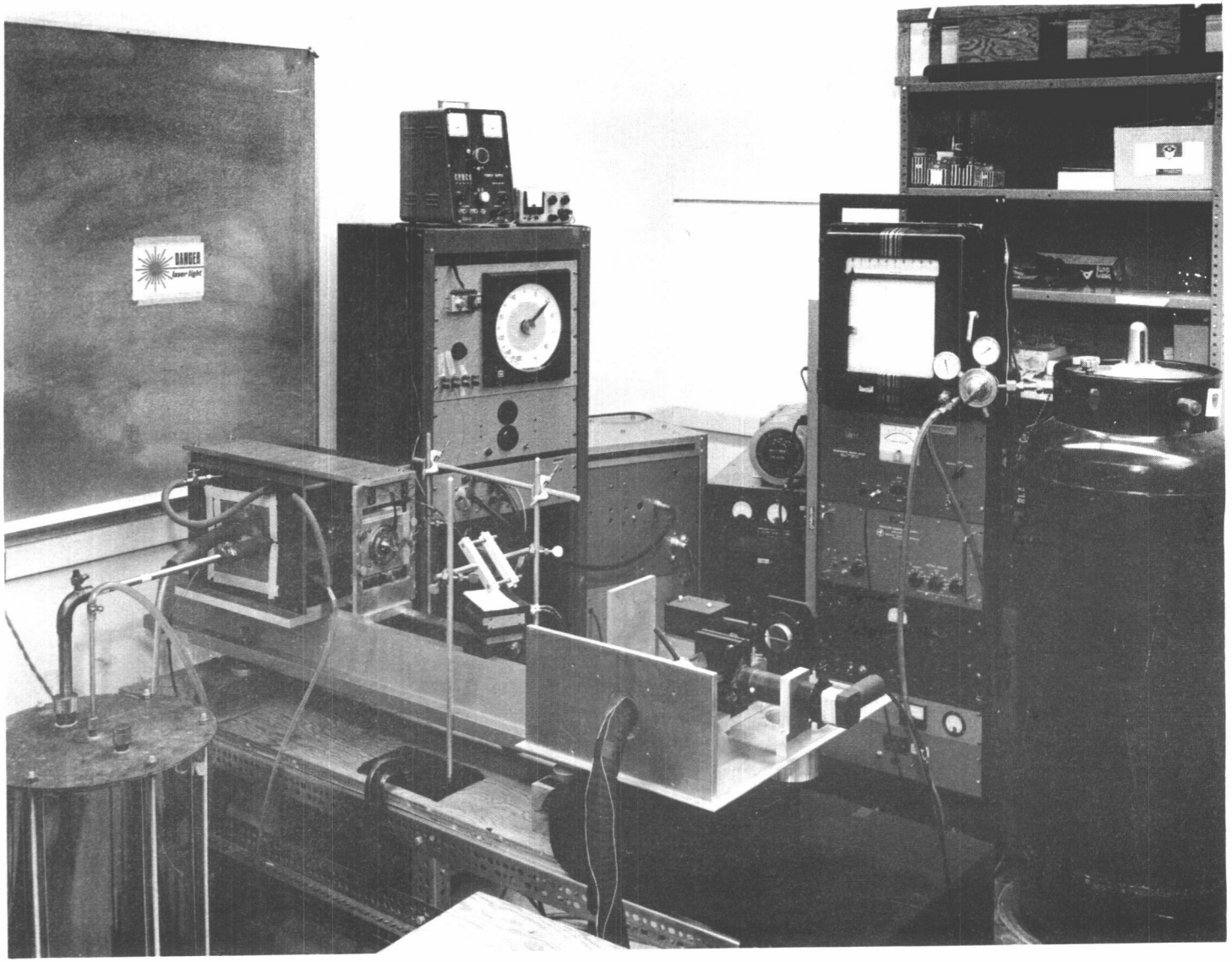

FIG. 2.1--Photograph of the pulsed, tunable ruby laser and related equipment.

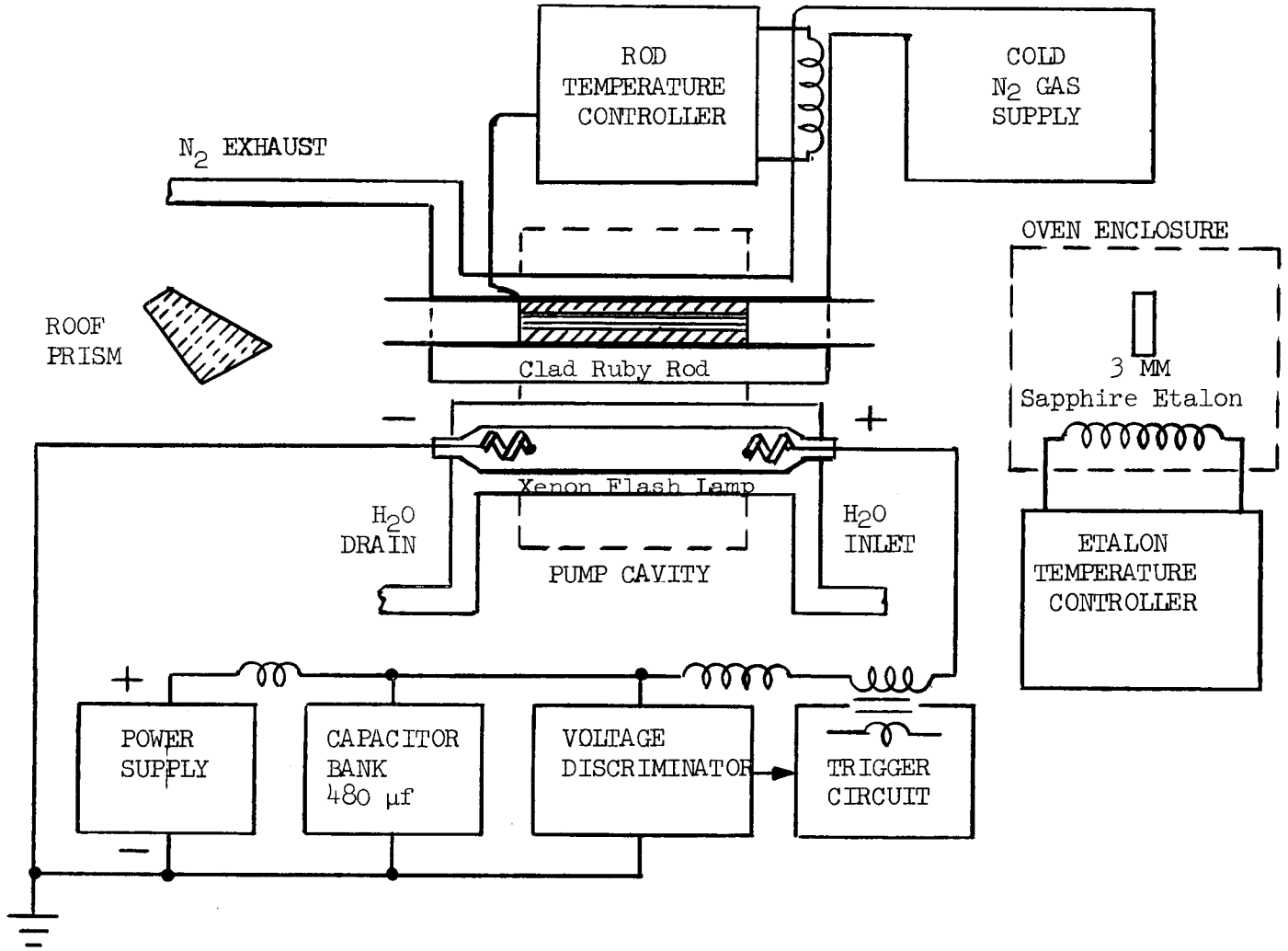

FIG. 2.2--Schematic diagram of the laser system.

the capacitors. Another relay automatically turned off the high voltage and discharged the capacitors through a bleeder resistor in case the flash lamp failed to fire and the voltage continued to climb. A schematic diagram of the discharge circuit is shown in Fig. 2.3.

2.2.2 Rod Cooling and Frequency Tuning

The cooling system for the ruby rod performed two functions. The first was simply to remove the heat which would otherwise build up in the rod with each successive pulse. The second was to control the frequency of the laser output by making use of the temperature-dependent shift of the ruby fluorescence line.[51] The cooling was accomplished by a continuous stream of nitrogen gas which was bubbled through a fifty-liter dewar of liquid nitrogen and passed over the rod through a fused silica cooling jacket. The use of a sapphire-clad ruby rod (Linde Crystal Products, Division of Union Carbide Corp.) with a 0.250 inch diameter core and an outer diameter of 0.442 inch provided additional thermal ballast and cooling surface area, as well as lowering the input energy at the oscillation threshold of the laser. The temperature, and hence the wavelength, could be controlled reasonably well by adjusting the nitrogen flow rate. This method, however, was inconvenient and also could not compensate for slow fluctuations in the temperature from pulse to pulse. The situation was greatly improved by increasing the flow rate slightly and placing a heater consisting of several feet of coiled nichrome wire in the nitrogen stream just ahead of the rod. The temperature sensed by a copper-constantan thermocouple in close contact with the rod was displayed on an indicating potentiometer (Leeds-Northrup "Speed-O-Max"). Geared to the indicator dial was a variable resistor forming part of a bridge circuit (see Fig. 2.4). The current from the bridge was amplified and used to operate a relay which controlled the heater. The sensitivity of the system was such that the temperature difference between opening and closing of the relay was about one degree C . A second variable resistor in the bridge circuit allowed the operating temperature to be selected anywhere over the range of the indicator dial. The control system operated so that if the temperature tended to drift downward,

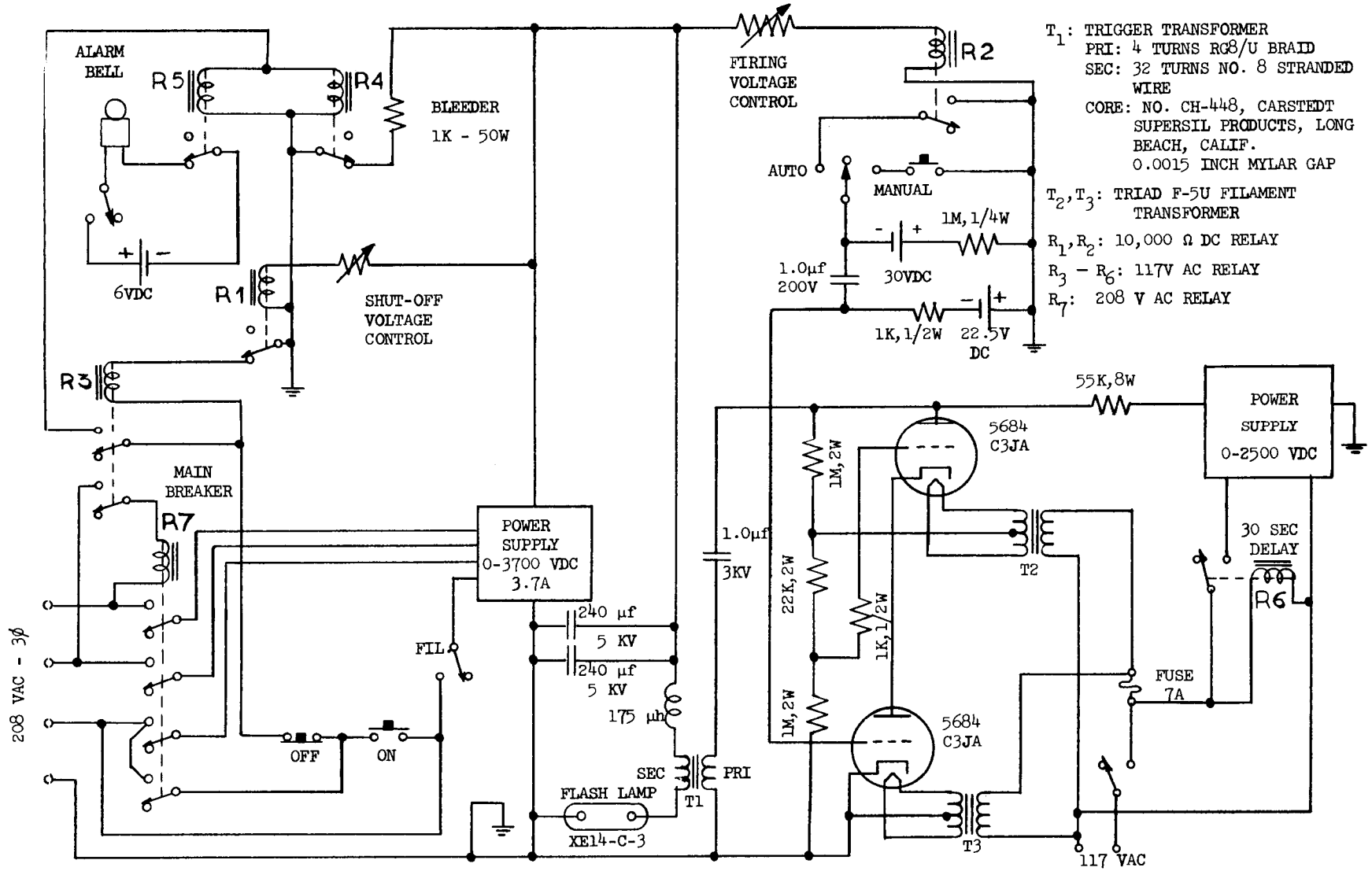

T_1: TRIGGER TRANSFORMER
PRI: 4 TURNS RG8/U BRAID
SEC: 32 TURNS NO. 8 STRANDED WIRE
CORE: NO. CH-448, CARSTEDT SUPERSIL PRODUCTS, LONG BEACH, CALIF.
0.0015 INCH MYLAR GAP

T_2, T_3: TRIAD F-5U FILAMENT TRANSFORMER

R_1, R_2: 10,000 Ω DC RELAY

R_3 – R_6: 117V AC RELAY

R_7: 208 V AC RELAY

FIG. 2.3--Laser flash lamp energy discharge and control circuits.

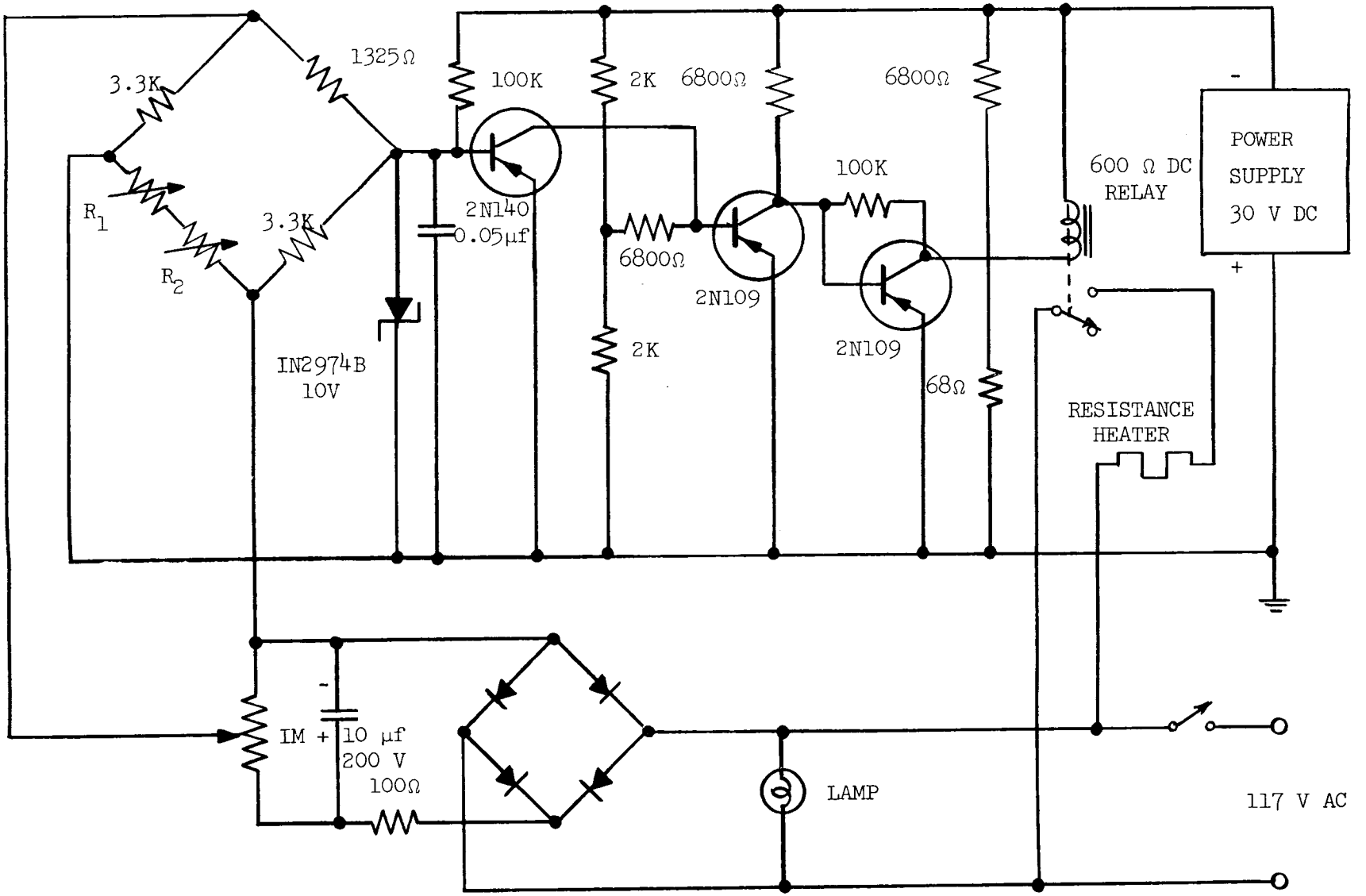

R_1: 10 KΩ PRECISION VARIABLE RESISTOR GEARED TO TEMPERATURE INDICATOR

R_2: 5 KΩ PRECISION VARIABLE RESISTOR FOR SELECTION OF OPERATING TEMPERATURE

FIG. 2.4--Automatic control circuit for laser rod temperature.

the heater would remain on during a longer proportion of each pulse cycle to combat the drift. It should be noted that the temperature sensed by the thermocouple was somewhat lower than the true rod temperature at the moment of the pulse. This was due partly to the fact that the thermocouple was in thermal contact with the cooler nitrogen stream as well as the rod, and partly to the finite thermal conductivity of the rod and response time of the instrument. This made the indicated temperature a function of operating conditions such as pulse rate and energy, as well as a function of the true rod temperature. Therefore, although temperature sensing could be used as a means for frequency control under a given set of operating conditions, it could not provide an absolute frequency calibration. This was accomplished by means of techniques which are discussed in Section 2.4.1.

2.2.3 Control of Spectral Width and Stability

Unfortunately, lasers under ordinary operating conditions are not so ideally monochromatic as we would like for them to be. This arises from the fact that the fluorescence lines themselves have finite frequency widths. Laser oscillation can in principle take place at any frequency within this width for which (1) the round-trip gain in the medium exceeds the round-trip loss, and (2) the round-trip phase shift is zero.[6] The latter condition is satisfied for all frequencies $f = mc/2L$, $m = 1,2,\ldots$, where L is the optical length of the resonator between the two end reflectors. Hence, there exists a set of axial modes of oscillation separated by a frequency interval of $\Delta f = c/2L$. This is illustrated in Fig. 2.5a, along with the possible laser oscillation frequencies which can arise. In particular, it has been shown that, for the ordinary ruby laser, oscillation does in fact occur in many such modes simultaneously,[52] as well as sequentially jumping from mode to mode[53] during the course of a pulse. In addition, the heating of the rod during the pulse can shift the fluorescence line and change the optical length of the cavity,[54] further complicating the spectral output. It was found in the course of our experiments that this behavior made the free-running ruby laser unsuitable for selectively exciting individual bromine lines.

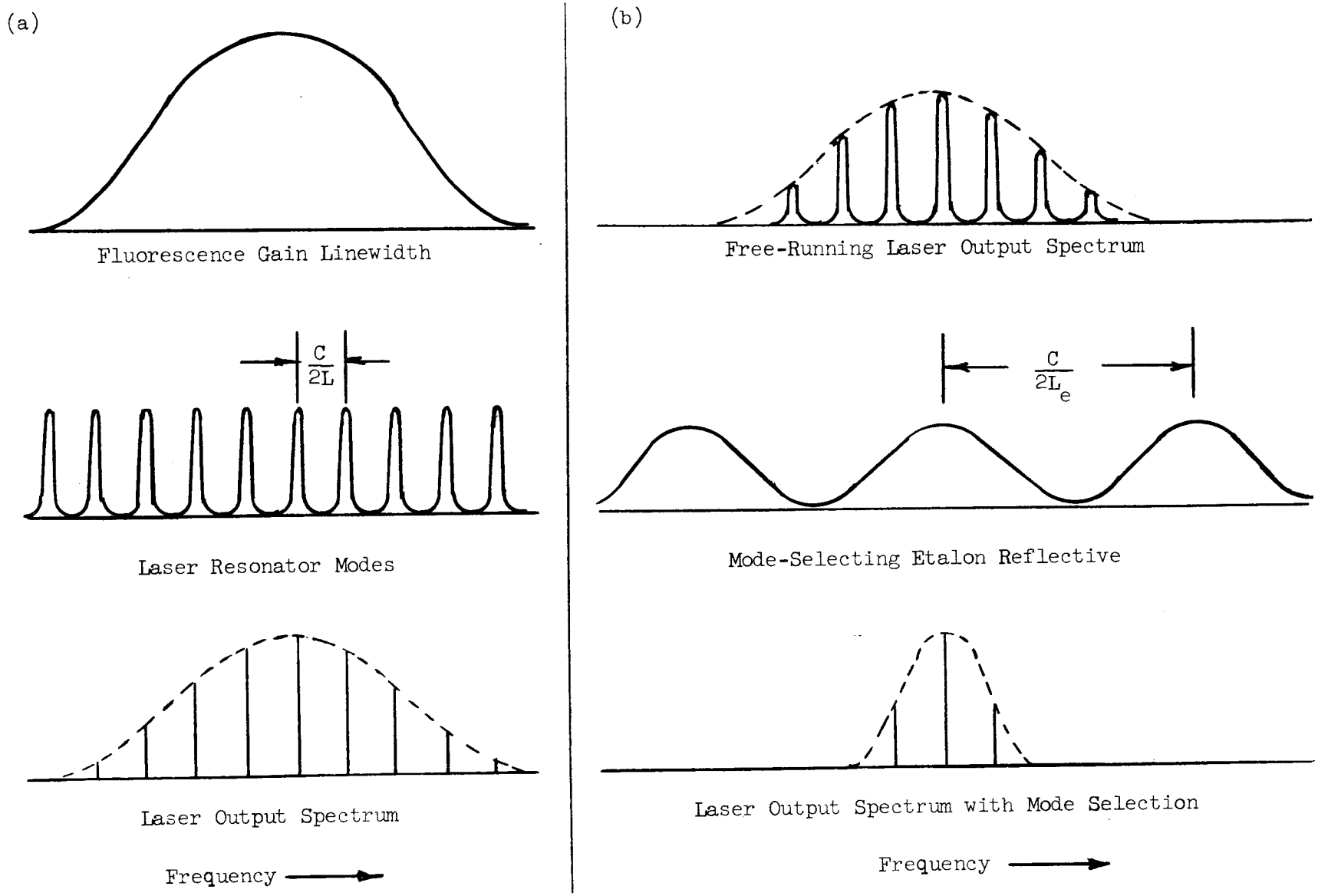

FIG. 2.5--(a) Fluorescence gain linewidth, resonator modes, and resulting output spectrum of a free-running laser.
(b) Narrowing of laser output spectrum resulting from the use of a mode-selecting etalon for one end reflector.

This situation was corrected by replacing the output mirror of the laser with an uncoated sapphire optical flat. The interference between the light waves reflected at the two parallel faces of this flat was such that the combined reflectivity was frequency dependent. This behavior is that of a Fabry-Perot etalon.[55] As with the laser cavity, the etalon has resonances which are spaced by $\Delta f_e = c/2L_e$ where L_e is the optical thickness of the etalon. Thus, there are reflection maxima spaced Δf_e apart, with minima, where the reflection cancels, midway between each pair of maxima. The peak reflectivity is given by

$$\left(\frac{I_R}{I_0}\right)_{\text{maximum}} = \frac{4R}{(1+R)^2} \quad ,$$

where R is the reflectivity of an individual face. Since, for the uncoated flat, the reflectivity arises only from the dielectric interface between the sapphire and air, we have

$$R = \frac{(n-1)^2}{(n+1)^2} \quad ,$$

where n is the refractive index of the sapphire. The result of this periodic frequency dependent reflectivity is to reduce the feedback coupling for most of the laser cavity modes. Only a fraction of them remain with low enough round-trip loss to oscillate, as shown in Fig. 2.5b. The use of such a technique to restrict the number of oscillating laser modes has been discussed in the literature.[56,57]

The resonant frequencies of a solid etalon can be shifted readily by varying the temperature. This shift can be calculated in the following way. Expressed in wave numbers, the frequencies of the etalon modes are given by

$$\nu_e = \frac{m}{2nd}$$

where $m = 1,2,\ldots$, n is the refractive index, and d is the actual thickness of the plate. In general, a change in temperature can produce both a change in the thickness proportional to the coefficient of linear expansion, and a change in the refractive index. Hence, we have

$$\frac{\delta \nu_e}{\delta T} = \frac{\partial \nu_e}{\partial d}\frac{\delta d}{\delta T} + \frac{\partial \nu_e}{\partial n}\frac{\delta n}{\delta T}$$

$$= -\frac{m}{2nd^2}\frac{\delta d}{\delta T} - \frac{m}{2n^2 d}\frac{\delta n}{\delta T}$$

$$= -\nu_e\left(\frac{1}{d}\frac{\delta d}{\delta T} + \frac{1}{n}\frac{\delta n}{\delta T}\right) \quad .$$

Since the quantity $1/d \; \delta d/\delta T$ is just the coefficient of linear expansion, the entire temperature effect is independent of the thickness of the etalon.

Sapphire was chosen because of its excellent thermal properties, and because its peak reflectivity was sufficiently high to provide mode discrimination over a convenient range of pump energies. It has a refractive index of 1.76 with a temperature coefficient of 1.3×10^{-5} per degree C , and an expansion coefficient of 6.76×10^{-6} per degree C .[58] From these values we calculate a peak reflectivity of 26% and a temperature shift of the etalon resonances of

$$\frac{\delta \nu_e}{\delta T} = -14.16 \times 10^{-6} \; \nu_e \; \text{cm}^{-1}/^{\circ}\text{C} \quad ,$$

which for ruby laser light at 14,400 cm^{-1} is equal to -0.204 $\text{cm}^{-1}/^{\circ}\text{C}$. The flat was 3 mm thick, which made the interval between modes equal to 0.95 cm^{-1} . Thus, the etalon could be tuned over its free spectral range in a temperature interval of approximately 5°C, making it possible to place only one etalon resonance within the gain profile of the fluorescence line. As long as this condition could be maintained, the

etalon would effectively reduce the spectral width of the laser output. An additional advantage in using the etalon was that the laser would continue to oscillate at the frequency determined by the etalon resonance, in spite of small shifts in the center frequency of the ruby fluorescence line. This would result in a great improvement in spectral stability, as the thermal stabilization of the passive etalon was inherently much less difficult than the thermal stabilization of the active ruby rod, which was continually subjected to the violent pulses of flash lamp radiation.

To accomplish this, the etalon was housed in an insulated oven enclosure, with strict temperature regulation provided by a proportional controller (Model V1523, Reeves-Hoffman Division, Dynamics Corporation of America, Carlisle, Pennsylvania) with a range of $\pm 10^{\circ}C$ and a published stability within $0.01^{\circ}C$. The laser light entered and left the oven enclosure through low-scatter Suprasil[1] Brewster-angle windows. Since the sapphire etalon was oriented at zero degrees, its reflectivity did not depend upon the polarization of the light.

2.3 PERFORMANCE OF THE RUBY LASER

After the laser was constructed, preliminary experiments were conducted to determine its performance characteristics. The results were consistent with expectations.

To measure the frequency shift of the laser output as a function of rod temperature, a portion of the beam, suitably attenuated with interference filters, was admitted through the entrance slit of a Jarrell-Ash high resolution scanning spectrometer. An RCA 7265 Photomultiplier tube served as a detector, and its output signal was amplified and displayed on a chart recorder. The spectrum was scanned slowly while the laser was repetitively pulsed, with the result that the laser pulses were detected and recorded at their appropriate wavelength. The instrument automatically provided wavelength calibration marks on the chart at convenient intervals. Runs were made for indicated temperatures of $-40^{\circ}C$,

---

[1] Trade name, Amersil Quartz Division, Engelhard Industries, Inc., Hillside, N. J.

-60°C, and -80°C, and for several values of pulse repetition rate and input energy. The results are plotted in Fig. 2.6. The fact that the frequency depended upon other parameters besides the indicated temperature resulted from the time lag of the latter with respect to the actual rod temperature, as discussed in Section 2.2.2.

The output energy of the laser was measured in two ways. First, the relative energy was measured by splitting off part of the beam with a glass microscope slide, attenuating it, passing it through a narrow-pass interference filter, and detecting it with an RCA type 925 vacuum photodiode. The resulting signal was processed by a simple integrating circuit, the voltage output of which was measured with a vacuum-tube voltmeter. A schematic of this arrangement is shown in Fig. 2.7. The measured voltage was proportional to the average power delivered by the laser. A figure proportional to the energy output per pulse was obtained by dividing by the pulse repetition rate. A more direct, but less convenient, measurement of the absolute energy per pulse was made by admitting single pulses into a calibrated thermopile ("Laser Rater," TRG, Inc., Melville, N. Y.). The output voltage was measured by a microvoltmeter. The relative energy measurements were converted to absolute energy by comparison with the thermopile measurements at several points. Figure 2.8 shows the resulting dependence of the output energy on input energy for two sets of temperatures and two pulse rates. Threshold input energy increased with temperature and was about 240 J at -80°C. The error bars indicate only the spread in the experimental data, but do not take into account inaccuracies in the conversion from relative to absolute energies due to the thermopile. These, however, are believed to be no greater than ±10%. For subsequent experiments the laser was generally operated at a higher input energy, with a correspondingly greater output energy. Calibrations were made at those times in the same manner as described above. The output pulse duration was typically about 0.5 msec, during which spiking behavior characteristic of ruby lasers was observed.[52,53]

The spectral width and stability of the laser output, as well as the thermal tuning properties of the sapphire mode-selecting etalon, were measured by means of an analyzing Fabry-Perot etalon placed in the

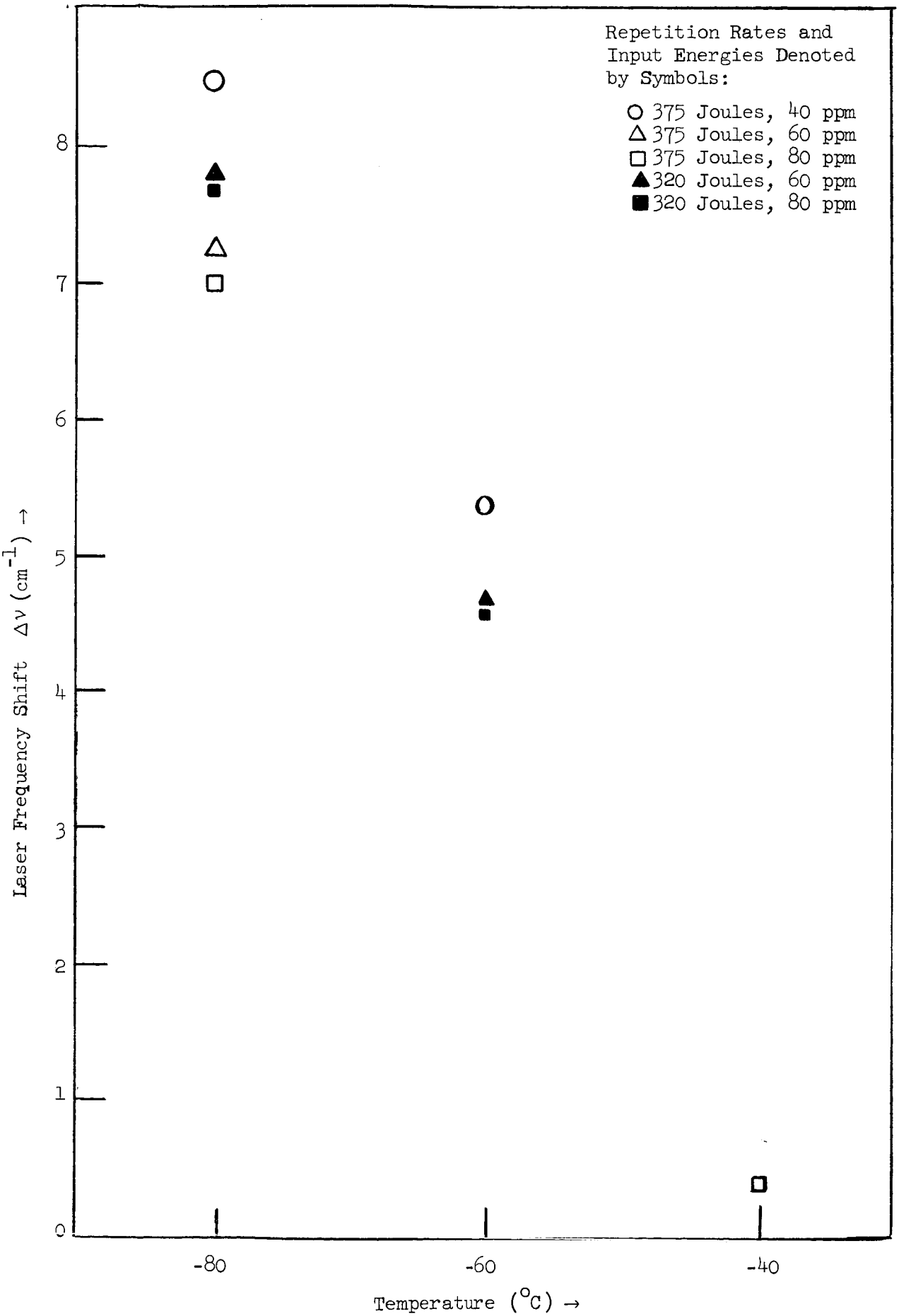

FIG. 2.6--Measured shift of laser frequency as a function of indicated rod temperature for various repetition rates and input energies.

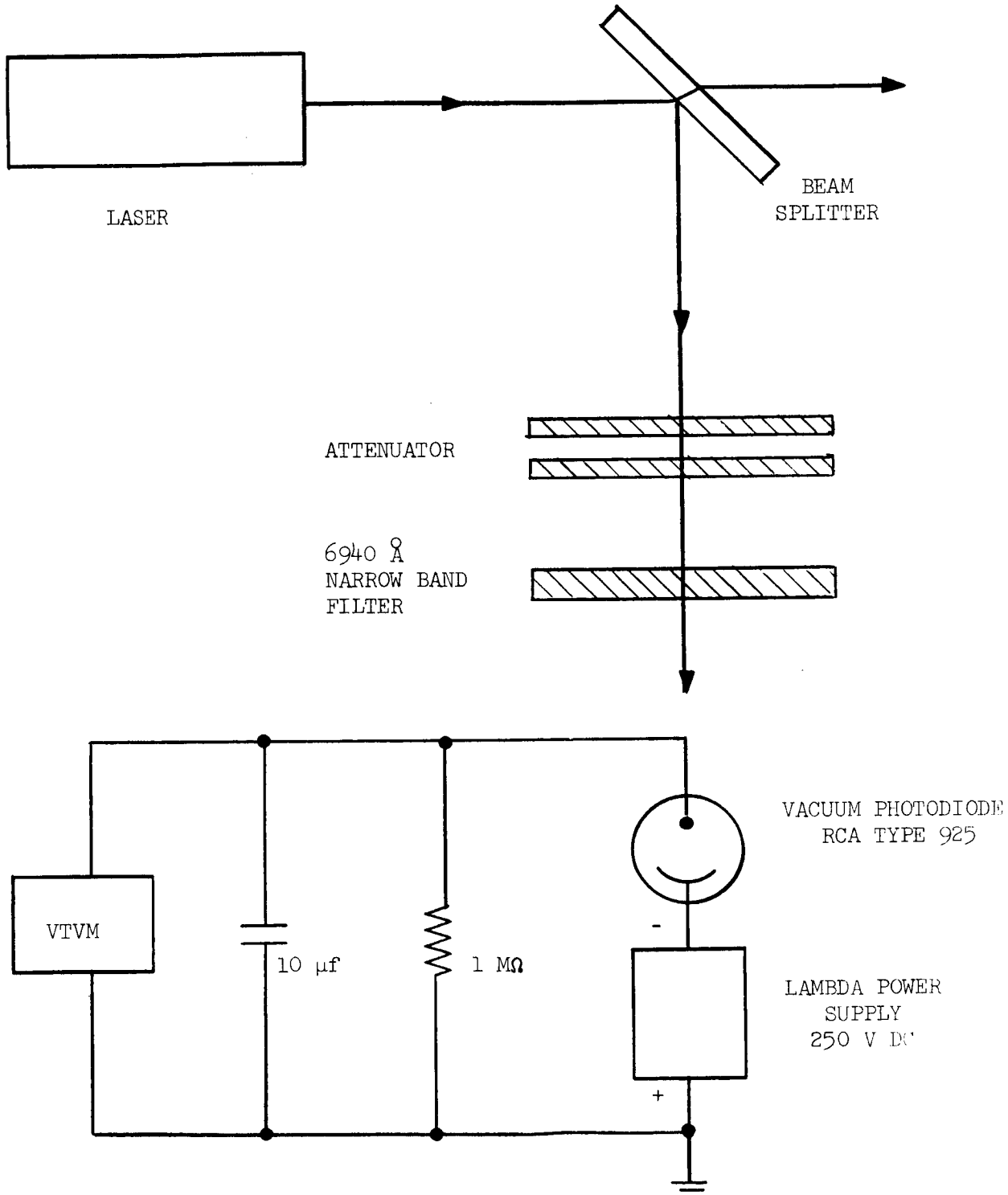

FIG. 2.7--Schematic arrangement of laser energy monitoring apparatus.

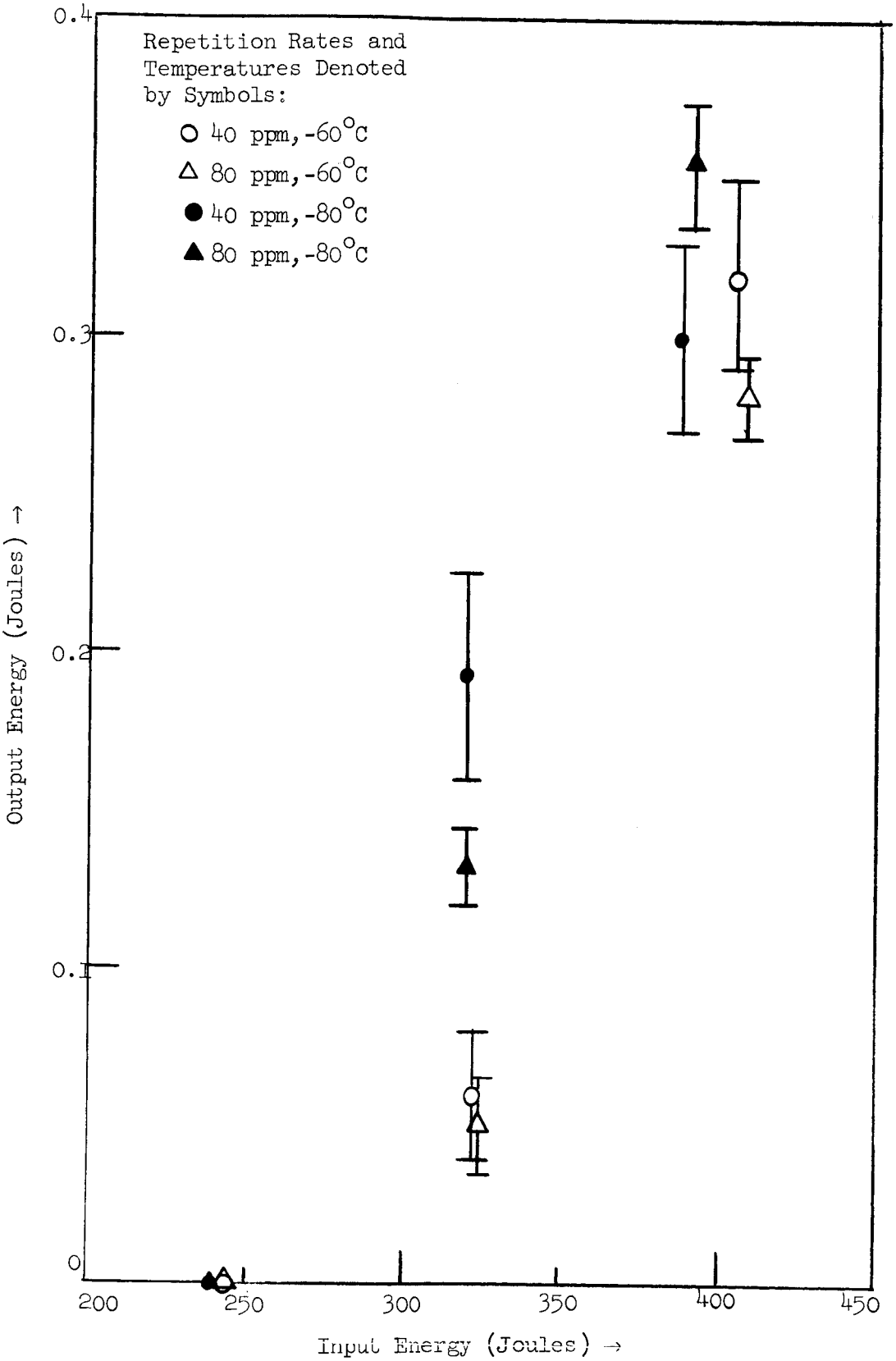

FIG. 2.8--Laser output energy per pulse as a function of input energy measured at various rod temperatures and pulse repetition rates.

path of the beam behind a diffusing ground-glass screen. The resulting interference fringes were recorded on polaroid film. This arrangement is shown schematically in Fig. 2.9. The analyzing etalon used in most of these measurements was a solid fused quartz flat with dielectric reflective coatings on its parallel faces.[1] Its thickness was such that the distance between fringes of successive order corresponded to a spectral range of approximately 0.25 cm^{-1}.

The result of such a measurement is shown in Fig. 2.10. The left-hand side is the fringe pattern produced by the superposition of one hundred consecutive ruby laser pulses. The fringe width indicates a spectral width and stability within about 0.04 cm^{-1}. Fringes resulting from more than this number of pulses, or from single pulses, indicated materially the same linewidth, so long as the mode-selecting etalon was allowed to remain at a constant temperature. This stability was maintained even when the indicated temperature of the ruby rod drifted over a five degree range. Rod temperature changes greater than this caused the laser oscillation to occur at two resonances of the etalon separated by about 1 cm^{-1}, and for even larger changes the laser frequency shifted entirely to the second resonance. On the other hand, the frequency of the laser could be tuned smoothly by changing the etalon temperature. It was possible to achieve oscillation at only a single etalon resonance even when the laser was operated at input energies greater than twice threshold. The right-hand side of Fig. 2.10 shows for comparison the fringe pattern from a highly monochromatic and stable helium-neon laser (Model No. 119, Spectra-Physics, Inc., Mountain View, Calif.), using the same analyzing Fabry-Perot etalon. The width of these fringes is due almost entirely to the limited resolution of the analyzing etalon itself. After correcting the observed ruby laser fringe width for this instrumental fringe width, the actual spectral width of the ruby laser output is somewhat less than 0.04 cm^{-1}. From the dimensions of the laser the spacing of the individual cavity modes was calculated to be about 0.01 cm^{-1}. It was not possible to decide on the basis of the fringe patterns if oscillation occurred in more than one of these during a pulse. The time-resolved spiking behavior,

[1] Manufactured by Laboratory for Science, Oakland, California.

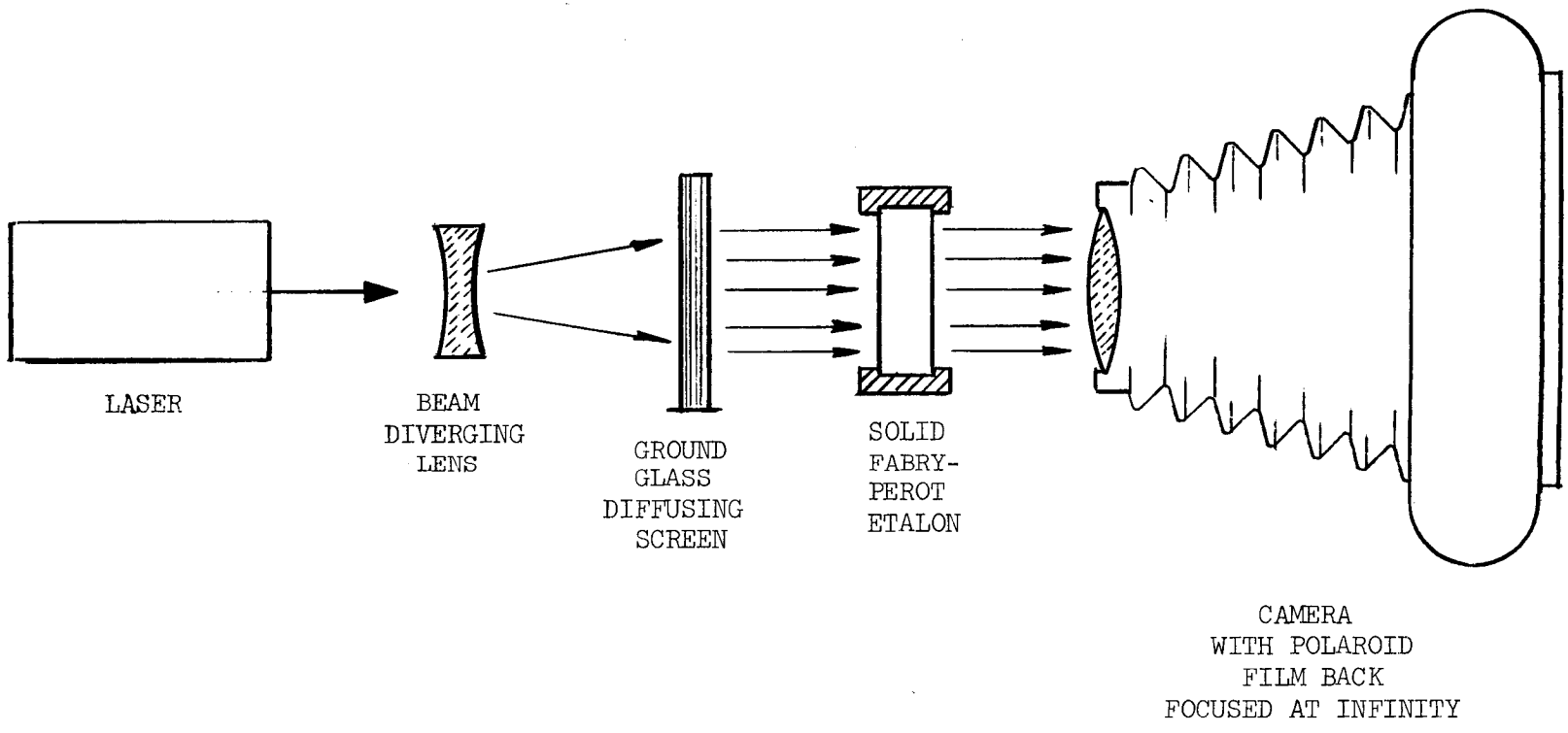

FIG. 2.9--Schematic arrangement for photographing interference fringes of laser spectrum.

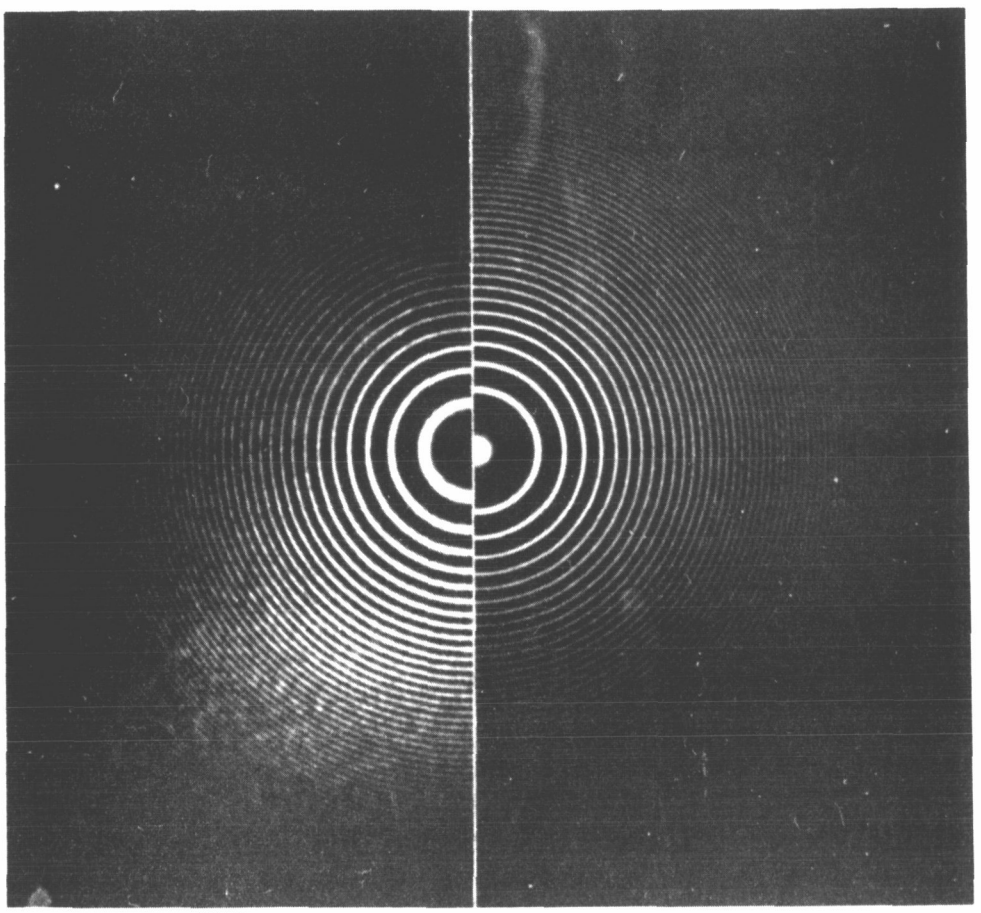

FIG. 2.10--Interference fringes on the left-hand side produced by 100 consecutive pulses of the ruby laser; fringes on the right show output of Spectra-Physics 119 single-frequency helium-neon laser. The spacing between adjacent fringes corresponds to a spectral range of 0.25 cm^{-1}.

however, indicated that this was the case. Also, rapid temperature fluctuations in the ruby during the pulse would be expected to cause changes in the cavity optical length, with resultant shifts of the cavity modes across the etalon resonance. With a conventional mirror instead of the mode-selecting etalon, the laser oscillation occurred over a width of about 0.35 cm^{-1}. Hence, the upper limit of 0.04 cm^{-1} obtained with the etalon represents a significant spectral narrowing of the laser output.

The reliability of the laser was an extremely important consideration, since the proposed experiments potentially involved runs lasting several hours, requiring tens of thousands of consecutive pulses. This problem was solved only after a number of different approaches were tried unsuccessfully. The described system evolved through careful selection and combination of many individual components. The result was stable and reliable operation, with hardly any interruption due to breakdowns, over a total period of some hundreds of thousands of pulses.

2.4 LASER PHOTOCHEMISTRY TECHNIQUES

In addition to developing a suitable laser, it was necessary to devise methods for using it as efficiently as possible to catalyze the reaction, as well as methods for monitoring the course of the reaction. The purpose of this section is to describe these techniques and their relation to the overall experiment. Figure 2.11 shows schematically the arrangement of the apparatus, which will be discussed in detail below.

2.4.1 Energy and Wavelength Monitoring

Obviously, the laser wavelength and the energy per pulse had to be known during the course of a reaction because changes in either of them could affect the results drastically. The energy was measured by the indirect method using a photocell and an integrating circuit, as described in Section 2.3. As far as wavelength was concerned, the important consideration was the position of the laser output with respect to the bromine absorption lines. This was measured in a manner similar to that described in Section 2.3. However, instead of using the spectrometer wavelength

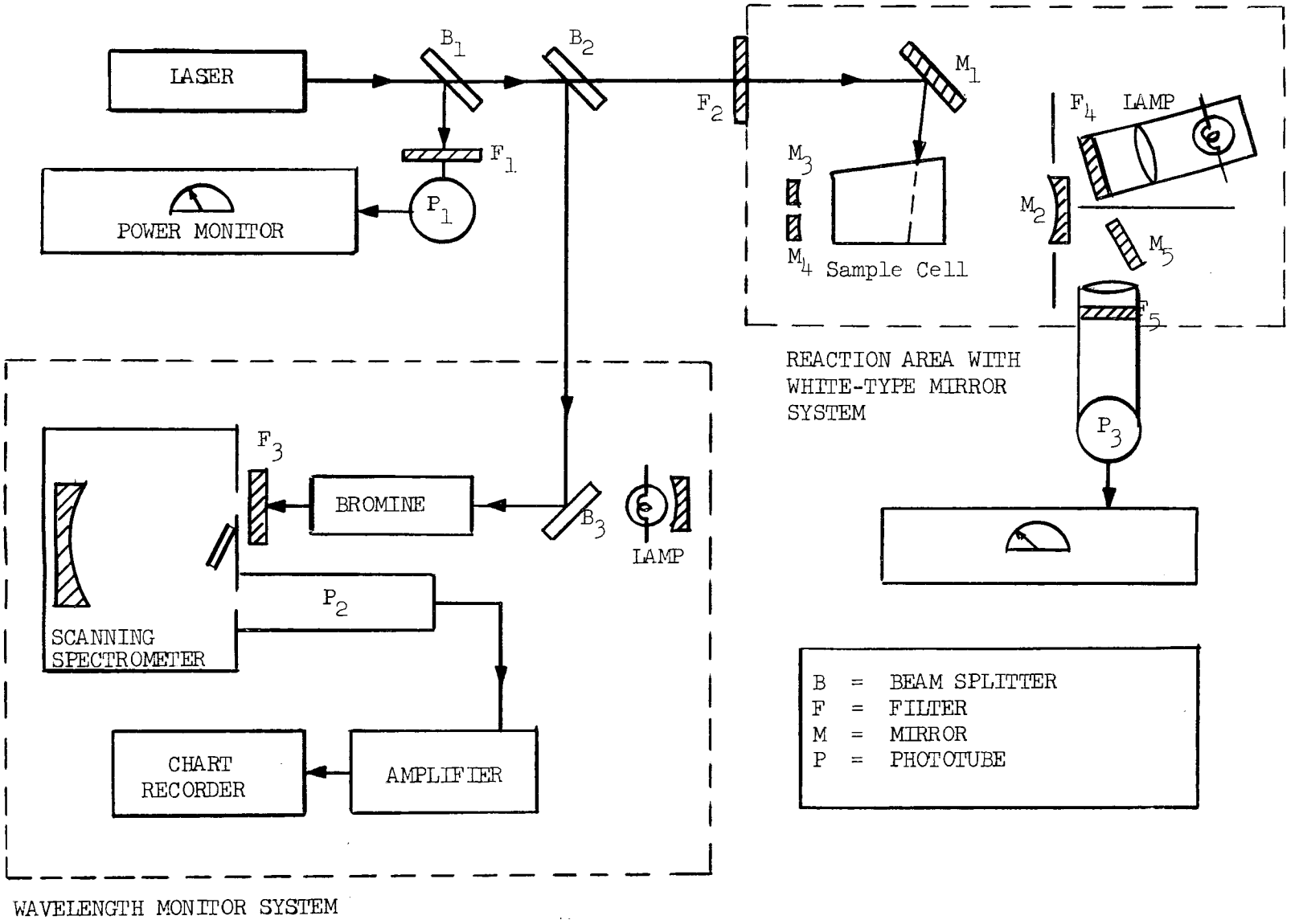

FIG. 2.11--Schematic diagram of overall arrangement of equipment for laser photocatalysis experiments.

marker, a long absorption cell filled with bromine was placed in front of the spectrometer. Light from a low-voltage tungsten projection lamp (Sylvania Tru-flector) was passed through the cell into the spectrometer simultaneously with the pulses of laser light. Thus the absorption spectrum of bromine was recorded on the chart paper, with the laser pulses superimposed at the appropriate wavelength as the spectrum was scanned. The temperatures of the rod and of the mode-selecting etalon were then adjusted to bring the laser wavelength into coincidence with the desired absorption line. The wavelength region of interest was scanned repetitively during the course of the experiment to double-check the temperature stability of the rod. Since the mode-selector temperature was extremely stable at all times, it was necessary only to guard against the appearance of a second oscillation occurring about 1 cm^{-1} away from the desired line, which was easily detectable by means of this technique.

2.4.2 Reaction Cell

For reasons which will be discussed in later chapters, it appeared to be desirable to work with small samples of gases in doing the reactions. Very little of the light energy from the laser beam could be absorbed in a single pass through these samples, and thus most of the energy would be wasted. One obvious way to make more efficient use of the available energy was to reflect the emerging beam back through the sample repeatedly. This was accomplished by making use, with slight modifications, of a special cell which had been designed for laser-excited Raman spectroscopy (Perkin-Elmer Corp., Norwalk, Conn., Part No. 211-0537 for Model LR-1 Laser Excited Raman Spectrometer). This 2.5 ml cell was constructed entirely of optically contacted fused silica approximately in the shape of a rectangular parallelepiped. There was a slight wedge angle between the upper and lower faces, which were multi-layer dielectric reflective coated except for a small area which permitted the laser beam to enter. This geometry caused a beam entering at the proper angle to be multiply reflected through the cell in such a way that the absorption path length was increased to approximately 1.5 meter. The cell was held in a kinematic mounting assembly (Perkin-Elmer Corp., Part No. 211-0535) which was adjustable

for optimum orientation. A graded seal connected it to a pyrex side tubing which led to a vacuum stopcock and a tapered ground-glass joint. The cell could be easily detached from the mounting assembly and connected to a mating joint on a gas-handling system, which is described in Section 2.5. The reaction cell and its mounting assembly are shown in Fig. 2.12.

2.4.3 Optical Alignment

The multiple-pass cell arrangement made alignment of the laser beam more critical than would be the case for a single pass. In addition, the external reflectors forming the laser cavity itself needed to be aligned carefully. Clearly, attempts to perform this alignment under pulsed conditions, even with a high repetition rate, would be slow and frustrating. This was avoided by using an inexpensive continuous-running helium-neon laser (Optics Technology, Inc., Palo Alto, Calif., Model No. 170), which provided a well-collimated beam at a wavelength of 6328 Å.

The alignment procedure for the ruby laser consisted of passing the He-Ne laser beam through two apertures on the optical bench which defined the beam axis, and then aligning the pump cavity of the laser so that the beam passed through the ruby rod, and so that the weak reflection from the ends of the rod produced a spot concentric with the initial beam at the output aperture of the gas laser. Then the roof prism and the sapphire etalon were attached to the optical bench and adjusted so that they also reflected the beam directly back upon itself. Before the ruby laser could oscillate, it was necessary to make a small additional adjustment in the prism orientation to correct for dispersion in its refractive index in going from 6328 Å to 6940 Å. This was facilitated by using a micrometer screw on the prism mount.

Next, the reaction cell was aligned by passing the He-Ne laser beam along the same axis in the opposite direction. The cell, attached to its mount, could be moved horizontally at right angles to this axis along a track, which in turn was secured to the optical bench. An adjustable 45° prism was positioned so as to deflect the laser light downward into the cell. All of these components were aligned so that the beam entered the

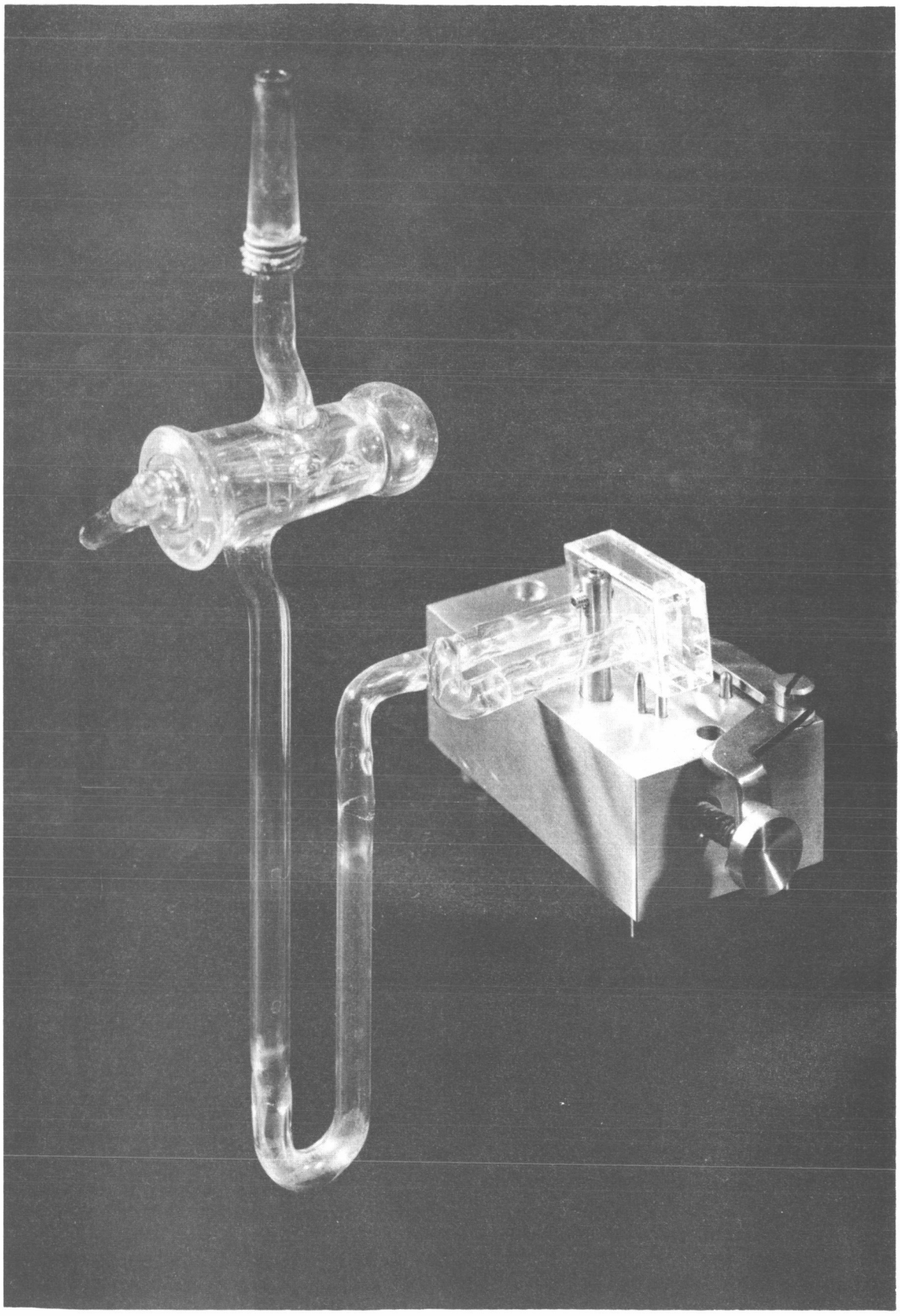

FIG. 2.12--Photograph of reaction cell and kinematic mounting assembly.

cell properly and was multiply reflected to fill the volume as uniformly as possible. Additional adjustments were usually necessary after the ruby laser was turned on, but these were generally minor.

2.4.4 Monitoring the Reactions

The technique chosen for determining the reaction rate was the optical measurement of the disappearance of bromine molecules from the cell. Basically, this was done by using a light source with a wavelength which was absorbed by the bromine molecules, but not by the other gases in the cell, and a photodetector to measure the transmission of this light through the cell. This arrangement was calibrated against known partial pressures of bromine, which in turn were determined from temperature-vapor pressure tables.[59] One important consideration was that the monitor light intensity had to be low enough so as not to induce a significant reaction itself.

In order to increase the sensitivity of the monitoring system, the monitor light was multiply-passed through the cell at right angles to the laser beam. This was accomplished by means of external mirrors in a configuration originally designed by White.[60] Some of the mechanical mounting features described by McCubbin and Grosso[61] were incorporated in the construction. Up to sixteen passes of the light were readily obtained. The light source was a microscope lamp, the intensity of which was monitored with a silicon photodiode and regulated by a variac. It was operated below its normal current by placing a two-ohm resistor in series with it. A pair of glass filters with similar bandpass characteristics (Corning No. 5-57 and No. 5-58) allowed only blue light to fall on the cell and to be detected by the photomultiplier. This eliminated spurious signals caused by the red laser light. The type 931A photomultiplier was operated with a regulated power supply at 1000 V dc. The output current was filtered to remove excess high frequency noise, and was measured with a Hewlett-Packard Model No. 425A Micro Volt-Ammeter. The system was quite stable, and was capable of detecting changes in bromine concentration of the order of 1%. A schematic of this arrangement is shown in Fig. 2.13.

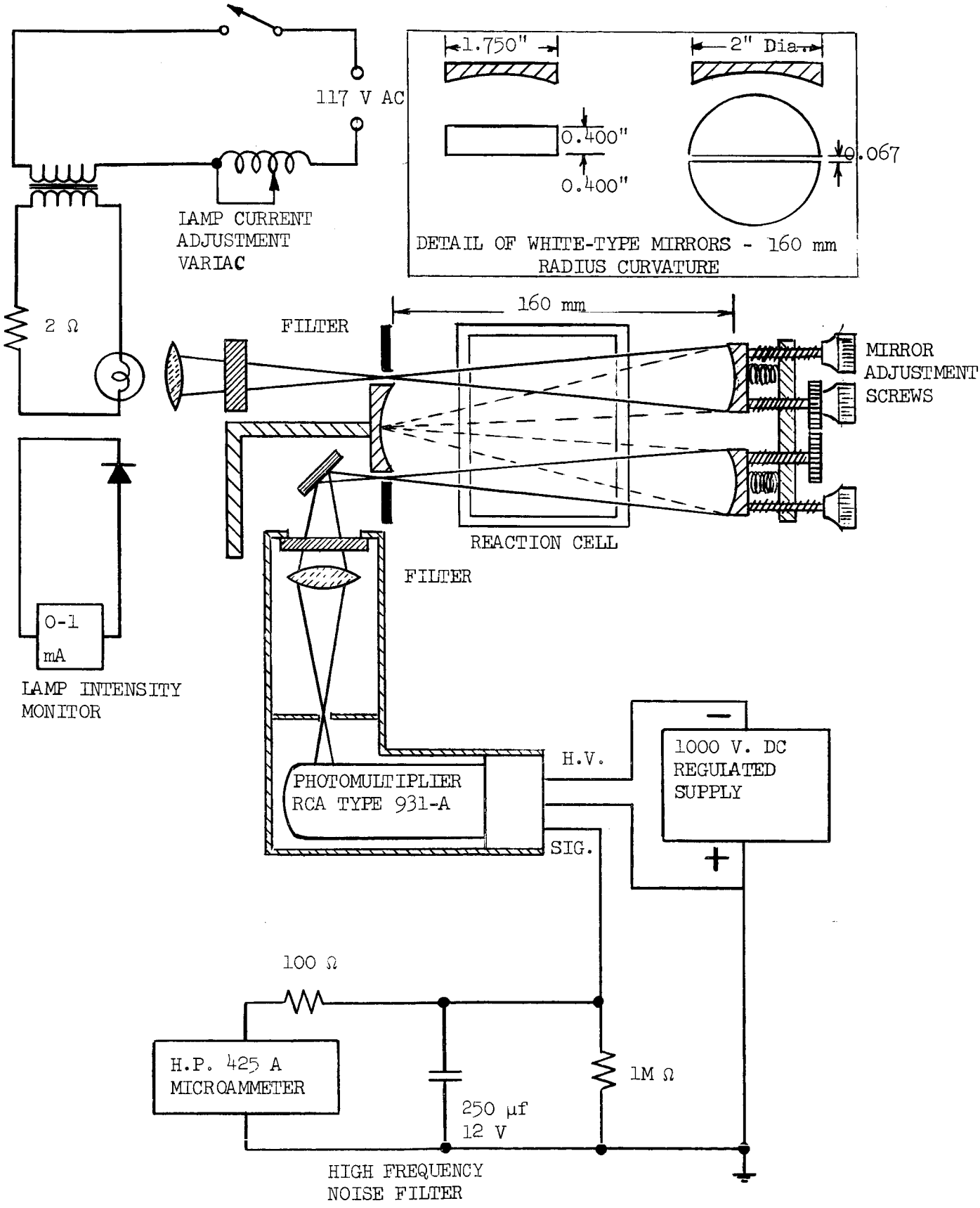

FIG. 2.13--Schematic diagram of system for optical monitoring of reaction rate.

The entire reaction cell and monitoring system were covered with a light-tight box to prevent room lights from affecting the reaction or the monitoring system. A shutter could be opened to admit the laser light through a red glass cut-off filter (Corning No. 2-64). A photograph of the reaction cell in position with the monitoring system and other related optical equipment is shown in Fig. 2.14.

2.5 PREPARATION AND HANDLING OF CHEMICALS

The corrosive nature of bromine necessitated the use of an all-glass system for handling the chemicals. Since most of the reactions were sensitive to oxygen and water vapor, the system had to be evacuated prior to use. For convenience the system could be easily dismantled and reconstructed using interchangeable ground glass joints. High vacuum stopcocks were used throughout. Apiezon type N and type L lubricants were used for the stopcocks and joints, respectively. Sidearms could be attached to the system by means of additional ground glass joints. The system was evacuated with a mechanical roughing pump and with a three-stage glass diffusion pump, which were connected to the system through a liquid nitrogen cold trap. The roughing pump vacuum was measured with a thermocouple gauge, and could be maintained at ~ 20 microns Hg . A mercury manometer for measuring the pressures of noncorrosive gases was connected to various parts of the system through stopcocks. It could also be connected to air or to the roughing pump and used in conjunction with a quartz-spiral null-type Bourdon gauge (Worden Instruments, Inc., Houston, Texas) for indirectly measuring the pressure of bromine or of a reacting mixture of gases. Because of the poisonous and corrosive nature of many of the reactants and products, the pump exhaust was directed into a laboratory fume hood. The gas-handling system is shown in Fig. 2.15.

Mallinckrodt Analytical Reagent grade bromine was used in the experiments. It was placed in a side tube which was attached to the vacuum system and then subjected to several freeze-pump cycles to remove the air. Then it was dried by vacuum distillation to another side bulb through a phosphorous pentoxide tube. This process was repeated several

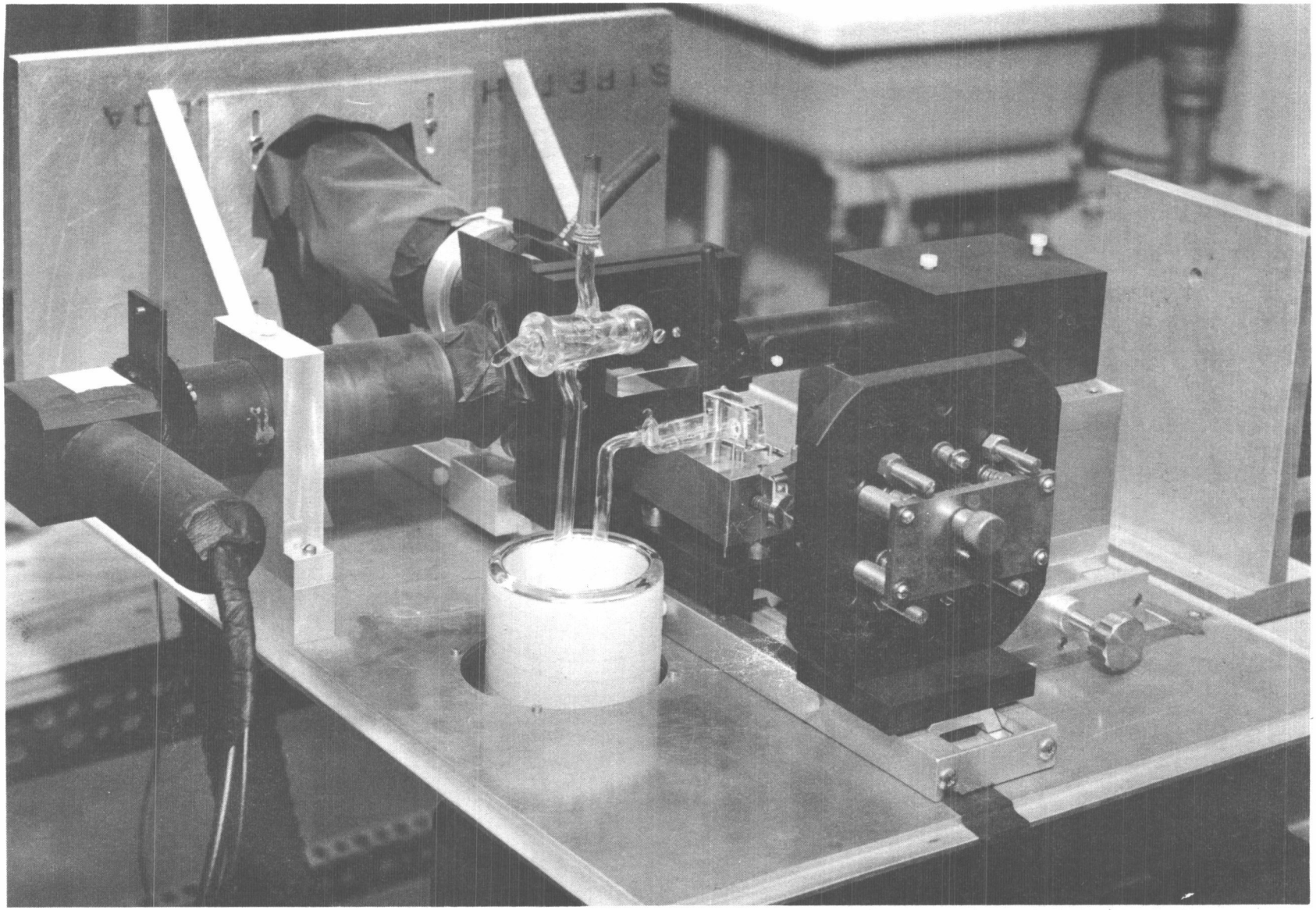

2.14--Photograph of reaction monitoring equipment with reaction cell in position.

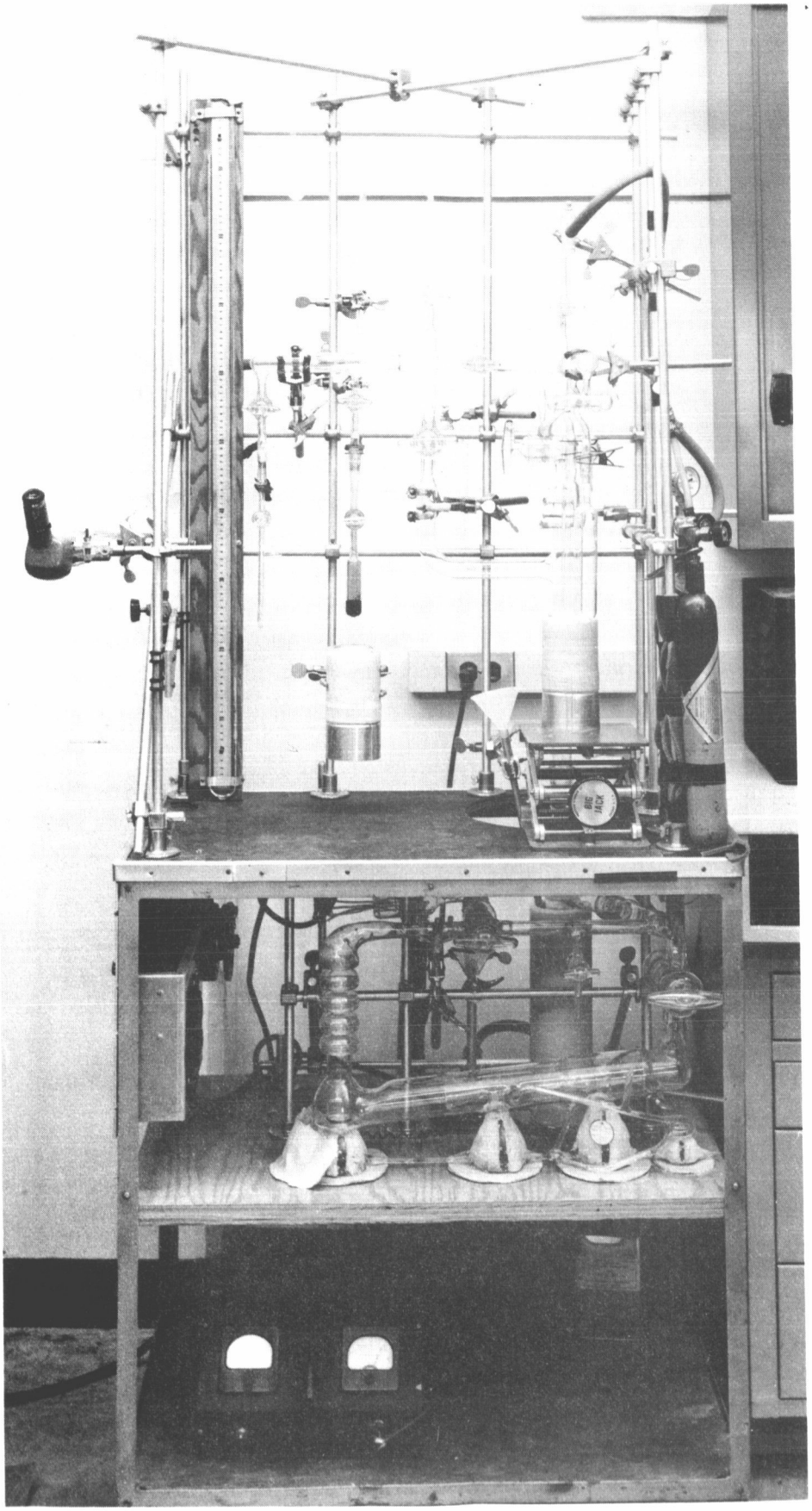

FIG. 2.15--Photograph of gas handling system.

times, after which the bromine was fractionally distilled, retaining only the middle fraction, which was stored in an evacuated side tube and was periodically purified by the same method. The same procedure was also followed for the other gases.

At the beginning of a reaction, the reaction cell was first filled with bromine and then evacuated. Then the second filling was made to the desired pressure, using the Bourdon gauge-manometer combination for pressure monitoring. Additional gases were placed in the cell by first filling a large ballast chamber of the system until the manometer indicated the desired sum of the partial pressures of gases being filled and those already in the cell. Then the stopcock to the cell was opened and the gas flowed in under its own excess pressure. When the pressures equalized, the stopcock was quickly closed and the final pressure was recorded. After a reaction, the contents of the cell were trapped into a side tube, to be discarded, or else sealed off and analyzed.

2.6 ANALYTICAL PROCEDURES

The identification of reaction products was accomplished mainly through the use of gas chromatography and mass spectrometry. In the former, a small sample (fraction of a microliter to a milliliter or so) is injected into a stream of inert carrier gas, which then passes at a controlled flow rate and temperature through a long column. The column contains loosely packed solid material (the "support") on which there is a thin film of liquid. The molecules of the gas sample tend to become adsorbed on the liquid film, which causes them to lag behind the carried gas flow. After some finite "retention time," the sample reaches the other end of the column, where it is detected. In general, different molecules have different retention times. Thus, if a sample contains a mixture of N different components, they will arrive at the detector at N different times. The detector output then appears as N separate peaks on a recorder chart, if the times are sufficiently resolved. This is generally accomplished by the proper choice of support and liquid materials, column dimensions, flow rate, and temperature. Components can be identified in some cases by comparing their retention times with

known substances. In addition, most gas chromatographs have provisions for collecting samples after the detector during desired peaks. These samples can then be submitted to further analysis. This technique of preparative chromatography is especially useful for separating the components of a mixture, which might otherwise lead to ambiguous results when analyzed by mass spectrometry or other means. Gas chromatography in general is a powerful technique for establishing purity and identity on the basis of very minute samples.

Two instruments were used in various phases of the investigation. One was a Perkin-Elmer Model 801 chromatograph with a 0.25 inch by 6 ft. SE-30 column and an electron-capture detector. This was particularly useful for the analysis of very small samples. The valuable assistance of Dr. H. W. Brewer of the Department of Anaesthesia in the Stanford Medical School is gratefully acknowledged in making this instrument available and making many helpful suggestions regarding its use. The other instrument was a Varian Aerograph model A-90-P3 with a 0.25 inch by 20 ft. Carbowax 20-M column and a thermal conductivity detector, which was more convenient for preparative chromatography. The author is grateful to J. A. Dale of the Stanford Chemistry Department for his assistance with this instrument.

In a mass spectrometer, the relative number of ions for each mass-to-charge ratio is determined. Since most of the ions are singly charged, the data represent the relative abundances of particles of different molecular mass. In the analysis of this data, it is necessary to take into account the splitting of the original molecule into various fragment ions which are recorded along with the entire molecular ion. Each molecular species has a characteristic fragmentation pattern, by means of which the structure of the parent molecule may be deduced. This pattern also depends in part upon the conditions under which the ions are produced and detected.

Mass spectra taken on a CEC instrument in the Stanford Chemistry Department were used to analyze reactants and products for a number of purposes during the investigation. First, they were used to identify impurities which were troublesome in one of the reactants. Second, they

established the identity of the reaction products. Third, they were used to search for enrichment in the product with respect to a specific bromine isotope. For this application the instrument was sensitive enough to detect less than a 1% change in isotope abundances.

2.7 OPTICAL SPECTROSCOPY

Considerable work on the absorption spectrum of bromine was done preliminary to the main photochemical experiments. Spectrographic plates were made on a Bausch and Lomb Dual Grating Spectrograph, and spectra were recorded photoelectrically using Jarrell-Ash 1-meter and 1.8-meter scanning spectrometers having Ebert-mounted gratings. Several 1-meter long pyrex tubes with optical end windows were used to contain the various bromine samples. These tubes contained excess liquid bromine in side arms , which could be immersed in a temperature bath to control the vapor pressure of the gas. Sylvania Tru-flector low voltage projection lamps were used as light sources for most of the work. Wavelength calibrations, where needed, were provided by neon and krypton standard lamps, and by a thorium iodide electrodeless discharge.

III. SPECTRUM OF BROMINE

3.1 INTRODUCTION

The choice of bromine for the photocatalysis experiments was influenced by the availability of the ruby laser at the wavelength of one of its absorption bands. Although previous photochemical investigations of bromine had been performed, all of them had been done with light of shorter wavelengths, where the absorption spectrum was continuous. In this chapter we shall review some of the principles which underlie molecular absorption spectra. The spectrum of bromine will be described, emphasizing the features in the wavelength region of the ruby laser. The spectroscopy of bromine which was performed in the course of this investigation will then be discussed.

3.2 GENERAL DESCRIPTION OF THE SPECTRUM OF BROMINE

The spectroscopy of diatomic molecules is discussed in detail by Herzberg.[62] The total internal energy of a molecule arises from three sources, which can be treated independently in first approximation. The first is the energy due to the electrons. This has its counterpart in the electronic energy of a free atom, and gives rise to discrete quantum states. As the two atoms approach each other to form the molecule, the wave functions and energies of the atoms join smoothly to those of the molecule. Each electronic state provides a potential in which the two nuclei move. Some of these potentials are completely repulsive, corresponding to unstable molecules. Others are repulsive at short distances for high kinetic energies of the nuclear motion, but are attractive for some range of internuclear separations, leading to the formation of stable molecules. For these stable molecules, the nuclei vibrate along the axis connecting them in the electronic potential. This motion is the second source of molecular energy, giving rise to a set of quantized vibrational energy levels for each stable electronic

state. The third type of energy arises from the rotation of the molecule in space about its center of mass. This splits each vibrational level into quantized rotational energy levels. It is clear that the vibrational and rotational energies of molecules have no counterpart for atoms. The combined energy of a diatomic molecule can then be expressed as

$$E_{molecule} = E_{electronic} + E_{vibrational} + E_{rotational} \quad .$$

Each of these contributions can be expressed in terms of quantum numbers and certain parameters which can be used to relate experimental data to quantum mechanical theory. The vibrational energy levels are given approximately by

$$E_{vib} = \omega_e \left(v + \frac{1}{2}\right) - \omega_e x_e \left(v + \frac{1}{2}\right)^2 + \ldots \quad ,$$

where v is the vibrational quantum number, and ω_e , $\omega_e x_e$ are parameters which, in general, are different for different electronic states. The first term is just the expression for the energy of a harmonic oscillator, while the second term includes the second-order corrections due to anharmonicity. Similarly, the rotational energy can be written approximately as

$$E_{rot} = B_e J(J + 1) - D_e J^2(J + 1)^2 - \alpha_e\left(v + \frac{1}{2}\right) J(J + 1) + \ldots \quad ,$$

where J is the rotational quantum number, and B_e , D_e , and α_e are again parameters which are characteristic of the electronic state. The first term here is the energy for a rigid rotator, which is corrected for centrifugal stretching by the second term, and for vibrational stretching by the third term.

The known vibrational and rotational parameters for the lowest-lying stable electronic states of the bromine molecule are listed in Table 3.1. The potential energies of these states as a function of internuclear distance are shown in Fig. 3.1. A few of the vibrational levels of the ground electronic state are also shown in the figure. The notation for the molecular electronic states is analogous with that used for atoms, with the difference that now the symbols refer to components of the respective angular momenta which lie along the internuclear axis. Thus Σ , Π , Δ , etc., refer to orbital electronic angular momentum components of $\Lambda = 0$, 1 , 2 , etc., along this axis. Similarly, the pre-superscript gives the multiplicity arising from the axial component Σ of the total electron spin, and the following subscript is the quantum number for the axial component Ω of total electronic angular momentum. The symbols "+" and "-" refer to symmetry properties of the wave functions with respect to a plane intersecting the two nuclei, and "g" and "u," for gerade and ungerade, denote even or odd inversion symmetry about the center-of-mass for homonuclear molecules. As shown in the diagram, dissociation of a molecule from either the $^1\Sigma_g^+$ state or the $^3\Pi_{1,u}$ state produces two bromine atoms in their ground $^2P_{3/2}$ state, whereas dissociation from the $^3\Pi_{0,u}^+$ state produces one $^2P_{3/2}$ atom and one excited $^2P_{1/2}$ atom.

In a radiative transition of a molecule from one electronic state to another, certain selection rules are obeyed. The electronic selection rules regarding spin and orbital angular momentum are similar to those for atomic transitions. For heavy molecules such as bromine, however, spin-orbit coupling relaxes these rules somewhat. A stricter rule is that, for homonuclear molecules, the symmetry gerade or ungerade must change in a transition. During an electronic transition, the vibrational and rotational quantum numbers may also change. For the rotational number, this change is restricted to $\Delta J = 0$, ± 1 with $\Delta J = 0$ forbidden if $\Omega = 0$ in both electronic states. The change in vibrational number is not so severely restricted. The relative intensities of transitions between various lower vibrational states v'' and upper states v' are

TABLE 3.1

BROMINE SPECTROSCOPIC PARAMETERS

(Units are cm^{-1})

Electronic State:	$^1\Sigma_g^+$	$^3\Pi_{1,u}$	$^3\Pi_{0,u}^+$
E_e^*	0	13,814	15,891.3
E_d^{**}	~16,070	~16,070	~19,735
ω_e	323.2	(170.7)	169.71
$\omega_e x_e$	1.07	(3.69)	1.913
B_e	0.08091	--	0.0595
α_e	0.000275	--	0.000625
D_e	--	--	--
Reference:	Brown[44]	Darbyshire[39]	Brown[44]

Notes:

*Electronic energy at the equilibrium internuclear distance, measured from the energy minimum of the ground state potential (see Fig. 3.1).

**Dissociation energy, also measured from the lowest point of ground state potential.

Quantities in parentheses ( ) based on vibrational quantum numbering assignment of Darbyshire.[39]

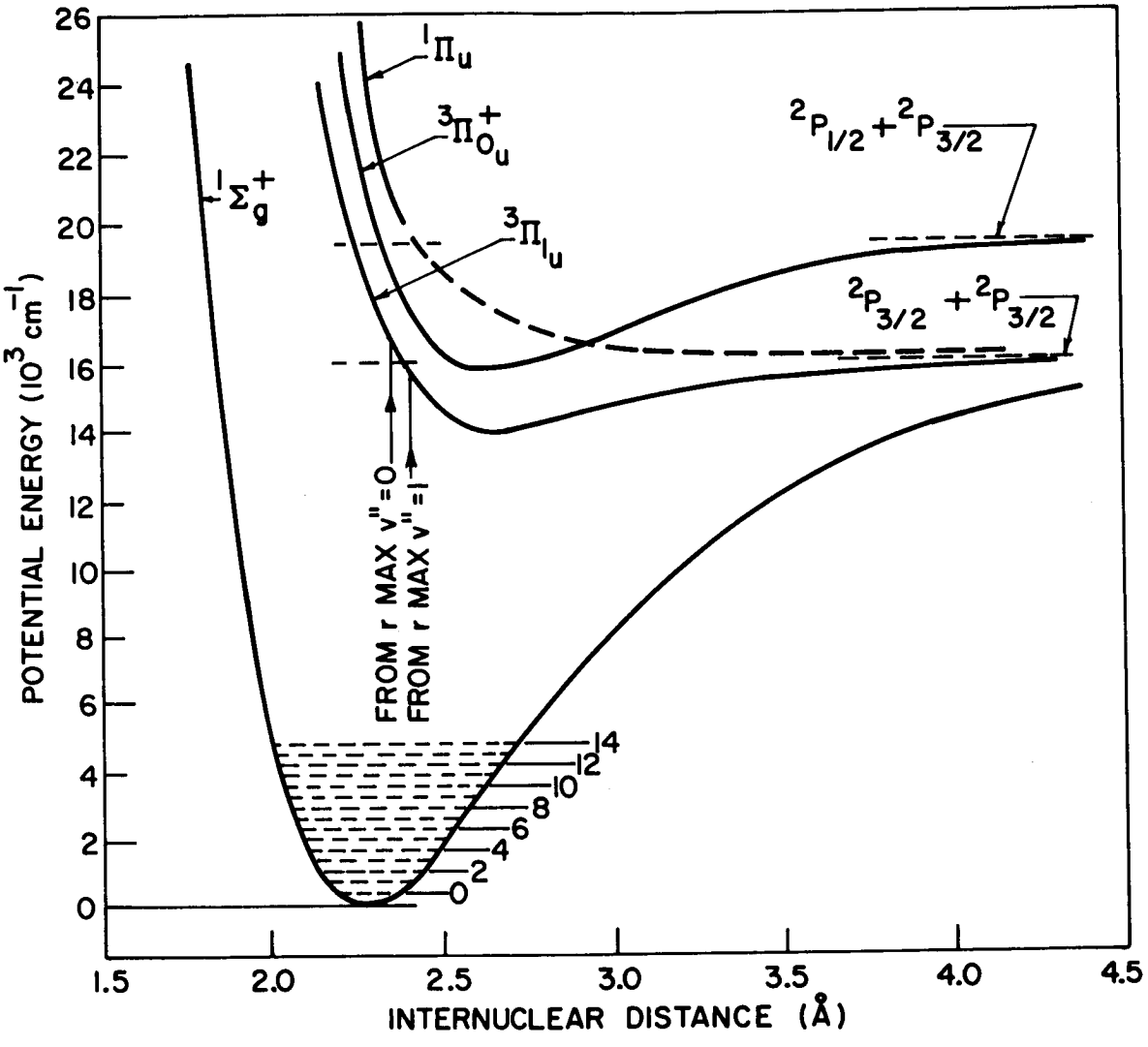

FIG. 3.1--Potential energy diagram of the Br_2 molecule (Rees[47]).

determined by the Franck-Condon principle. The main idea is that the nuclei do not have time to move during the sudden electronic transition. Hence, the relative position of the nuclei does not change, so that transitions are "vertical" on the energy diagram of Fig. 3.1. The relative velocity, and thus the kinetic energy, also cannot change appreciably during the transition. A highly probable transition, therefore, would be between vibrational levels, the classical turning points (both with zero kinetic energy) of which are located vertically one above the other. This principle can be developed from a quantum mechanical basis, also. It has been applied in showing on Fig. 3.1 the probable transitions to the $^3\Pi_{1,u}$ state from the lowest two vibrational levels of the ground electronic state of bromine.

When a molecule absorbs a photon of the appropriate energy to excite it to a level below the dissociation energy, it remains stable. The absorption spectrum in this energy range then consists of many individual lines arranged in bands corresponding to various Δv and ΔJ changes. If transitions take place at higher energies, the molecule can then be excited to an unstable region of the upper electronic potential, where it immediately dissociates. In this case the spectrum no longer has vibrational and rotational structure, and is simply a continuum. A spectrum may have overlapping bands and continuum at the same wavelength, as transitions may be allowed from lower vibrational levels of the lower state to a stable region of the upper state, and also from more highly excited vibrational levels of the ground state to an unstable portion of the upper state. In addition, when two or more upper states exist with nearly the same energy, as in the case of bromine, transitions to both states may overlap for some wavelengths.

The relative intensities of the various bands and of the continua are determined not only by the selection rules, but also by the initial populations. In absorption at thermal equilibrium, these follow a Boltzmann distribution among the vibrational levels.

Bromine has two isotopes of mass number 79 and 81, respectively,[41] which form three different isotopic species of molecules. Since the relative abundances of the atomic isotopes are 50.57% for ^{79}Br and 49.43% for ^{81}Br, the approximate abundances of the molecular species are:

Isotope	Abundance
79-79	25%
79-81	50%
81-81	25%

We expect differences in the spectra of these different isotopic molecules because of the effects of nuclear mass on the energy levels.[63] The largest of these effects is the vibrational isotope shift. A heavier oscillator should be expected to vibrate more slowly than a lighter one under the same force constant. We represent this formally by making the following modifications to the vibrational parameters in going from Br_2^{79-81} to one of the pure isotopes:

Br_2^{79-81}	Pure Isotopes
ω_e	$\rho\omega_e$
$\omega_e x_e$	$\rho^2\omega_e x_e$

where $\rho = (\mu/\mu_i)^{1/2}$ and μ, μ_i are the reduced masses of Br_2^{79-81} and of the pure isotopic molecule, respectively.

In addition, the isotope effect changes the moment of inertia for rotational motion. The formal substitution in this case is just the following:

Br_2^{79-81}	Pure Isotopes
B_e	$\rho^2 B_e$
α_e	$\rho^3\alpha_e$
D_e	$\rho^4 D_e$

There is an isotope shift of the electronic levels, also, but this is much smaller than the vibrational and rotational effects.

As a result of these isotope shifts, the spectrum of natural bromine is three times as complicated as that of a single isotope. On the other hand, the isotope effects can be exploited in several ways to provide useful information about the static properties and the dynamic behavior of the molecules.

A number of previous investigations have contributed to the present understanding of the spectrum of bromine. The vibrational-rotational structure of the $^3\Pi_0 \leftarrow {}^1\Sigma_g^+$ absorption bands was analyzed by Brown.[44] Transitions between these two states were observed in emission by Plumley.[45] A band-head analysis for the $^3\Pi_{1,u} \leftarrow {}^1\Sigma_g^+$ system was performed by Darbyshire[39] from absorption data. A complete rotational analysis was never done for this system, and it has never been observed in emission. Measurements of the continuous absorption spectrum by Acton, Aickin, and Bayliss[40] were used by Mulliken[46] in developing the theory of halogen spectra. Rees[47] later used this theory and the earlier experimental data to construct potential energy curves for bromine. A Raman spectrum was reported by Stammreich.[48]

3.3 SPECTRUM OF Br_2 AT THE RUBY LASER WAVELENGTH: RESULTS OF EARLIER INVESTIGATIONS

The absorption spectrum of bromine at the ruby laser wavelength is particularly interesting. This wavelength corresponds to a wave number of 14,400 cm^{-1}, which lies in the band system from the $^1\Sigma_g^+$ ground state to the $^3\Pi_{1,u}$ excited state. Thus, the stable excited molecules which are produced have energies below that required for dissociation. From the vibrational analysis of Darbyshire[39] it could be determined that the strongest transitions at 14,400 cm^{-1} originate at the lower vibrational levels $v'' = 2$ and $v'' = 3$. The upper levels would then lie about 500 cm^{-1} to 800 cm^{-1} away from dissocation. However, the $^3\Pi_{1,u} \leftarrow {}^1\Sigma_g^+$ bands had not been rotationaly analyzed, so it was not possible to determine either the rotational or the vibrational numbering for a given individual line. Hence, the $\sim$ 300 cm^{-1} uncertainty could not be reduced.

It was not established whether or not a weak underlying continuum accompanied the individual lines at 14,400 cm^{-1}. The continuous absorption spectrum of bromine had been investigated experimentally by Acton, Aikin, and Bayliss,[40] and theoretically by Mulliken[46] and by Rees.[47] It was known to consist of contributions from transitions to the $^3\pi^+_{o,u}$ and the $^3\pi_{1,u}$ states above their dissociation energies, as well as to the repulsive $^1\pi_u$ state. It was possible that transitions from the sparsely populated vibrational levels of $^1\Sigma^+_g$ might give rise to a continuum at 14,400 cm^{-1}. There was experimental evidence against the existence of a continuum somewhat farther to the red,[32] but no measurements had been made in this region.

The known features of its spectrum thus made bromine an interesting molecule for selective excitation by means of a ruby laser. The fact that this laser light could produce stable excited molecules below the lowest dissociation energy would make it possible to investigate molecular processes by using photochemical techniques, if a suitable reaction could be found. The results of such an investigation might then help to resolve some of the uncertainties regarding the spectrum.

3.4 RESULTS OF PRESENT INVESTIGATION

Conventional spectroscopic techniques were used to study the absorption spectrum of the continuum and the $^3\pi_{1,u} \leftarrow {}^1\Sigma^+_g$ bands of bromine. Samples studied included natural Br_2 at various concentrations, and in mixtures with other gases. Samples of the pure $Br_2^{79\text{-}79}$ and $Br_2^{81\text{-}81}$ isotopes were obtained on loan from the Oak Ridge National Laboratory and were also examined by means of conventional absorption spectroscopy. Laser excitation was used in observing absorption in individual lines of natural Br_2, as well as in an attempt to observe fluorescence from the $^3\pi_{1,u}$ state. Most of the techniques have been described in Chapter II. Results are presented and discussed in the following sections.

3.4.1 Continuous Absorption Spectrum

Absorption spectra of natural Br_2 at several pressures were recorded at several wavelengths, and were compared with light transmission through the system with all the Br_2 removed. The base-line for the line absorption was estimated and its contribution was subtracted to obtain the continuous absorption. The resulting absorption coefficient α was calculated from Lambert's law[9]

$$I_t = I_0 e^{-\alpha L} \quad ,$$

where I_t and I_0 are the transmitted and incident light intensities, and L is the absorption path length through the sample.

The results of these measurements are shown in Fig. 3.2, which shows the continuous absorption coefficient of Br_2 at its room temperature vapor pressure of 186 torr,[59] as a function of wavelength. The absorption coefficient was proportional to bromine concentration, in accordance with Beer's law.[9] Uncertainties in distinguishing overlapping wings of the lines from the true continuum are responsible for the apparent leveling-off at longer wavelengths (solid line in Fig. 3.2). Hence these measurements could not determine whether the continuum actually ceased to exist at these wavelengths (dashed line in the figure). It was concluded, however, that the continuum at 6940 Å was very weak if it existed at all.

3.4.2 Isotopic Identification of Individual Lines

The absorption spectra of the two pure isotope samples and of natural bromine were scanned in the region from 6934 Å to 6943 Å using a high resolution spectrometer with a neon standard lamp for wavelength calibration. The results are shown in Fig. 3.3. Certain strong lines of the pure isotopes can be identified readily in the spectrum of natural Br_2, and a few of these are labeled on the figure. The extremely close spacing of the lines underscores the difficulty of performing selective excitation experiments on this system.

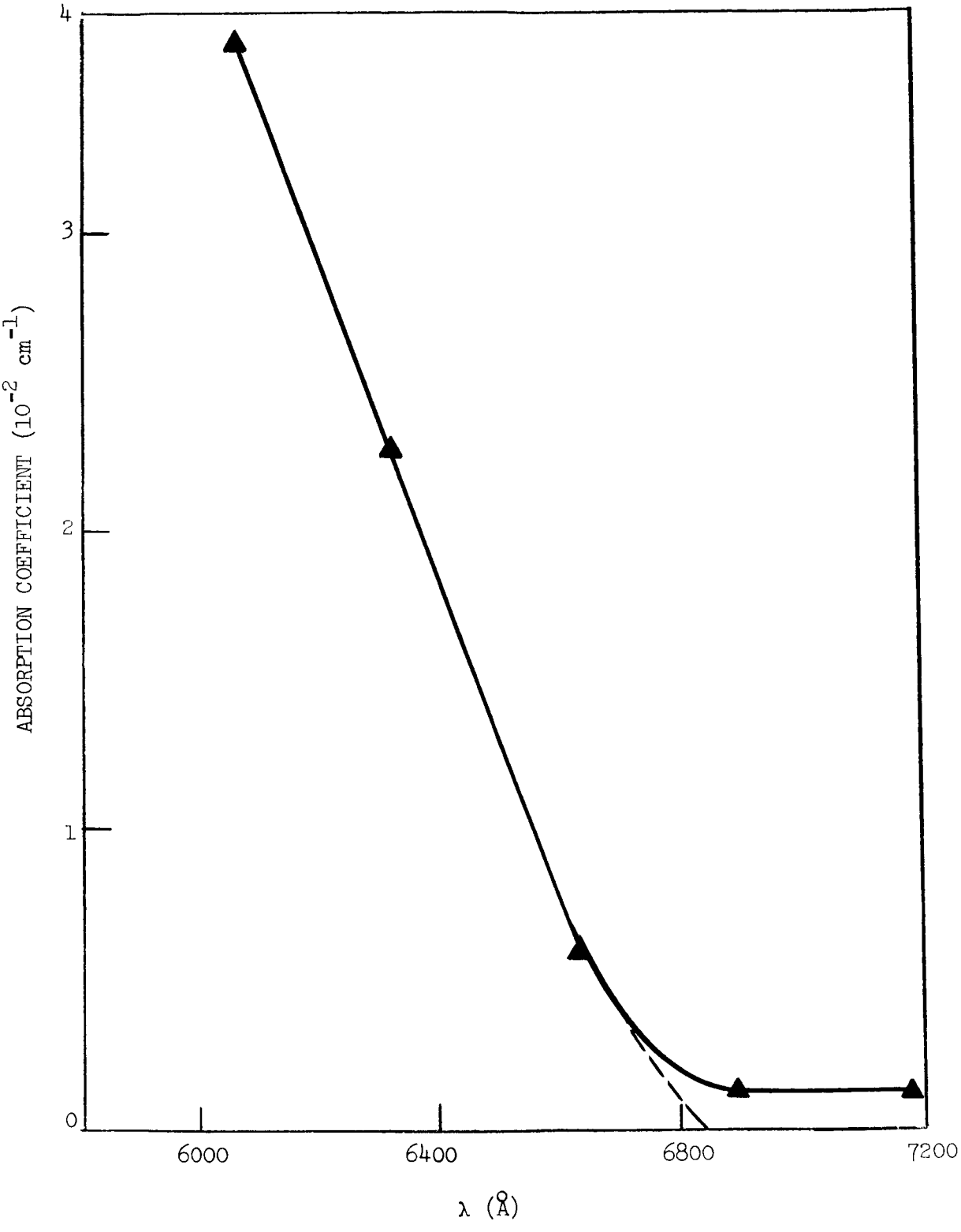

FIG. 3.2--Continuous absorption spectrum of Br_2 in 6000-7000 Å region.

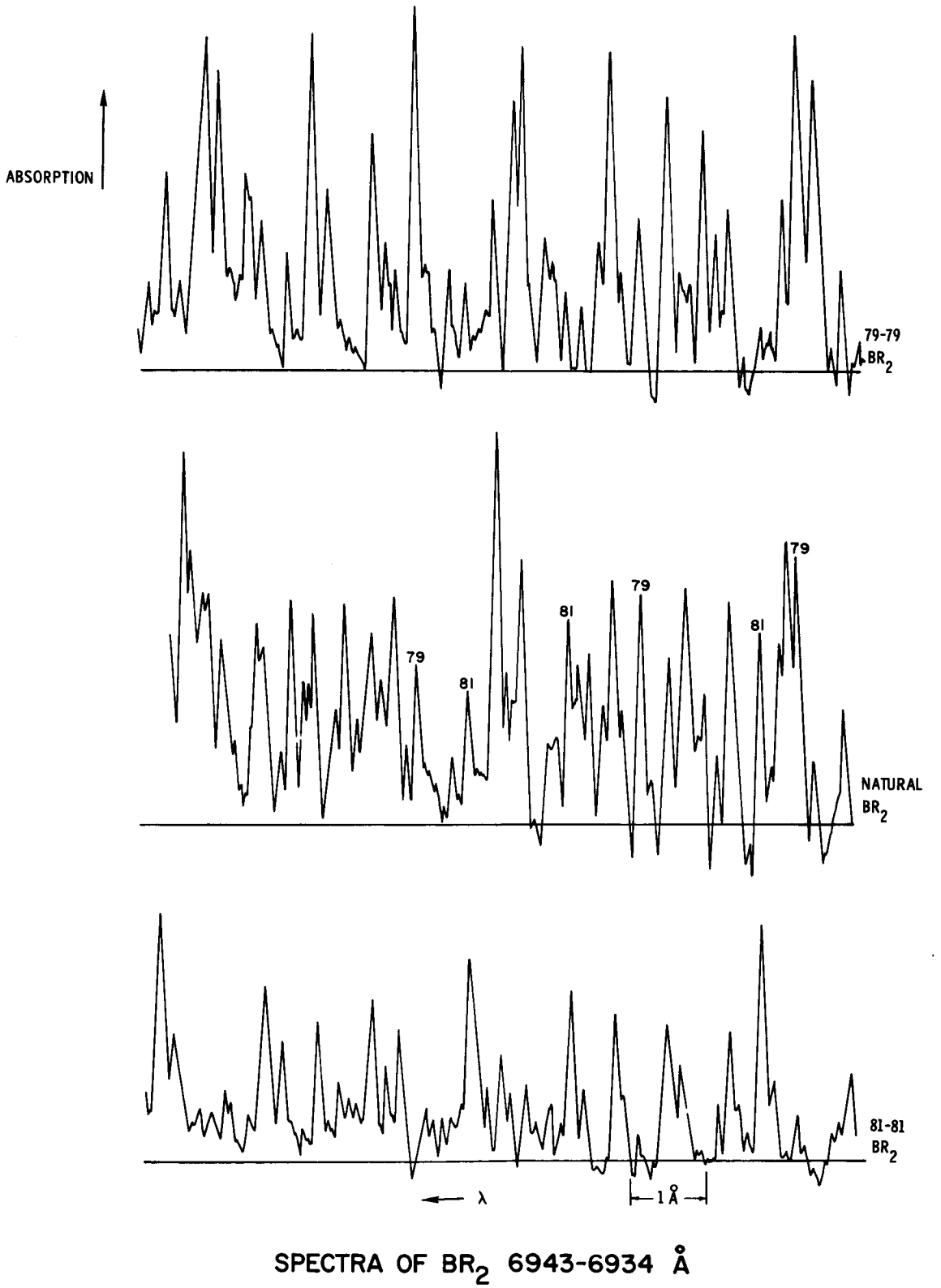

FIG. 3.3--Spectra of the pure bromine isotopes and natural Br_2 shown on same wavelength scale in the 6940-Å region.

3.4.3 Strengths and Widths of Individual Lines

The observed width of an absorption line in a gas comes about for a number of reasons. One cause of apparent width is the limited resolving power of the instrument. Another cause is the distortion in line shape brought about by the overlapping wings of neighboring lines. The true width of the line has two primary sources.[64] The first is inhomogeneous, or Gaussian broadening due to the thermal distribution of Doppler shifts from the individual molecules. The second is homogeneous, or Lorentzian broadening due to the finite lifetimes of all the molecules in the quantum states involved in the transition. In a gas at the pressures encountered in this investigation, the lifetime is determined by the mean time between molecular collisions. Since this lifetime is pressure dependent, the overall effect is called "pressure broadening." A rough approximation for the relationship of these individual types of broadening to the observed linewidth is

$$\Delta\nu^2_{\text{observed}} \cong \Delta\nu_I^2 + \Delta\nu_N^2 + \Delta\nu_D^2 + \Delta\nu_P^2 \quad ,$$

where

$\Delta\nu_I$ = Instrumental linewidth

$\Delta\nu_N$ = Effect of neighboring lines

$\Delta\nu_D$ = Doppler linewidth

$\Delta\nu_P$ = Pressure linewidth

The instrumental linewidth was estimated by measuring the apparent width of the farthest resolved hyperfine component of the 5461 Å emission line from a low pressure mercury lamp. This gave an instrumental resolution of $\Delta\nu_I \cong 0.065 \text{ cm}^{-1}$.

Doppler linewidths can be calculated from the expression

$$\Delta\nu_D = \frac{2(2R \ln 2)^{1/2}}{c} \nu_0 \left(\frac{T}{M}\right)^{1/2} ,$$

where R is the gas constant, T is the absolute temperature, and M is the molecular weight. For Br_2 at $300^\circ K$ this turns out to be $\Delta\nu_D \cong 0.015$ cm^{-1} when $\nu_0 = 14{,}400$ cm^{-1} .

The linewidth due to pressure broadening is $\Delta\nu_P = (Z_1 + Z_2)\,\pi c$, where Z_1 and Z_2 are the mean number of collisions per second of a molecule in the lower and upper states, respectively, of the transition. For the lower state in bromine, Z_1 can be calculated from kinetic theory by means of the expression[65]

$$Z_1 = 4n\sigma^2 \left(\frac{\pi kT}{m}\right)^{1/2}$$

where

n = number of molecules per cm^3

σ = collision diameter to be defined

m = mass of molecule

T = absolute temperature

k = Boltzmann constant .

For bromine, σ is generally accepted to be 4.27 Å.[66] At $300^\circ K$, the above expression leads to a value for bromine of $Z_1 \cong 5 \times 10^6 P$ collisions per second, where P is the pressure in Torr.

There is reason to believe that the increase in effective collision diameter in excited Br_2 may cause Z_2 to be 2 to 4 times as large as Z_1.[67] Thus if we take Z_2 as 3 times Z_1, we obtain

$$\Delta\nu_P \cong 2.1 \times 10^{-4} P \text{ cm}^{-1} .$$

The problem of overlapping neighboring lines was particularly troublesome because of the close spacing of these lines in bromine. This was handled by comparing the observed widths of several lines at different pressures with the widths predicted on the basis of the above calculations, ignoring the effects of neighboring lines. The pressures used were the vapor pressures of Br_2 in equilibrium with liquid Br_2 at room temperature (~ 186 Torr) at 0°C (~ 70 Torr).[59] These led to calculated values of $\Delta\nu_P$ of

$$\Delta\nu_{P_{\text{room}}}^{\text{calc.}} \cong 0.04 \text{ cm}^{-1}$$

and

$$\Delta\nu_{P_0}^{\text{calc.}} \cong 0.015 \text{ cm}^{-1} .$$

The total predicted linewidths, ignoring neighboring lines, were then

$$\Delta\nu_{\text{room}}^{\text{calc.}} = 0.077 \text{ cm}^{-1}$$

$$\Delta\nu_0^{\text{calc.}} = 0.068 \text{ cm}^{-1} .$$

The data indicated pressure broadening of approximately double the predicted amount. The discrepancy was probably due to a combination of neighboring line effects and larger collision diameters in the upper state. Hence, the overall linewidths appeared to be

$$\Delta\nu_{room}^{obs.} \approx 0.1 \text{ cm}^{-1}$$

$$\Delta\nu_{0}^{obs.} \approx 0.07 \text{ cm}^{-1} \quad .$$

The true linewidths, obtained by correcting for the instrument resolution, were then

$$\Delta\nu_{room}^{corr.} \approx 0.08 \text{ cm}^{-1}$$

$$\Delta\nu_{0}^{corr.} \approx 0.04 \text{ cm}^{-1} \quad .$$

The widths of the absorption lines were measured when part of the bromine pressure was replaced by one of the organic gases used in the reaction experiments. The effect was not observably different from that caused by the same total pressure of pure bromine.

The peak absorptions of a number of lines were measured and corrected for instrumental effects in a similar manner. The absolute values obtained may be in error by 50% , but this does not seriously affect the conclusions of the photocatalysis experiments. Relative absorption strengths were considerably more accurate. The numerical results for individual lines will not be presented here, but will be introduced where appropriate in the discussion of the results. The peak absorptions of the prominent lines in the natural Br_2 spectrum of Fig. 3.3 were typically 10% to 25% per meter at a bromine pressure of 186 Torr.

3.4.4 Vibrational Structure of the $^3\Pi_{1,u}$ State

Previous vibrational analyses by Brown[44] and by Darbyshire[39] left some uncertainty in the absolute vibration quantum numbers and vibrational parameters for the $^3\Pi_{1,u}$ state of bromine. A complete rotational analysis by Brown determined these values accurately for the $^1\Sigma_g^+$ state and the $^3\Pi_{0,u}^+$ state, but such an analysis was not performed for the $^3\Pi_{1,u} \leftarrow {}^1\Sigma_g^+$ bands. An additional complication was the fact that the 0,0 band was missing in the latter system because of the Franck-Condon principle. In such a case it was still possible to determine the vibrational structure from the wave numbers for the band origins ($J = 0$) and their isotope shifts. However, since the band origins themselves were not determined, the band heads were used instead. Darbyshire measured the average positions of a large number of band heads, but determined isotope shifts for only three of them. However, on the basis of his data he concluded that there should be an increase of 6 to 8 units in the arbitrary quantum numbers originally assigned by Brown. The presently accepted vibrational parameters for the $^3\Pi_{1,u}$ state of bromine are based on his assumption that the increase should be 7 units.

In the present work, because of the availability of the pure isotope samples, it was possible to measure isotope shifts for eighteen band heads from the lower vibrational levels $v'' = 1, 2$, and 3, in the region 14,150-15,400 cm^{-1}. The average positions of these band heads agreed well with Darbyshire's data.

Vibrational parameters were calculated from the average band head positions, and the corresponding isotope shifts were predicted, assuming several different vibrational numerations. Calculations were performed on an IBM 7090 computer. The predicted isotope shifts were then compared with the data for consistency. The results tended to favor an increase in v' of 6 units from the arbitrary numeration. However, the experimental error due to the use of band heads, and not band origins, was too large to exclude Darbyshire's assumption of a 7 unit increase. The comparison between calculated and experimental isotope shifts of the upper vibrational level is shown in Fig. 3.4. The v' numbering assumes the increase to be 6 units, with predicted isotope shifts given by the solid

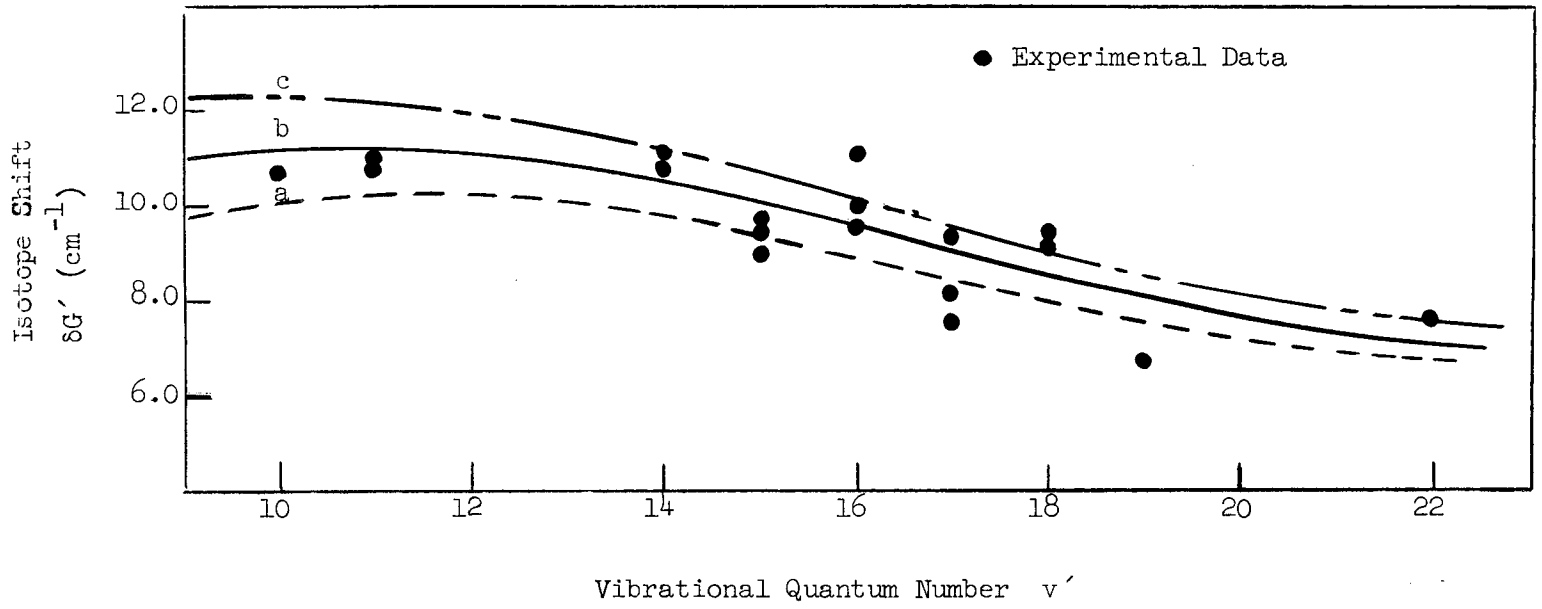

FIG. 3.4--Isotope shifts of vibrational levels in the $^3\Pi_{1,u}$ electronic state of Br_2 . The solid curve b shows calculated shifts based on the vibrational quantum numbering shown. The broken curves a and c show shifts predicted by assuming an increase or a decrease in the numbering by one unit.

curve. The broken curves a and c are predicted by increases of 5 and 7 units, respectively. The correct numbering will probably be determined only by the accurate measurement of band origins, resulting from a complete rotational analysis.

3.4.5 Laser Absorption Spectroscopy of Bromine

Experiments were performed in which the absorption of laser light by a column of bromine was measured as the laser was tuned stepwise across two of the prominent absorption lines of natural Br_2. The purpose of these experiments was to explore the feasibility of this technique for absorption spectroscopy, as well as to check the line-width and tuning accuracy of the laser. The laser energy and wavelength were monitored as described in Chapter II. However, this time a second photocell detected the laser energy after it had passed three times through the one-meter absorption cell containing the bromine. The signals from the two photocells were then integrated using a Tektronix Type "O" operational amplifier and were displayed simultaneously on a Tektronix 555 Dual Beam Oscilloscope and recorded on Polaroid film. The ratio of the heights of the two traces, normalized to the conditions with the bromine removed, indicated the amount of absorption. These data are summarized in Fig. 3.5, along with the profiles of the respective lines obtained by conventional spectroscopy. In spite of the crudeness of the experiment, the agreement between the two methods was satisfactory. Such an agreement could not be observed in similar experiments performed before mode-control techniques were employed on the laser. Minor refinements in the technique could make the laser a useful instrument for high resolution absorption spectroscopy.

3.4.6 Attempted Laser-Excited Fluorescence

The use of monochromatic light to excite emission from molecules has been recognized as a powerful technique for studying energy level structures and energy transfer processes.[68] A number of such investigations of iodine fluorescence excited by sharp lines from mercury or sodium lamps have been conducted.[69] The use of a tunable laser as a

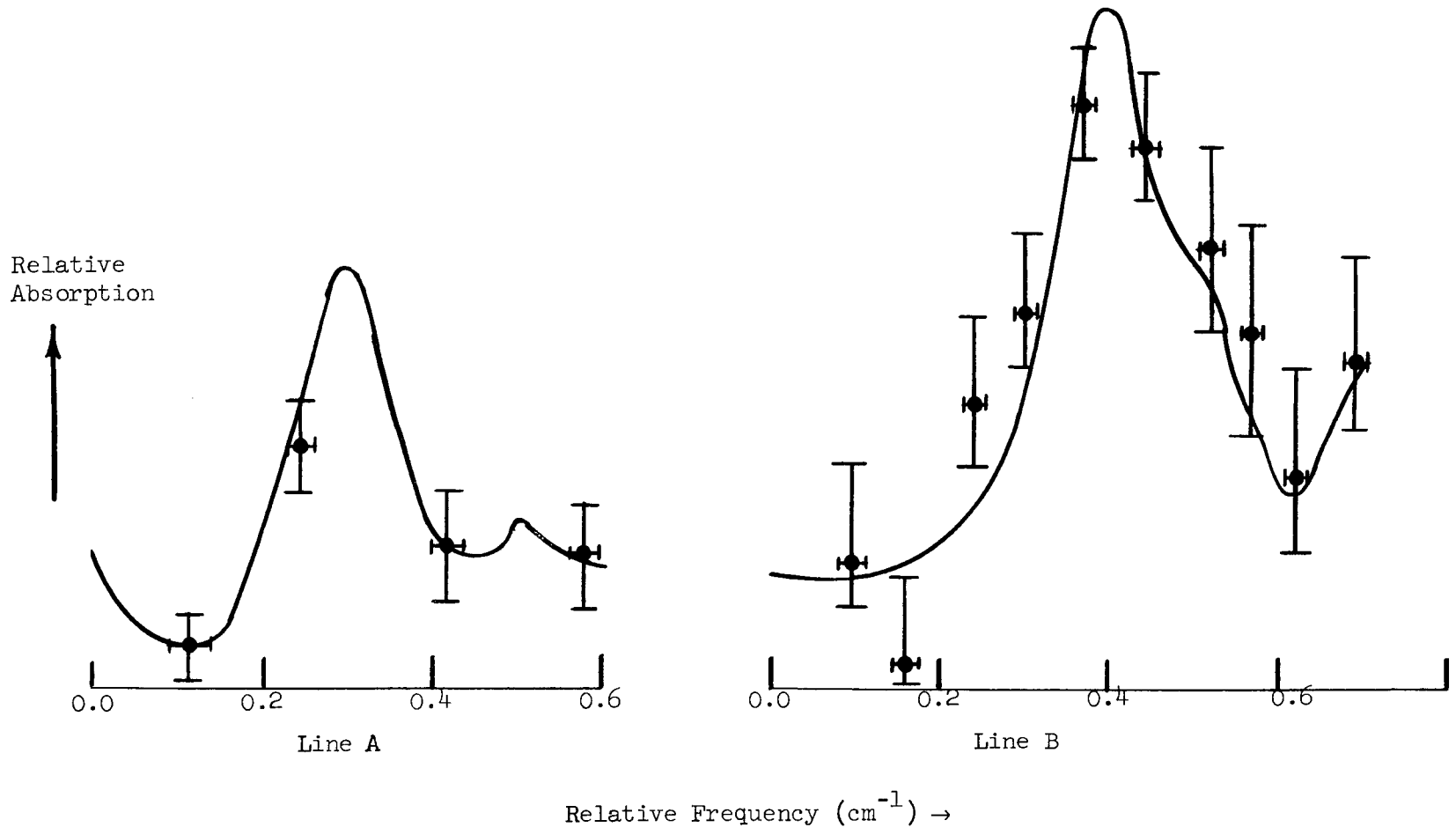

FIG. 3.5--Absorption in two regions of Br_2 spectrum obtained by tuning the ruby laser. The solid curves show the spectra as measured conventionally with a high resolution spectrometer.

source would clearly enable the technique to be extended to molecules whose absorption lines do not fortuitously coincide with one of the conventional atomic emission lines. Excitation of emission in the $^3\pi_{1,u} \rightarrow {}^1\Sigma_g^+$ bands of bromine by means of the ruby laser was attempted in order to demonstrate this extension.

Emission from the $^3\pi_{1,u}$ state of Br_2 had not previously been observed under any conditions. Plumley[45] observed $^3\pi_{0,u}^+ \rightarrow {}^1\Sigma_g^+$ emission photographically using the 5461 Å line of an intense mercury arc. This required an exposure time of some 70 hours, which indicated that the fluorescence was about 300 times weaker than that of iodine under similar conditions. Calculations based on Mulliken's theoretical analysis of the halogen spectra[46] suggested that the $^3\pi_{1,u}$ emission might be still weaker by a factor of 20 or so. In spite of these pessimistic predictions, it was felt that this emission might be observable by using intense laser light and taking advantage of the efficient excitation geometry of the reaction cell (see Chapter II). The image of the cell interior was focused on the entrance slit of a spectrograph which had an effective aperture number of $f/4$. Exposures were made on hypersensitized infra-red plates over the wavelength range of 7000 to 12,000 Å during 25,000 consecutive laser pulses, with no observable fluorescence.

It is now known from the photocatalysis experiments that nonradiative relaxation from the $^3\pi_{1,u}$ to the $^1\Sigma_g^+$ state occurs extremely rapidly. This greatly reduces the chance of observing emission. Even so, it is conceivable that the use of more sophisticated detection techniques, such as photon counting,[70] might enable the $^3\pi_{1,u}$ fluorescence to be studied.

3.4.7 Summary

Spectroscopic investigations of bromine using conventional and laser techniques were conducted preliminary to the photochemical studies. Isotopic labeling of prominent absorption lines near 14,400 cm^{-1} was accomplished, as well as a probe of line profiles using the laser as a source. Linewidths were measured and compared with theoretical predictions, and peak absorption

strengths were estimated. Measurement of the continuous absorption was done, but was limited by the problem of overlapping individual lines. Additional isotope shifts for the $^3\Pi_{1,u} \leftarrow {}^1\Sigma_g^+$ band heads were measured, and essentially confirmed an earlier analysis of the vibrational structure. The attempt to observe laser-excited emission from the $^3\Pi_{1,u}$ state was not successful.

IV. PHOTOCATALYSIS OF BROMINE REACTIONS: EXPERIMENTAL RESULTS

4.1 INTRODUCTION

The type of reaction chosen for the photocatalysis experiments was the addition of bromine to the double bonds of unsaturated organic molecules. These are known as alkenes, olefins, or ethylenic molecules, ethylene being the simplest molecule with this structure.[71] Figure 4.1 illustrates schematically the structure of ethylene and bromine, along with their addition product, dibromoethane.

Earlier studies of such reactions with both thermal[72] and photochemical[32,37,38] activation showed that the addition did not take place in a single elementary step. Instead, the overall reaction was the result of a complex set of processes initiated by dissociated bromine atoms. This mechanism is known as a "free radical chain." Denoting the olefin by "X", we may represent the elementary steps as follows:

Activation: (1) $Br_2 \rightarrow 2Br$

Propagation: (2) $Br + X \rightleftarrows XBr$

(3) $XBr + Br_2 \rightleftarrows XBr_2 + Br$

Termination: (4) $Br \overset{\text{wall}}{\rightarrow} \frac{1}{2} Br_2$

(5) $Br + Br + M \rightarrow Br_2 + M$

(6) $XBr + M \rightarrow$ Deactivation ,

where M denotes any molecule in the system which can carry away the excess energy released by the recombination of atoms. According to this mechanism, the bromine atom produced by dissociation in (1) combines with the olefin in (2) to form XBr, which is a free radical. This is a relatively unstable species, having an unpaired electron, and so it

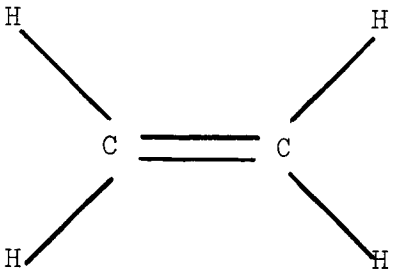

ETHYLENE

BROMINE

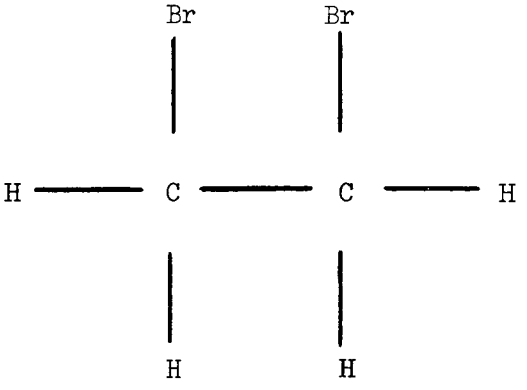

1,2-DIBROMOETHANE

FIG. 4.1--Structures of ethylene, bromine, and dibromoethane.

must eventually either dissociate in the reverse of (2), or else react with a bromine molecule in (3) to form the stable product, XBr_2, plus a free bromine atom. The latter may then continue the "chain" by reacting with another olefin in (2). The overall process does not result in a net removal of bromine atoms, so it can potentially be repeated indefinitely. However, the competing processes (4), (5), and (6) remove the reactive atoms and radicals by recombination, so that there is a finite average quantum yield ("chain length") of product molecules formed per initially activated atom. Since the process as a whole is exothermic, the reverse reaction in (3) would be expected to be very slow, at least initially.

The kinetics of these free radical chain reactions have been treated by a number of authors.[73-76] If we neglect for the moment the termination process (6), the initial rate of the overall reaction can be expressed in terms of the reactant concentrations and rate constants of the elementary steps (2) and (3) as

$$\frac{d\,[XBr_2]}{dt} = \frac{k_2 k_3\,[Br]\,[X]\,[Br_2]}{k_3\,[Br_2] + k_{-2}} \quad . \qquad (4.1)$$

The brackets [ ] in Eq. (4.1) denote concentrations, and the k's are the rate constants for the individual steps, with the minus sign designating the rate constant for the reverse reaction.

The concentration [Br] itself depends upon the methods of activation and termination. In thermal reactions it is established by the thermodynamic equilibrium between collisional dissociation and recombination processes. In this case the concentration of bromine atoms is related to the concentration of bromine molecules by

$$[Br] = K_{eq}^{1/2}\,[Br_2]^{1/2} \quad ,$$

where K_{eq} is the equilibrium constant

$$K_{eq} = \frac{k_1}{k_{-1}} \quad ,$$

with reaction (1) now being considered reversible.

Under photochemical activation, the concentration [Br] can be given by a simple expression only if certain approximations are made. The most common of these is the "steady-state" approximation, the applicability of which is discussed by Benson.[74] What is done is to assume that the concentrations of the intermediate species (atoms and radicals) are maintained at a constant value, which is small compared with the concentrations of the original reactants and final products. This is a valid approximation as long as the light source has sufficiently low intensity and is steady in time. It is obviously not applicable under intense, pulsed laser excitation without modifications, which will be discussed later.

The explicit form for the steady-state concentration of bromine atoms depends upon which of the terminating processes dominates. The general expression for the time dependence of this concentration is

$$\frac{d\,[Br]}{dt} = 2I_a - k_4\,[Br] - 2k_5\,[M]\,[Br]^2 \quad , \qquad (4.2)$$

where the first term reflects the assumption that the number of atoms generated is twice I_a, the number of photons absorbed per unit time per unit volume. This will be true only for direct dissociation in the wavelength region of continuous absorption. The second term depends upon diffusion to the walls, which dominates at low pressures, and is linear in [Br]. The third term arises from recombination on a third body, and thus increases with increasing pressure. The relative importance of the two terms also depends on such conditions as the geometry of the reaction cell, the nature of the third body, and the light intensity.

With these considerations in mind, and setting $d[Br]/dt = 0$ in accordance with the steady-state approximation, we obtain for low pressures

$$[Br] \approx \frac{2I_a}{k_4} \quad , \tag{4.3a}$$

and for high pressures

$$[Br] \approx \left(\frac{I_a}{k_5[M]}\right)^{1/2} \quad . \tag{4.3b}$$

Combining with Eq. (4.1), we obtain expressions for the overall rate at low pressures

$$\frac{d[XBr_2]}{dt} \approx \frac{2k_2 I_a[X][Br_2]}{k_4([Br_2] + k_{-2}/k_3)} \quad , \tag{4.4a}$$

and at high pressures

$$\frac{d[XBr_2]}{dt} \approx k_2\left(\frac{I_a}{k_5[M]}\right)^{1/2} \frac{[X][Br_2]}{[Br_2] + k_{-2}/k_3} \quad . \tag{4.4b}$$

A useful way to express these rates is in terms of the quantum yield, or chain length, which is the reaction rate divided by the absorption rate:

$$Q \approx \frac{2k_2}{k_4} \cdot \frac{[X][Br_2]}{[Br_2] + k_{-2}/k_3} \tag{4.5a}$$

or

$$Q \approx k_2\left(\frac{1}{k_5 I_a[M]}\right)^{1/2} \frac{[X][Br_2]}{[Br_2] + k_{-2}/k_3} \quad . \tag{4.5b}$$

We note from Eq. (4.5b) that for sufficiently high pressure, as the light intensity increases, the chain length becomes shorter, although the overall reaction rate continues to increase. The inclusion of process (6) causes an additional decrease in the quantum yield with increasing pressure.

The quantum yields for some bromine-olefin reactions are known to be very high. For the addition of bromine to ethylene, 10^5 or more product molecules have been formed for each absorbed photon, at reactant pressures of the order of 30 mm.[38] Quantum yields of 10^3 to 10^4 for reactions with other olefins are not uncommon.[37] One of the problems encountered in this investigation was to find a reactant which would combine with bromine with a sufficiently low quantum yield, so that the thermal background reaction rate would be small, and so that the effects of other slower processes to be studied would not be masked.

Free radical chain reactions also have the property of being strongly inhibited by the addition of small amounts of certain gases, notably nitric oxide.[76] The presence of a small quantity of oxygen also has an inhibiting effect on the addition of bromine to olefins, and has been observed to cause an "induction period" at the beginning of a reaction.[32]

The gas-phase addition of bromine to trans-1,2-dichloroethylene was studied by Müller and Schumacher,[37] using light at 5461 Å from a mercury lamp. Schmitz, Schumacher, and Jäger[38] used the mercury lines at both 4358 Å and 5461 Å to catalyze the addition of bromine to ethylene. Kistiakowsky and Sternberg[32] studied the same reaction in a number of spectral regions using a tungsten filament lamp and bandpass filters. They concluded that all the photochemical addition reactions of bromine to olefins, as well as all the other observed photochemical reactions of bromine[33-36] were due entirely to direct dissociation into atoms upon absorption of light in the continuous absorption region. Their experimental evidence, as well as calculations by McDowell,[77] showed that the activity at longer wavelengths was due to direct dissociation of vibrationally excited $^1\Sigma_g^+$ molecules, and not to subsequent collisional dissociation of molecules excited in individual lines to the $^3\pi_{1,u}$ state. However, the longest wavelength observed for this was 6800 Å, and no experiments had

been attempted in the 6940 Å region, where continuous absorption was expected to be considerably weaker.

If light at 6940 Å catalyzed the addition of bromine to an olefin, one of several alternative mechanisms could be responsible. The first would be continuous absorption superimposed on the bands, so that direct dissociation would take place, as in the earlier investigations. A second alternative would be formation of a stable excited $^3\Pi_{1,u}$ molecule by absorption in an individual line, with subsequent collisional dissociation into free atoms. A third possibility would be dissociation by absorption of two photons. A fourth process could be a heating effect which would increase the number of bromine atoms in equilibrium with the bromine molecules. The fifth alternative would be the direct addition of the excited molecule to the olefin in a single elementary process, without dissociation into atoms.

The objectives of the present experiments were then: (1) to discover if laser light at 6940 Å would catalyze a reaction between bromine and an olefin; (2) to determine whether or not it was an addition reaction; (3) to identify the mechanism; and (4) to explore energy transfer processes and any other effects which might take advantage of the selective method of excitation. The remainder of the present chapter will be devoted primarily to the description of the experimental results. These will be examined in detail and interpreted in terms of the various individual dynamic processes in Chapter V.

4.2 SELECTION OF REACTANTS

As noted in the previous section, it was desirable to find chemicals which would react with bromine much more slowly than, for example, ethylene, which had a quantum yield of about 10^5. Various olefins were tried, both in dark reactions and in conventional light, to obtain rough estimates of their reaction rates. The details of this survey will not be discussed. However, it is worthwhile to mention several general principles which led to the eventual selection of the reactants.

First, although there are exceptions, many olefins become less reactive in addition reactions when one or more of their hydrogen atoms are replaced by halogen atoms. In order of increasing effectiveness, these are iodine, bromine, chlorine, and fluorine. This is probably related to the increased electronegativity (electron-withdrawing character) of the halogens compared with hydrogen. The result is that they may decrease the electron energy available at the double bond for attaching another atom. The relative electronegativities of the halogens and hydrogen,[71] and the corresponding bond energies with carbon,[78] are shown in Table 4.1. It can be seen that in the particular case of fluorine substitution, not only is the electronegativity much greater, but the C-F bond has a higher binding energy than C-H. It has been found that organic polyfluorides are especially stable, even though the monofluorides are not.[79] This has been explained in terms of a decrease of the C-F bond distance from 1.42 Å in monofluorides to 1.35 Å in polyfluorides.

TABLE 4.1

ELECTRONEGATIVITIES AND BOND ENERGIES

Atom	Relative Electronegativity	Bond Energy with Carbon (Kcal/mol)
H	2.1	87.3
I	2.5	45.5
Br	2.8	54.0
Cl	3.0	66.5
F	4.0	107.0

Another consideration was that the reaction product, once formed, should be as stable as possible. This would be particularly important when investigating the possibility of a direct addition of the excited bromine molecules to the double bond. When atoms or molecules react,

the excess energy of activation must somehow be carried away for the product to become stabilized. In an addition reaction, this cannot be done by the translational kinetic energy of the product alone, or else conservation of momentum is violated. Hence the energy must be dissipated (a) by fluorescence, which is rare, (b) by a third body which then acts as a recombination center (the wall of the container may act as a third body), or (c) by redistribution among the internal degrees of freedom of the product molecule. In order for this last mechanism to be efficient, it is important for the product to have many such internal degrees of freedom. The number of modes of vibration for a polyatomic molecule is $3N-6$, where N is the number of atoms in the molecule. Thus it would be desirable to use a large molecule for the reactant.

Naturally, an important additional requirement was that neither the reactant nor its addition product with bromine could absorb the laser light.

The result of the preliminary experiments was the tentative selection of two fluorocarbons, which had the desired properties outlined above. Perfluoro-2-butene was found to react with bromine very negligible in the dark. In ordinary room lights the reaction took place very slowly. A related chemical, 1,1,1,2,4,4,4-heptafluoro-3-chloro-2-butene, was also found to react very slowly with bromine. It yielded a product with a somewhat lower vapor pressure, which made it more convenient for separation from the initial reactants by fractional distillation. The perfluorobutene was obtained as a gas from the Mathieson Company; the heptafluorochlorobutene was obtained in liquid form from the Columbia Organic Chemical Company. Both chemicals were furnished as mixtures of the cis and trans isomers. The structural forms for both isomers of these two fluorocarbons are shown in Fig. 4.2. Their physical properties are listed in Table 4.2.

The chemistry of fluorocarbons had been discussed in detail by several authors.[80,81] It has been shown that bromine adds to the fluorinated olefins without substitution for fluorine. Also, the speed of the addition decreases as more trifluoromethyl ($-CF_3$) groups are attached to the carbon atoms forming the double bond. The trifluoromethyl

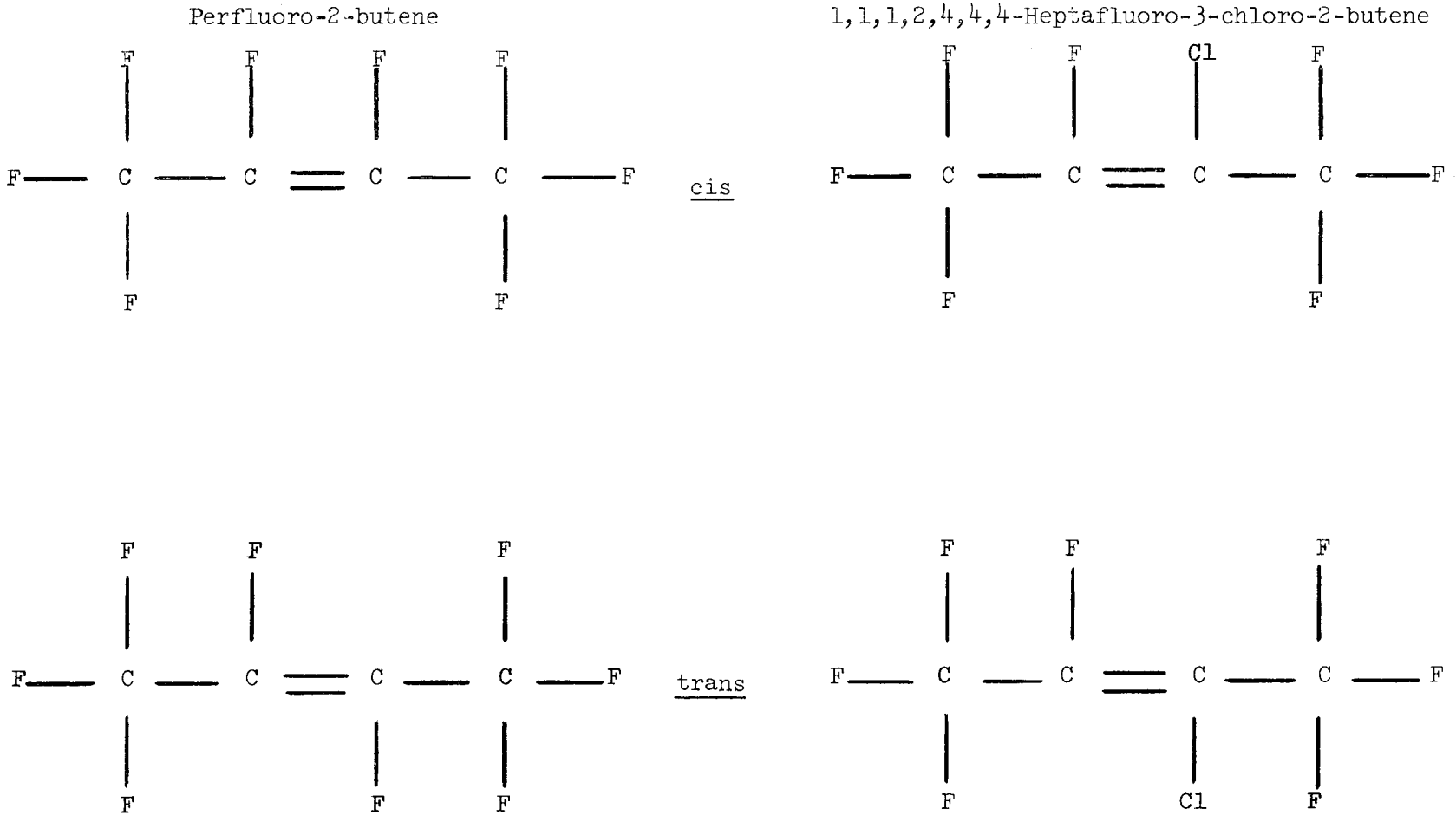

FIG. 4.2--Structures of cis and trans isomers of perfluoro-2-butene and 1,1,1,2,4,4,4-heptafluoro-3-chloro-2-butene (schematic).

TABLE 4.2

PROPERTIES OF SELECTED FLUOROCARBONS[81]

Name	Perfluoro-2-butene	1,1,1,2,4,4,4-heptafluoro-3-chloro-2-butene
Formula	$CF_3CF = CFCF_3$	$CF_3CF = CClCF_3$
Molecular Weight	200	216,218
Boiling Point	0°C (740 mm)	32.2°C (760 mm)
Density*	1.5297 (0°C)	1.5482 (20°C)
Refractive Index**	--	1.2946 (20°C)

*Density at given temperature relative to density of water at 4°C.

**Refractive index at given temperature for wavelength of sodium D-lines.

group is known to be a very efficient electron withdrawer. For instance, bromine adds in order of increasing difficulty to $CF_2 = CFCF_2CF_3$, $CF_3CF = CFCF_3$, and $CF_2 = C(CF_3)_2$. Hence, the selection of $CF_3CF = CFCF_3$ and the related $CF_3CF = CClCF_3$ appeared to be justified on a theoretical as well as an experimental basis.

4.3 EXPERIMENTS USING CONVENTIONAL LIGHT

Before proceeding with the laser photocatalysis experiments, reactions of bromine with the two selected fluorocarbons were carried out using light in the wavelength region of continuous bromine absorption. This was done in order to obtain estimates of the quantum yield under these conditions for comparison with the results using laser light. The experiments were conducted using the same reaction cell that was used in the laser experiments, in order to take into account the effect of cell geometry. The light source used was simply the ordinary room light, which was furnished entirely by fluorescent lamps. This provided a repeatable light intensity, with a spectral distribution which was absorbed by the bromine predominantly in the continuum. The reactions were monitored by observing the decrease in pressure by means of the Bourdon gauge-manometer combination described in Chapter II. The system was calibrated by observing the reaction of bromine with trans-1,2-dichloroethylene, which had been studied in detail previously by Müller and Schumacher.[37]

In the following sections the results using dichlorethylene will first be presented and discussed. The reactions using heptafluorochlorobutene and perfluorobutene will then be described.

4.3.1 Trans-1,2-Dichloroethylene

Bromine and trans-1,2,-dichloroethylene were purified according to the procedures outlined in Chapter II. The reaction cell was filled with an initial partial pressure of 10 mm of each reactant. The rate of pressure decrease was observed with the Bourdon gauge and extrapolated to zero time to obtain the initial rate, which was estimated to be 5 mm/minute. Since the room-temperature vapor pressure of the product, dibromodichloroethane, was only 0.7 mm, the actual initial rate of the reaction was 2.5 mm/minute.

The quantum yield corresponding to this reaction rate could be estimated from the results of Müller and Schumacher.[37] Corrections first had to be made for differences in pressure, reactant concentrations, temperatures, and cell geometry. Their results showed a quantum yield of 1.2×10^4 molecules per absorbed photon, for initial concentrations of 100 mm of each of the reactants at a temperature of 90°C.(1) The total pressure of 200 mm was in an intermediate region between those where Eqs. (4.5a) and (4.5b) were valid for their experiments. However, they performed a series of experiments, in which the pressure effect was shown explicitly, by keeping the reactant concentrations constant and varying the total pressure with an inert gas. These showed that the quantum yield would be expected to decrease by a factor of 3 or 4 as the pressure was decreased from 200 mm to 20 mm.

At a pressure of 20 mm, chain termination in their apparatus proceeded almost entirely by diffusion to the walls. The same held true in our cell, the dimensions of which were much smaller than theirs. With this mechanism the quantum yield is proportional to the mean time required for a bromine atom to diffuse to the wall. This time is proportional to pressure, and also to the square of the distance traveled. Hence a scale factor must be introduced to account for the differences in cell geometries. Müller and Schumacher used a cylindrical cell which was approximately 10 cm long and 5 cm in diameter.[82] The rectangular cell used in our experiments measured approximately 0.5 cm × 2 cm × 2.5 cm. Using 5 cm as characteristic of the larger cell, and 1 cm for the smaller one, the quantum yield would then be reduced by a scale factor of 25. Thus, the overall effect of pressure and cell geometry would be to reduce the yield by a factor of 75 to 100.

The dependence of the quantum yield on the bromine and dichlorothylene concentrations, in accordance with Eq. (4.5a) can be rewritten more simply as

$$Q = \frac{k\, P\, [Br_2]\, [C_2H_2Cl_2]}{[Br_2] + k'} \quad . \qquad (4.6)$$

(1) The quantum yield of 1.1×10^3 molecules/hν , quoted by Müller and Schumacher, was incorrect, based on their own data.

It was found by Müller and Schumacher that k was nearly independent of temperature, whereas k′ was found to be 140 mm at 90°C, 220 mm at 110°C, and 330 mm at 130°C. By fitting this to the usual exponential temperature dependence and extrapolating, a value for k′ of approximately 18 mm was obtained for a temperature of 295°K. The temperature decrease also resulted in an increase in molecular concentration for a given pressure. This was taken into account by adjusting the reactant pressures in Eq. (4.6), which were then used to compute the relative yields. This calculation led to a further decrease in quantum yield by a factor of 8.4. When this was combined with the effect of pressure and cell size, a reduction factor of the order of 750 was obtained. Thus the reaction rate of 2.5 mm/minute corresponded to a quantum yield of roughly 16 molecules per photon.

This result appeared to be consistent with the estimated amount of light being absorbed by the bromine. It was not convenient to make a direct comparison of the reaction rate at 100 mm partial pressures of the reactants because it was too rapid under those conditions. It was verified that the addition of nitric oxide strongly inhibited the reaction, as expected from its free radical chain character.

4.3.2 Perfluoro-2-butene

The results of reactions of bromine with perfluoro-2-butene in room light are summarized in runs numbered 2-8 in Table 4.3. Run 1 was the reaction with dichloroethylene described in the previous section. In run 2 nearly the same pressures were used, but C_4F_8 was substituted for $C_2H_2Cl_2$. The reaction rate, and thus the quantum yield, was found to decrease by a factor of more than 2000. In runs 3 through 6, a considerably higher partial pressure of C_4F_8 was used, while the bromine concentration was maintained at approximately 11 mm. Sulfur hexafluoride, an inert gas, was added in runs 4 through 6 to increase the total pressure. Quantum yields were estimated from the observed rates by comparison with run 1. These were in reasonable agreement with the quantum yields calculated by means of Eq. (4.6), using the yield observed in run 2 as a basis.

TABLE 4.3

SUMMARY OF REACTIONS IN CONVENTIONAL LIGHT

Run	Olefin Reacted	Partial Pressures (mmH_g) Olefin	Br_2	Total Pressure (mmH_g)	Initial Reaction Rate (mm/min)	Quantum Yield (molecules/$h\nu_{abs}$) From Observed Rate	Calculated
1.	$C_2H_2Cl_2$	10	10	20	2.5	--	16*
2.	C_4F_8	12	11	23	0.0011	0.007	--
3.	C_4F_8	50	11	61	0.022	0.154	0.084
4.	C_4F_8	50	11	100	0.027	0.19	0.14
5.	C_4F_8	50	11	178	0.033	0.23	0.25
6.	C_4F_8	51	11	248	0.048	0.33	0.35
7.	C_4F_8	84	60	144	0.25	0.355**	--
8.	C_4F_8	85	60	290	0.40	0.56	0.70
9.	C_4ClF_7	90	60	150	0.125	0.18	--
10.	C_4ClF_7	60	30	100	0.09	0.25**	--

*Quantum yield calculated as described in Section 4.3.1 from data of Müller and Schumacher,[37] and used for comparison with subsequent runs.

**Estimate based on assumptions that light absorption is linear in bromine concentration and that Eq. (4.3a) is applicable.

Runs 7 and 8 were performed at higher reactant concentrations, with SF_6 being added again in run 8. The order-of-magnitude agreement with extrapolations from runs 2 through 6 was satisfactory. The detailed dependence upon the bromine concentration, however, was not studied. The increased bromine concentration would affect the overall rate by increasing the light absorption, as well as increasing the quantum yield. At such a high concentration, it was also likely that quadratic chain termination was important, due to the greater frequency of binary collisions of two bromine atoms. This is suggested by the slower than linear pressure dependence in runs 7 and 8. The main conclusion of this series of experiments was that C_4F_8 reacted with bromine quite slowly in ordinary light.

4.3.3 1,1,1,2,4,4,4-Heptafluoro-3-chloro-2-butene

Experiments in room light with C_4ClF_7 gave results very similar to those obtained with C_4F_8. These are summarized in runs numbered 9 and 10 in Table 4.3. Some reactions with C_4ClF_7, which were done prior to the experiments with $C_2H_2Cl_2$ and C_4F_8, showed rather long induction periods (up to 17 hours) before noticeable reaction occurred. This was indicative of the presence of some chain inhibitor, probably oxygen, in the reaction cell. As additional runs were made without opening the cell to air, the induction period became shorter, and eventually was not observed at all. This induction effect, together with the fact that addition of NO inhibited the reaction, was evidence of the chain nature of the reaction between bromine and C_4ClF_7.

The reactants and products in some of the runs using C_4ClF_7 were analyzed by means of gas chromatography and mass spectrometry. The gas chromatograms showed that an additional component was present in samples after reactions, which was not present in the starting materials. This component was then isolated by fractional distillation, and was submitted to mass spectrometric analysis after ascertaining its purity by running another chromatogram. The mass spectrum of this product component showed it to be $C_4Br_2ClF_7$, the expected addition product, which was not detected in the mass spectrum of the starting materials. Due to fragmentation in

the mass spectrometer as discussed in Chapter II, ions with other masses were also detected. These, however, were consistent with the respective structures of C_4ClF_7 and $C_4Br_2ClF_7$. The isotopic distribution due to the presence of the ^{79}Br and ^{81}Br isotopes, as well as the ^{35}Cl and ^{37}Cl isotopes, aided in establishing unambiguous identification of the product. Thus, it was concluded that the reaction observed was indeed addition of bromine to the double bond. The mass distributions of fragments for C_4ClF_7 and $C_4Br_2ClF_7$ are reproduced in Figs. 4.3(A) and 4.3(B) respectively. An enlarged insert in Fig. 4.3(C) shows the detailed distribution of bromine and chlorine isotopes in the complete $C_4Br_2ClF_7$ molecule at atomic mass numbers 374 through 380.

The experiments in room light confirmed that bromine, when excited by light in its continuous absorption region, added to the double bonds of C_4F_8 and C_4ClF_7. The mechanism was a free radical chain, with a quantum yield on the order of unity for both reactants under the experimental conditions employed. The following sections will describe the results of experiments in which ruby laser light was used to catalyze the reactions.

4.4 LASER PHOTOCATALYSIS EXPERIMENTS

Both C_4F_8 and C_4ClF_7 were used in the laser photocatalysis experiments. About 25 runs were made in all, during which no essential difference in behavior between these two reactants was observed. Therefore, results which are described are equally applicable to both reactants, unless otherwise indicated. The procedures and techniques used in these experiments have already been outlined in Chapter II.

In nearly all the experiments, the initial partial pressure of C_4F_8 or C_4ClF_7 was approximately 200 mm. Initial bromine pressures between 7 mm and 12 mm were used. Thus, throughout the course of each reaction, the concentration of the fluoro-olefin, as well as the total pressure, remained more or less constant. Measurements of the reaction rates were made as the laser frequency and intensity were varied, and as the concentration of bromine changed. The effect of adding nitric oxide was also

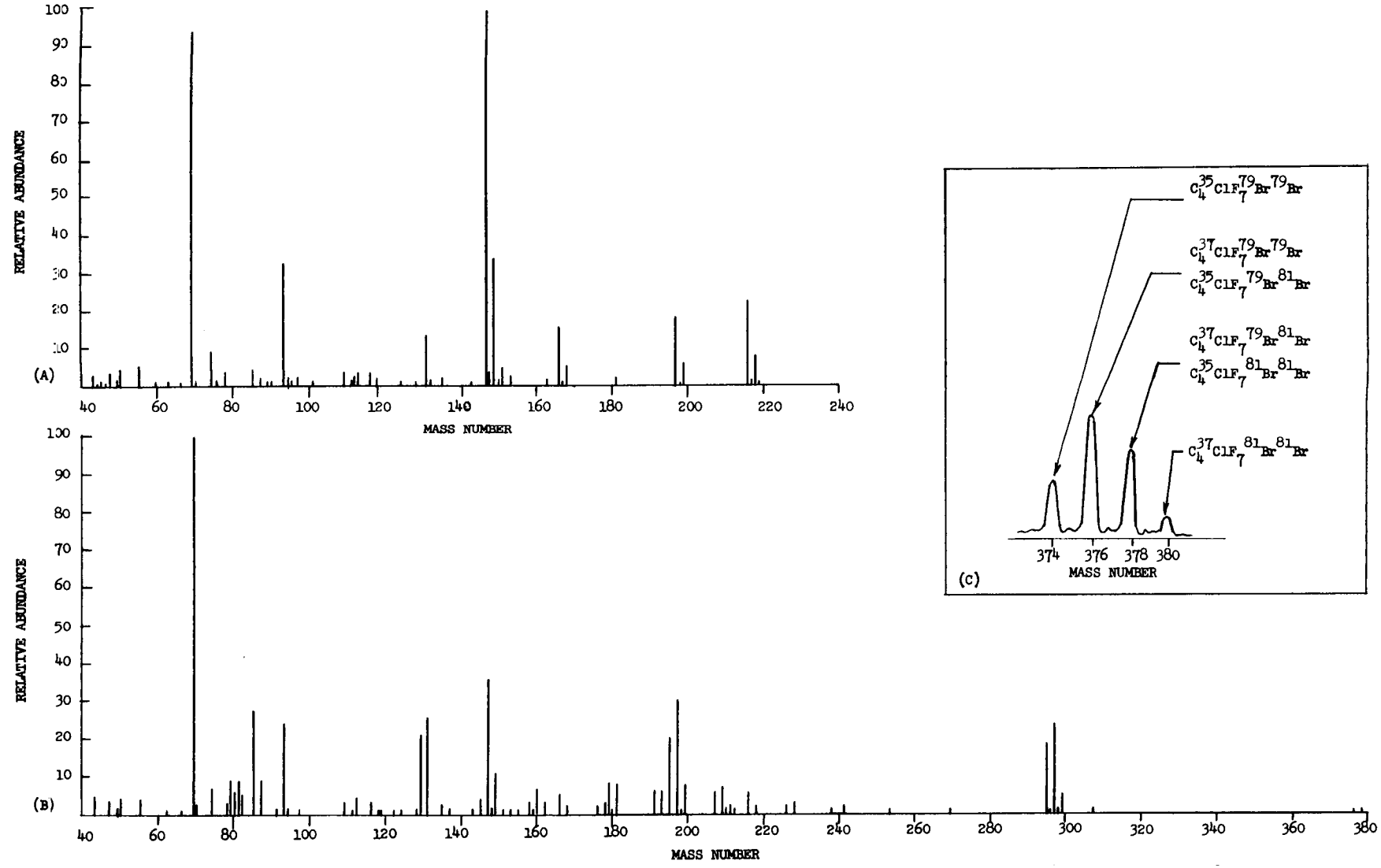

FIG. 4.3--Mass spectra of (A) C_4ClF_7 and (B) $C_4ClBr_2F_7$. The insert (C) shows the detailed isotopic distribution of masses in the region of the complete $C_4ClBr_2F_7$ molecule, which helped to confirm its identification.

observed. Gas chromatographic and mass spectrometric analyses were made to identify the reaction product and to detect isotope effects.

4.4.1 Dependence on Laser Frequency and Intensity, and Bromine Concentration

The experimental results showed that the reaction rate depended strongly on the individual absorption lines of bromine, as the laser frequency was tuned across a spectral range which contained a number of these lines (near 14,400 cm^{-1}) in the $^3\pi_{1,u} \leftarrow {}^1\Sigma_g^+$ band system. This was the first evidence of any photochemical activity associated with line absorption in bromine. Even the residual reactivity observed between the individual lines could be attributed to overlapping wings of these lines, rather than to underlying continuous absorption. In any case, the results proved that the continuum, if it existed, was extremely weak. In addition, by inserting calibrated attenuating filters into the laser beam, it was found that the rate depended approximately linearly on the incident light intensity.

Finally, as the concentration of bromine molecules decreased, so did the reaction rate. This was attributable to two causes: first, the reduction in the amount of light absorption; and second, the reduction in quantum yield due to its dependence on the Br_2 concentration. At the dilute partial pressures of Br_2 in the laser catalyzed reactions, the light absorption was expected to depend linearly on this partial pressure. The dependence of the quantum yield on Br_2 concentration, given by

$$Q \propto \frac{[Br_2]}{[Br_2] + k'} \quad ,$$

would be linear, if k' were large enough, for low Br_2 concentration, but would become independent of $[Br_2]$ at high concentrations. The low-concentration approximation appeared to fit the experimental data more satisfactorily, resulting in a $[Br_2]^2$ dependence of the reaction rate, since the rate was proportional to light intensity.

The combined dependence of the reaction rate on laser wavelength λ , incident light intensity I_0 , and bromine concentration is illustrated in Fig. 4.4. The results of ten runs with C_4F_8 are shown, which are typical of the overall results. The absorption spectrum of bromine is shown on the same wavelength scale for comparison. The actual reaction rates were normalized by dividing by $I_0[Br_2]^2$, as indicated on the figure.

4.4.2 Estimated Quantum Yield

The measured reaction rate when the laser wavelength coincided with the most prominent Br_2 absorption line was about 7.0×10^{-4} mm per pulse, at a laser output energy of approximately 0.5 Joule per pulse, and a Br_2 partial pressure of 7mm. The peak absorption in this line was approximately 25% per meter in pure bromine at a pressure of 186 mm. Thus, the same line should absorb about one per cent at its peak over the absorption path inside the cell, under the conditions of the reaction. Optical losses were estimated at 50%, resulting in an incident light energy per pulse of 0.25 Joule. This in turn led to an absorbed light energy of 0.25×10^{-2} Joule . Since each Joule of light at 14,400 cm^{-1} is approximately equal to 3×10^{18} photons, the number of absorbed quanta per pulse was about 0.75×10^{16} .

Each millimeter of gas pressure at room temperature corresponds to a density of about 3.27×10^{16} molecules per ml. Since the volume of the cell was approximately 2.5 ml., each millimeter of pressure in it consisted of 8×10^{16} molecules. Thus the observed reaction rate corresponded to 5.6×10^{13} molecules per pulse, resulting in an estimated overall quantum yield of 0.75×10^{-2} molecule per photon. This was clearly much smaller than the quantum yield expected for light in the wavelength region of continuous absorption and under steady-state conditions, but at the same reactant concentrations. An extrapolation from the room light reaction results in Table 4.3 showed that this should be about one molecule per photon.

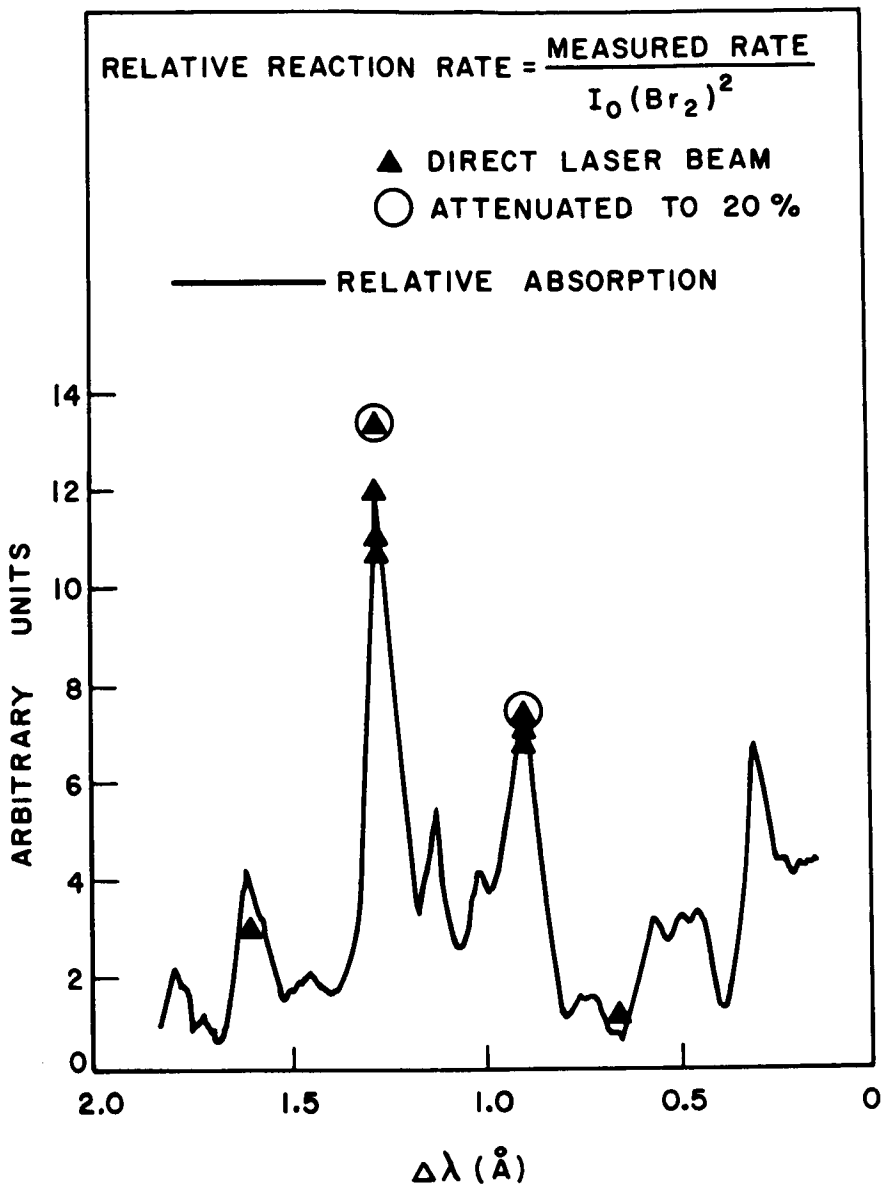

FIG. 4.4--Dependence of the reaction rate in laser light on the individual absorption lines of Br_2, showing relative rates and relative absorption on the same wavelength scale. The normalization of the relative reaction rates reflects the observed dependence on incident light intensity I_0, and on bromine concentration.

4.4.3 Effect of Adding Nitric Oxide

In one run, a few mm of nitric oxide were added to the reaction mixture. When laser light was again admitted to the reaction cell, the light transmission, indicated by the reaction rate monitoring system, decreased instead of increasing, until a steady value was reached. Upon blocking the laser beam, the light transmission slowly increased to its previous value, with a recovery time on the order of a few minutes. This effect was attributed to the formation of NOBr by the combination of the NO with Br atoms. If NOBr absorbed more strongly than Br_2 in the blue region of the monitoring light, it would account for the decrease in light transmission. Unfortunately, very little quantitative information could be found concerning the absorption spectrum of NOBr , but it was known to absorb blue light rather strongly. The rapid formation of NOBr probably depleted the supply of Br atoms, preventing any appreciable reaction with the fluorocarbon. The NOBr in turn must have been unstable with respect to binary collisions, so that the process

$$2NOBr \rightarrow 2NO + Br_2$$

caused a steady-state concentration to be reached under the influence of the laser light. When the laser beam was blocked, the NOBr continued to decompose, restoring the original concentrations of NO and Br_2 .

Based upon this interpretation, the effect of adding NO to the system was evidence that Br atoms were responsible for the reaction of bromine with the fluorocarbon. While this appears to be the only explanation consistent with the experimental results, it cannot be taken as conclusive proof of the mechanism. Although inhibition of a reaction by NO is considered by many investigators to be evidence of a free radical chain mechanism, many of the details are still open to controversy.[76]

4.4.4 Identification of the Reaction Product

Samples of laser-reacted material were analyzed by means of the gas chromatograph. They were found to contain the same component which had been identified as the product of addition of bromine to the double bond in samples reacted in ordinary light. In addition, laser-reacted samples produced mass spectra which showed the presence of $C_4Br_2ClF_7$. It was thus concluded that the laser reaction consisted of addition of bromine to the double bond of the fluorocarbon, just as did the reaction in ordinary light.

4.4.5 Isotope Effects

In view of the apparently very short lengths of the chains involved in the addition of bromine to C_4F_8 or C_4ClF_7, it was thought that this reaction might be used to separate the two isotopes of bromine. The general conditions under which photochemical separation of isotopes is possible are the following:[20]

(1) a difference in the absorption spectrum of the species,

(2) a light source capable of selectively exciting only one species,

(3) a chemical reaction involving only the excited species.

Requirements (1) and (2) were met by the identification of lines belonging to the pure isotopic molecules in the spectrum of natural bromine (see Section 3.4.2), and by the demonstration of selective photocatalysis when the laser was tuned to individual absorption lines. Requirement (3) would be met if the reaction product contained only the originally excited bromine. However, in the free radical chain mechanism, as shown at the beginning of this chapter, the process

$$(3) \qquad XBr + Br_2 \rightarrow XBr_2 + Br$$

adds the second bromine atom with no selectivity, so that the maximum expected isotopic enrichment is 50%. With continued chain propagation, the percentage enrichment becomes smaller, in inverse proportion to the

quantum yield. However, since the quantum yields in the present reactions of bromine were quite small, it might be possible to obtain a significant enrichment.

A number of runs were made in which either the pure $Br_2^{79\text{-}79}$ or $Br_2^{81\text{-}81}$ isotope was selectively excited. The products of these runs were analyzed with the mass spectrometer. No detectable isotopic enrichment occurred. This was attributed to a very fast reaction

$$(7) \qquad Br^* + Br_2 \rightarrow Br' + Br^* \quad ,$$

which resulted in isotope scrambling, but no net chemical change. Estimates based on a previous study of this exchange reaction[72] showed that it took place about 10^5 times more rapidly than the addition of bromine to the fluorocarbon. The kinetics of the exchange are such that it would dominate unless the pressure of the fluorocarbon were on the order of thousands of atmospheres, clearly an unfeasible situation.

4.5 SUMMARY

Reactions of bromine with two unsaturated fluorocarbons were carried out with activation both by ordinary light and by light from a pulsed, tunable ruby laser. In the latter case, the photochemical activity depended strongly upon excitation of individual bromine absorption lines, and not upon an underlying continuum. The reaction rate depended linearly on the incident laser light intensity. Identification of the products established that the reactions consisted of addition of bromine to the double bonds of the fluorocarbons. Although the primary excitation resulted in the formation of stable excited molecules, and not dissociated atoms, the behavior of the subsequent reaction was consistent with a free radical chain mechanism, initiated by bromine atoms. The quantum yield of this chain, however, was estimated to be relatively small. It was

probably on the order of unity for steady-state excitation by light in the continuum, at the reactant concentrations used. The overall quantum yield under conditions of pulsed excitation by the ruby laser was estimated to be on the order of 10^{-2}. Reactions in which pure isotopes of bromine were selectively excited did not result in isotopic enrichment of the product. This could be attributed to rapid isotopic exchange reactions between bromine atoms and normal bromine molecules.

V. INTERPRETATION OF RESULTS

5.1 INTRODUCTION

In this chapter, the experimental evidence which was introduced in the preceding chapter will be examined, with a twofold purpose. First, insofar as is possible, the experimental results will be used to show which of the alternative mechanisms discussed in Section 4.1 is responsible for the observed reaction of bromine and the fluoro-olefins catalyzed by ruby laser light. Second, they will be used to draw conclusions as to the relative rates of certain competing dynamic processes in the system. In order to deal with processes which are initiated by pulsed excitation, it will first be necessary to develop expressions for the overall rates, to replace those which were formulated in the preceding chapter on the assumption of steady-state conditions. After this has been done, the various dynamic processes involving atoms and excited molecules will be examined. Each of the alternative hypotheses of Section 4.1 will be discussed to determine which of them is most consistent with the experimental evidence.

5.2 DYNAMIC RATES UNDER PULSED CONDITIONS

In the laser photocatalysis experiments, the active species (excited bromine molecules or dissociated atoms) initiating the reactions were generated in pulses of approximately 0.5 millisecond in duration, which were repeated at intervals of 0.75 second. This was clearly a condition under which the steady-state approximation[74] was not applicable. It is more appropriate, therefore, to discuss the behavior of the system in terms of the probabilities per unit time of the individual processes on a microscopic level, rather than in terms of steady rates. There are three general categories into which these processes fall. The first category includes radiative processes, absorption and emission, the

probabilities of which are affected only indirectly by the concentrations of the various atomic and molecular species. The second category includes transfer of the various forms of molecular energy, translational, vibrational, rotational, and electronic, by means of collisions between the molecules. Processes which involve chemical reactions are reserved for the third category. Clearly, the probabilities of the processes in the second and third categories depend strongly on the molecular concentrations.

Dynamic processes can also be classified according to their formal kinetics. First-order processes are those which, on the microscopic level, involve a single atom or molecule.[83] Likewise, second-order processes are events in which two particles participate. Many second-order processes involve one molecule each of two separate types, and thus they are first-order with respect to each individual type of molecule. Examples of first-order processes are absorption of photons, and spontaneous dissociation of molecules into atoms. The transfer of energy by collision is clearly a second-order process. However, if the particular type of transfer involves a molecular species which is present only in a dilute concentration, so that collisions between two of these molecules are very rare, the process is first-order with respect to that species. On the other hand, recombination of two like atoms to form a diatomic molecule is generally second-order with respect to these atoms (an exception is recombination at the walls), but the requirement of a third body to carry away excess energy makes the overall process obey third-order kinetics.

We shall now consider the behavior of systems undergoing both first- and second-order processes under pulsed conditions. We shall assume first that the pulse occurs instantaneously, and produces an initial population of some species (for instance, molecules in an excited electronic state). This population then decays by means of one or more dynamic processes, which we want to study. The supposition of an instantaneous pulse is a reasonably good approximation, so long as the actual pulse is much shorter than the subsequent decay time. Where this condition does not hold, the instantaneous initial population can be replaced, if needed, by an appropriate time integral over the duration of the pulse.

In this approximation, the time dependence of the concentration of a species undergoing a single first-order decay process is given by

$$-\frac{dc}{dt} = kc \quad , \tag{5.1}$$

where k is the rate constant for the process. Integrating Eq. (5.1) and denoting the initial concentration at $t = 0$ by c_0, we obtain

$$c = c_0 e^{-kt} \quad . \tag{5.2}$$

Clearly then, k is the probability per unit time that the process will occur for a single molecule, and the quantity

$$\tau = 1/k \tag{5.3}$$

is known as the characteristic time for the process; in a time τ the concentration c decreases by a factor e. Thus, this is the effective mean lifetime of the species with respect to the single-order process.

Now, if a number of competing first-order processes occur, the time dependence can be expressed as

$$-\frac{dc}{dt} = \sum_{n=1}^{N} k_n c \quad . \tag{5.4}$$

Here, the subscript refers to each of the N individual processes. If we define the quantity

$$K = \sum_{n=1}^{N} k_n \quad , \tag{5.5}$$

then integration of Eq. (5.4) produces the result

$$c = c_0 e^{-Kt} \quad . \tag{5.6}$$

The effective lifetime is now given by

$$\tau = \frac{1}{K} = 1 \Big/ \sum_{n=1}^{N} k_n \quad , \tag{5.7}$$

or

$$\frac{1}{\tau} = \sum_{n=1}^{N} \frac{1}{\tau_n} \quad . \tag{5.8}$$

Now let us consider the behavior of a system which undergoes a second-order process. The time dependence of a population can then be written

$$- \frac{dc_i}{dt} = k\, c_i\, c_j \quad . \tag{5.9}$$

Two special cases are now considered. In the first of these, the concentration c_j remains fixed during the process. This will be the case when c_j is very large, and represents a concentration which is essentially unaffected by the pulsed generation of c_i. Then we can define an effective first-order rate constant

$$k_{eff} = k\, c_j \quad , \tag{5.10}$$

and rewrite Eq. (5.9) as a first-order process involving only c_i, as

$$- \frac{dc_i}{dt} = k_{eff}\, c_i \quad , \tag{5.11}$$

which can then be treated in a manner identical to Eq. (5.1).

In the second special case, we consider a process in which two particles of type $\underline{i}$ combine with each other, so that Eq. (5.9) now is rewritten in the form

$$-\frac{dc}{dt} = k\,c^2 \quad , \tag{5.12}$$

where we omit the subscript for convenience. The probability per unit time for this process to occur is now no longer constant, but decreases as the population $\underline{c}$ decays. The concept of an effective lifetime τ is also no longer meaningful. Integrating Eq. (5.12) and again assuming an instantaneous initial population c_0, we now obtain

$$\frac{1}{c} = \frac{1}{c_0} + kt \quad , \tag{5.13}$$

or, equivalently,

$$c = \frac{c_0}{1 + c_0\,kt} \quad . \tag{5.14}$$

To complete this discussion of formal kinetics, we consider the following situation. A species is present, which is responsible for initiating a reaction, but is not used up in the process. This is the role played by bromine atoms in the free radical chain addition reaction with olefins. The chain reaction itself does not deplete the population of atoms, as they are continually regenerated. Two independent competing processes eventually lead to disappearance of the atoms. One of these processes is second-order, and dominates at sufficiently high concentrations. The other process is first-order, and takes over as the dominant mechanism at reduced concentrations. The rate at which products are formed in the chain reaction is then given by

$$\frac{dc_p}{dt} = k_c c_a \quad , \tag{5.15}$$

where c_p is the concentration of products, c_a is the concentration of initiating atoms, and k_c is the effective rate constant of the chain reaction, including the (nearly constant) concentrations of the other reactants, which, from Eq. (4.1), is given by

$$k_c = \frac{k_2 k_3 [X] [Br_2]}{k_3 [Br_2] + k_{-2}} \quad , \tag{5.16}$$

for the bromine-olefin reaction. If we now assume that c_a is reduced by a second-order process, it can be expressed by Eq. (5.14). Inserting this in Eq. (5.15), we obtain

$$\frac{dc_p}{dt} = \frac{k_c c_0}{1 + c_0 kt} \quad . \tag{5.17}$$

To obtain the total product yield per pulse, it is necessary to integrate Eq. (5.17). If this integral is taken from time $t = 0$ to $t = \infty$, it diverges. This is prevented by assuming a maximum cut-off time for the integral, which can be taken to be approximately the time at which the concentration is sufficiently reduced for the first-order decay process to become dominant. This results in the expression for the total product yield per pulse of

$$c_p = \int_0^{t_{max}} \frac{k_c c_0 \, dt}{1 + c_0 kt} \quad , \tag{5.18}$$

which has the solution

$$c_p = \frac{k_c}{k} \ln(1 + c_0 kt_{max}) \quad . \tag{5.19}$$

This logarithmic behavior of the total yield is clearly quite insensitive to changes in c_0 for $c_0 kt_{max} \gg 1$. This is in contrast to the result

expected for chain reactions terminated by a first-order process alone. In that case we obtain

$$c_p = \int_0^\infty k_c \, c_0 \, e^{-kt} \, dt \quad , \tag{5.20}$$

which has the solution

$$c_p = \frac{k_c \, c_0}{k} \quad , \tag{5.21}$$

and hence depends linearly on c_0 . It should be noted from Section 4.1 that the second-order termination mechanism leads to a square-root dependence on the excitation intensity under steady-state conditions, whereas it leads to the logarithmic dependence in the case of pulses. The consequences of these differences in behavior in the detailed analysis of the experimental results will be discussed in Section 5.5.

5.3 ABSORPTION OF PULSED LASER RADIATION

When the estimated quantum yield of the laser photocatalysis experiments was calculated in Section 4.2.2, it was tacitly assumed that saturation effects did not occur in the absorption process. This assumption requires some justification because it led to the conclusion that 0.75×10^{16} molecules were excited at every pulse. The total number of Br_2 molecules in the cell was about 0.56×10^{18} , so that about 1.34% of them were excited during the pulse duration of approximately 0.5 msec. It must be realized, however, that only half the bromine in the cell was the $Br_2^{79\text{-}81}$ isotopic species which was being excited, and, furthermore, that only a small fraction of this was present at any given time in the specific initial vibrational-rotational level of the ground state. If the quantum numbers for this level were known, the fractional population could be calculated readily for the room-temperature

Boltzmann distribution. However, since this information is not available, a reasonable estimate can be made as follows. The fraction of molecule $f_{v''}$ in a given v'' level at temperature T is given approximately by[39]

$$f_{v''} = e^{-v''\omega/kT}(1 - e^{-\omega/kT}) \quad , \qquad (5.22)$$

where ω is the vibrational parameter defined in Section 3.2, and is about 300 cm^{-1} for the $^1\Sigma_g^+$ state of bromine. At room temperature, $kT \approx 200\ cm^{-1}$; since the sharp line transitions of Br_2 near 14,400 cm^{-1} have $v'' = 2$ or 3 , the fractional population is then either 0.039 or 0.0086. This fractional population is further subdivided among the rotational levels J'' according to[84]

$$f_{J''} = \frac{B''}{kT}(2J'' + 1)\, e^{-B''J''(J''+1)/kT} \quad , \qquad (5.23)$$

where B'' is the rotational parameter for the $^1\Sigma_g^+$ state, and is approximately 0.08 cm^{-1}, as shown in Table 3.1. This fraction reaches a maximum for

$$J''_{max} = (kT/2B)^{1/2} - \frac{1}{2} \quad , \qquad (5.24)$$

which is $J''_{max} = 35$ for Br_2 . Inserting this value in Eq. (5.23), we obtain $f_{J''\,max} \cong 0.017$.

Judging from the prominence of this particular absorption line, it is reasonable to assume that the initial level is not far from J''_{max} . Combining the fractional populations resulting from the vibrational, rotational, and isotopic distributions, we find an overall fractional population of about 0.7×10^{-4} to 3.5×10^{-4} .

Thus it turns out that during the pulse about 40 to 200 times as many molecules are excited out of the initial state as are in it as thermal equilibrium.

In order to prevent saturation from occurring, it is clear that bromine molecules from other states must be transferred to this particular state more rapidly than they are excited out of it by the light. The mechanism for this is provided by rapid collisional transfer of vibrational and rotational energy by the $^1\Sigma_g^+$ ground-state bromine molecules. As shown in Section 3.4.3, the mean number of collisions per second which each ground-state bromine molecule undergoes in a sample of the pure gas is given approximately by

$$Z_1 = 5 \times 10^6 P \quad , \qquad (5.25)$$

where P is the pressure in mmHg . Experiments on pressure broadening of absorption lines indicated that this collision frequency did not change appreciably in a bromine-fluorocarbon mixture with the same total pressure. Thus, in the laser photocatalysis experiments, where the total pressure was about 200 mm, the gas-kinetic collision frequency was about 10^9 per second.

Ultrasonic absorption measurements[85] showed that collisional relaxation between the $v'' = 0$ and $v'' = 1$ levels of bromine require on the average 5600 gas-kinetic collisions at a temperature of 301°K.[66] The probability of collisional transfer of vibrational energy between adjacent vibrational levels follows the selection rule[86]

$$P_{v \leftrightarrow v-1} = v P_{1 \leftrightarrow 0}$$

where $P_{v \leftrightarrow v-1}$ denotes the probability of energy transfer between levels v and $v-1$. Hence relaxation between levels $v'' = 2$ and $v'' = 3$ should require on the average less than 2000 collisions. Thus, the vibrational population in one of these levels would be restored in a time on the order of 2μsec under our experimental conditions, which is 250 times faster than the laser pulse

Rotational relaxation within a vibrational state occurs much more rapidly than this. No experimental data are available for bromine, but ultrasonic measurements in N_2 and O_2 show that the probability per collision for rotation-translation energy transfer is about 0.1.[86] It is generally true of collisional energy transfer that for a particular type of process, the larger the energy the less probable the transfer becomes.[86] Therefore, in bromine, where the energy spacing between rotational levels is smaller, a greater probability of transfer is expected. Hence rotational relaxation would be expected to require on the average somewhat fewer than 10 gas-kinetic collisions. Under our experimental conditions, this would restore rotational equilibrium in about 10^{-8} second.

It can be concluded, therefore, on the basis of reasonable vibrational and rotational relaxation rates, that the assumption of no appreciable saturation effect is entirely justified. The extremely rapid rotational relaxation alone would be more than sufficient in the $v'' = 2$ state, where the overall population is higher. Likewise, vibrational relaxation alone would replenish the individual state as rapidly as the laser pulse depleted it. The combination of the two mechanisms is certainly sufficient to overcome any tendency to saturate at the experimental intensity level.

5.4 PROCESSES INVOLVING EXCITED BROMINE MOLECULES

After the bromine molecules were excited to the $^3\Pi_{1,u}$ state by the laser light, they could take part in a number of competing dynamic processes. The purpose of this section is to enumerate these processes and to estimate their probabilities.

5.4.1 Spontaneous Emission of Radiation

Calculations based on the theoretical work of Mulliken,[46] in his interpretation of the spectral data of Bayliss and co-workers,[40] indicated that the radiative lifetime of the $^3\Pi_{1,u}$ state was of the order of 10^{-4} sec. This process sets an ultimate limit to the lifetime of the $^3\Pi_{1,u}$ state, as it is independent of pressure or molecular concentration. It competes with other processes which have characteristic lifetimes of the same order of magnitude or greater.

5.4.2 Vibrational and Rotational Relaxation

Energy transfer processes within the $^3\Pi_{1,u}$ state can take place with a high probability per gas-kinetic collision. Since the concentration of excited bromine molecules under our experimental conditions was at most about 1.34% of all the bromine, which in turn was only about 3.5% of the total pressure, collisions between two excited molecules were rare. Therefore, practically all collisions of the excited bromine molecules were with the "heat bath" comprising the normal bromine and fluorocarbon molecules. In these collisions, the energy associated with the translational, vibrational, or rotational degrees of freedom of the excited bromine could be exchanged with any of the various degrees of freedom of the heat bath molecules. We are concerned here only with the internal degrees of freedom of the excited bromine molecules. Furthermore, it has already been established that rotational energy is transferred rapidly in ground state Br_2 molecules, and so it should be transferred even more rapidly in $^3\Pi_{1,u}$ molecules, where the rotational quanta are smaller.[86] Steinfeld and Klemperer[69] determined experimentally that rotational energy was transferred in excited iodine molecules on the average in practically every gas-kinetic collision. In addition, they determined that vibrational energy transfer occurred with the same high order of probability. For reasonably high vibrational levels of the $^3\Pi_{1,u}$ state of bromine, the spacing of these levels is only some 50 to 100 cm^{-1}. Theoretical calculations[87] using this value of energy spacing predict that vibrational energy transfer should occur very rapidly in excited bromine, with a probability per collision on the order of that for excited iodine molecules. With these high rates of energy transfer, it is reasonable to conclude that vibrational and rotational equilibrium within the $^3\Pi_{1,u}$ state is reached within 10 or 20 gas-kinetic collisions following excitation of the molecules to a single vibrational-rotational sub-level by means of the laser pulse.

5.4.3 Dissociation

When an excited molecule reaches an energy level within kT of the dissociation energy, it is easily capable of being dissociated by the next collision which it undergoes. The reverse reaction, i.e., the

recombination of two atoms to form an excited molecule, is much less probable, since it requires that both atoms first be brought together in a collision. The relative dominance of the dissociation process therefore perturbs the equilibrium populations of the upper vibrational states so as to make them lower than those expected from a simple Boltzmann distribution.[67] During the initial period before equilibrium is reached, there is a net transfer of excited molecules from lower to higher vibrational energy levels, and thence to dissociation. Non-equilibrium rate processes under such conditions have been discussed theoretically by a number of authors.[67,88] However, before considering the non-equilibrium dissociation rate for $^3\Pi_{1,u}$ bromine molecules, something should be understood about the equilibrium concentrations of bromine molecules and atoms.

Equilibrium constants for the dissociation of diatomic molecules can be estimated with reasonable accuracy from elementary statistical mechanics.[89] This calculation takes into consideration the changes in both energy and entropy between the typical bound molecule and the typical dissociated atom at a given temperature. The result is the expression

$$K_{eq.} = \frac{[X]^2}{[X_2]} = \frac{1.67\ e^{-D/RT}}{2\pi r_0^2 \xi} \text{ moles per ml} \quad , \quad (5.26)$$

for the relationship between the concentrations of atoms $[X]$ and of molecules $[X_2]$ in equilibrium at absolute temperature $T^{\circ}K$. In Eq. (5.26), D is the dissociation energy necessary to break the molecular bond, R is the gas constant; r_0 is the average internuclear radius, and ξ is the average vibrational amplitude for the molecules, both measured in $\mathring{A}$ units.(1)

(1) It might be naively assumed that the equilibrium concentrations of Br_2 molecules and Br atoms are determined only by the Boltzmann energy factor $e^{-D/RT}$, where D is the energy required to break the molecular bond. This, however, neglects the fact that a considerable increase in entropy occurs when a molecule dissociates into atoms. From a statistical mechanical viewpoint, this comes about because two atoms have access to a greater volume in phase space then does one molecule.[89]

For bromine molecules in the ground $^1\Sigma_g^+$ electronic state at room temperature, we have $r_0 \cong 2.284$ Å , $\xi \cong 0.12$ Å , and $D \cong 46$ Kcal/mole ($16{,}070\ cm^{-1}$). Inserting these values in Eq. (5.26), we obtain

$$K_{eq.}\ (Br_2 : {}^1\Sigma_g^+) \cong 10^{-33}\ \text{mole/ml} \quad .$$

A calculation from tabulated values of the bromine dissociation equilibrium constant[90] resulted in a value three times this large. However, the latter calculation assumed that bromine obeyed the ideal gas law, and therefore was subject to some error. A similar calculation for a temperature of 1400°K, where published data was available,[91] indicated a discrepancy by a factor of five in the same direction. Therefore, the result obtained from statistical mechanics is probably very nearly correct.

This shows that a very small fraction of bromine is dissociated under normal conditions at room temperature. For example, in the laser photocatalysis experiments the cell contained about 7 mm of bromine, or 3.8×10^{-7} mole per ml. From the equilibrium constant we calculate that only about 2×10^{-20} mole per ml of bromine atoms is present, so that less than one molecule in 10^{13} is dissociated.

The situation is entirely different when we now calculate the equilibrium constant for dissociation from the $^3\Pi_{1,u}$ state of bromine at room temperature. We assume that equilibrium between dissociated atoms and $^3\Pi_{1,u}$ molecules is established, and ignore relaxation processes involving the ground $^1\Sigma_g^+$ state, or the other excited molecular states. For $^3\Pi_{1,u}$ molecules we have the values $r_0 \cong 2.6$ Å , $\xi \cong 0.3$ Å , and $D \cong 2100\ cm^{-1}$, which is the depth of the $^3\Pi_{1,u}$ potential minimum below the dissociation energy level. This results in the equilibrium constant

$$K_{eq.}\ (Br_2 : {}^3\Pi_{1,u}) \cong 3.6 \times 10^{-6}\ \text{mole/ml} \quad .$$

Again taking the conditions of the laser photocatalysis experiment for our example, initially 5×10^{-9} mole/ml of Br_2 was excited to the $^3\Pi_{1,u}$ state by the light pulse. We assume that these become distributed at equilibrium between dissociated atoms and $^3\Pi_{1,u}$ molecules. Thus we have

$$\frac{1}{2}[Br] + [Br_2^*] = 5 \times 10^{-9} \text{ mole/ml} \quad , \qquad (5.27)$$

and, from the equilibrium condition

$$\frac{[Br]^2}{[Br_2^*]} = 3.6 \times 10^{-6} \text{ mole/ml} \quad . \qquad (5.28)$$

Solving these equations simultaneously, we arrive at an equilibrium value for the bromine atom concentration

$$[Br] \cong 9.9 \times 10^{-9} \text{ mole/ml} \quad ,$$

which means that 99% of the available excited molecules become dissociated. Hence, when the $^3\Pi_{1,u}$ state alone is considered, equilibrium is overwhelmingly in favor of dissociation. This fact alone, however, is not sufficient to explain the experimental results. It is necessary to estimate the rate of dissociation during the non-equilibrium period, in order to compare it with the rates of the other dynamic processes which compete in removing molecules from the $^3\Pi_{1,u}$ state.

Rates of dissociation and recombination of molecules have been studied recently in considerable detail using flash photolysis and shock tube techniques.[92] These experiments, however, have not led to any explicit information about dissociation from excited electronic states of the molecules. Again, though, reasonable estimates can be made by taking into account the difference in the activation energy

required for dissociation from the ground state and from the excited state. This activation energy leads to the same factor $e^{-D/RT}$ in the dissociation rate constant, which appeared in the expression given in Eq. (5.26) for the equilibrium constant. However, whereas the equilibrium constant is dependent only upon the temperature, and is essentially independent of the nature of the molecules comprising the "heat bath," this is no longer true of the rate constant. Experiments indicate wide variations in the effectiveness of various collision partners for this process. Furthermore, since the rate constants for dissociation k_d and recombination k_r are related through the equilibrium constant by means of

$$k_d = K_{eq.}\, k_r \quad , \tag{5.29}$$

the same variations in effectiveness are observed for the recombination process as well.

Givens and Willard[93] measured recombination rates of Br atoms to form ground state Br_2 following the flash photolysis of Br_2, using both Br_2 and Argon for collision partners. They found Br_2 to be by far the more effective, with a rate constant of $k_r(Br_2) = 2.6 \times 10^{11}$ $l^2 mole^{-2} sec^{-1}$, as compared with $k_r(A) = 2.0 \times 10^{9}$ $l^2 mole^{-2}$ sec^{-1} for Argon at 300°K. By means of Eq. (5.29) these can be converted into the respective dissociation rate constants, $k_d(Br_2) = 2.6 \times 10^{-19}$ l $mole^{-1}$ sec^{-1}, and $k_d(A) = 2.0 \times 10^{-21}$ l $mole^{-1}$ sec^{-1}. Attempts to relate these rate constants to those measured by Palmer and Hornig[94] at high temperatures in a shock tube met with a number of difficulties, which were discussed by Nikitin and Sokolov.[67]

If we now allow for the difference in activation energy for dissociation from the $^1\Sigma_g^+$ state and the $^3\Pi_{1,u}$ state, the resulting dissociation rate constants for excited bromine molecules become

$$k_d^*(Br_2) = 4.7 \times 10^{10} \text{ l mole}^{-1} \text{ sec}^{-1} \quad ,$$

and

$$k_d^*(A) = 3.6 \times 10^8 \text{ l mole}^{-1} \text{ sec}^{-1} \quad .$$

Although no explicit data were available for the fluorocarbons used in the present experiments, their effectiveness as collision partners should lie somewhere between those of argon and Br_2 . This is in agreement with measurements of recombination rates for iodine,[95] in which it was found that both C_3H_8 and C_5H_{12} were about ten times as efficient as argon for collision partners. We shall assume that the same is true of the fluorocarbons, which have a similar size and a similar number of vibrational modes, giving a rate constant

$$k_d^*(Fl) \cong 3.6 \times 10^9 \text{ l mole}^{-1} \text{ sec}^{-1} \quad .$$

Now the characteristic time for dissociation is given by

$$1/\tau_d^* = k_d^*(Br_2)[Br_2] + k_d^*(Fl)[Fl] \quad , \qquad (5.30)$$

in terms of the respective rate constants and concentrations. In the appropriate units, the latter are $[Br_2] = 3.8 \times 10^{-4}$ mole l^{-1} and $[Fl] = 1.09 \times 10^{-2}$ mole l^{-1} . Inserting these values in Eq. (5.30), we obtain

$$1/\tau_d^* = 5.7 \times 10^7 \text{ sec}^{-1} \quad .$$

This result indicates that about 17.5 gas-kinetic collisions are required, on the average, to dissociate a bromine molecule from the $^3\Pi_{1,u}$ state, using the ratio of bromine to fluorocarbon which was present in the laser photocatalysis experiments. This is approximately the same number of collisions which were estimated in the preceding section for achieving vibrational equilibrium within the $^3\Pi_{1,u}$ state. Hence, the two calculations are consistent within the framework of a model in which dissociation occurs freely for any molecule with the requisite energy, as part of an overall relaxation toward thermal equilibrium. It is concluded from the results of this section that this equilibrium lies in the direction of almost complete dissociation, and that it is attained in a very few gas-kinetic collisions. Other mechanisms which remove molecules from the $^3\Pi_{1,u}$ state must, therefore, also be very rapid, if they are to compete significantly with the dissociation process.

5.4.4 Chemical Reactions Involving Excited Bromine Molecules

A number of chemical processes involving $^3\Pi_{1,u}$ bromine molecules can be hypothesized, whether or not they actually do occur. These processes can be written formally as follows:

Substitution:	(M1a)	$Br_2^* + C_4F_8 \rightarrow C_4Br_2F_6 + F_2$
	(M1b)	$Br_2^* + C_4F_8 \rightarrow C_4BrF_7 + BrF$
Radical Formation:	(M2)	$Br_2^* + C_4F_8 \rightarrow C_4BrF_8 + Br$
Molecular Addition:	(M3)	$Br_2^* + C_4F_8 \rightarrow C_4Br_2F_8$
Isotopic Exchange:	(M4)	$Br_2^* + Br_2 \rightarrow 2Br^*Br$,

in which C_4F_8 is taken here to include C_4ClF_7 as well. It will be the purpose of this section to discuss these reactions.

Reactions (M1a) and (M1b) may be eliminated as being energetically unfavorable. According to the bond energies listed in Table 4.1, each C-Br bond substituted for a C-F bond requires the addition of 53 Kcal/mole. Furthermore, such substitution reactions have not been observed experimentally.[81]

Reaction (M2) is exothermic, so is not excluded by energetic considerations. On the other hand, by producing a pair of radicals, it would lead to the identical chain-reaction mechanism that would follow from the collisional dissociation process in Section 5.4.3. Complex formation of this sort is already thought to occur in many dissociation and recombination processes, but the matter is open to some controversy.[91-95] The detailed study of this mechanism was, however, not undertaken in the present investigation, although it could be studied by extension of the techniques developed here.

Reaction (M3), although energetically allowed, has never been observed in either photochemical or thermal reactions of Br_2.[76] Previous kinetic studies indicated that the mechanism was a free radical chain and not bimolecular addition. The reaction rates in the present study were also inconsistent with the kinetics of bimolecular addition reactions. The strong inhibition by nitric oxide was additional evidence against bimolecular addition. The most significant evidence, however, was the absence of isotopic enrichment in the reaction product when individual bromine isotopes were excited by the laser light. This is readily explained in a free radical reaction by the very rapid isotopic exchange[72]

$$(7) \qquad Br^{*} + Br_2 \rightarrow Br + Br^{*}Br \qquad ,$$

as discussed in Section 4.4.5. If, however, a significant amount of the product resulted from reaction (M3) above, then the lack of isotope enrichment must be attributed to competition from reaction (M4). The corresponding reaction between ground-state bromine molecules was discussed by Noyes.[96] The rate constant for it is calculated to be

$$k_{M4} = A_{M4}\, e^{-E_{M4}/RT} \qquad ,$$

where $E_{M4} = 10.4$ Kcal/mole , and $A_{M4} = 3.3 \times 10^{7}$ l mole^{-1} sec^{-1} . In the reaction between an excited Br_2 molecule and a ground-state molecule, enough activation energy is already available, so that the exponential factor may be taken to be nearly unity. Hence we make the approximation

$$k^{*}_{M4} \cong 3.3 \times 10^{7} \text{ l mole}^{-1} \text{ sec}^{-1} \quad ,$$

denoting by the asterisk the fact that one of the molecules is now in an excited state. With the Br_2 concentration of 3.8×10^{-4} mole/l , this leads to an exchange rate of

$$1/\tau^{*}_{M4} \cong 1.25 \times 10^{4} \text{ sec}^{-1} \quad .$$

This indicates that the exchange reaction is about three order of magnitude slower than dissociation rate for excited bromine, given previously as

$$1/\tau^{*}_{d} \cong 5.7 \times 10^{7} \text{ sec}^{-1} \quad .$$

Since the absence of isotopic enrichment implies that the rate of the molecular addition reaction (3) is slower than 1.25×10^{4} sec^{-1} , we conclude that molecular addition of $^{3}\Pi_{1,u}$ bromine to the fluoro-olefins is unable to compete with the rapid dissociation process, which leads in turn to the chain reaction.

5.4.5 Relaxation to the Electronic Ground State

The only remaining distinct process which can compete with dissociation in removing bromine molecules from the $^3\Pi_{1,u}$ state is collisional relaxation to the $^1\Sigma_g^+$ state. No data were available on this energy transfer process in Br_2 prior to the present investigation. In a number of other molecules, however, the corresponding processes were known to occur quite rapidly, despite substantial energy discrepancies, which had to be taken up by translation.[86] Deactivation of electronically excited NO by CO_2 was found to occur with even a greater probability than the gas-kinetic collision frequency.[68,97] Otherwise, the knowledge of this type of energy transfer is in general fragmentary.[86]

Certain conclusions about this deactivation process can be reached on the basis of the laser photocatalysis results. To understand how this comes about, it is first necessary to consider the processes involving dissociated Br atoms. This will be done in the next section, where the consequences with regard to molecular deactivation will also be discussed.

To summarize the information presented in this section, the following estimated rates have been obtained for processes involving Br_2 molecules in the $^3\Pi_{1,u}$ excited state:

(a) Spontaneous Emission $\sim 10^4\ sec^{-1}$

(b) Vibrational Energy Transfer $\sim 10^9\ sec^{-1}$

(c) Collisional Dissociation $\sim 5 \times 10^7\ sec^{-1}$

(d) Molecular Isotopic Exchange $\sim 10^4\ sec^{-1}$

(e) Molecular Addition to Double Bond $< 10^4\ sec^{-1}$.

5.5 PROCESSES INVOLVING BROMINE ATOMS

There are three different types of processes which involve bromine atoms. The first is the exchange reaction

$$(7) \qquad Br^* + Br_2 \rightarrow Br + Br^*Br \quad ,$$

which has already been discussed. The second is the chain addition reaction, consisting of the repeated consecutive elementary steps

$$(2) \qquad Br + X \leftrightarrows XBr \qquad ,$$

and

$$(3) \qquad XBr + Br_2 \rightarrow XBr_2 + Br \qquad .$$

Neither of these processes results in a net disappearance of Br atoms, which is governed by the two competing recombination reactions,

$$(4) \qquad Br \overset{wall}{\rightarrow} \frac{1}{2} Br_2 \qquad ,$$

and

$$(5) \qquad Br + Br + M \rightarrow Br_2 + M \qquad ,$$

as discussed at the beginning of Chapter IV.

The first of these recombination processes is first-order in the bromine atom concentration, whereas the second is second-order. The theory of the behavior of a system under the influence of two such competing processes was developed in Section 5.2. The resulting product yield per laser pulse for the chain reaction, as governed by the respective recombination processes was found to be expressed by

$$c_p = \frac{k_c}{k} \ln (1 + c_0 \, k t_{max}) \qquad (5.19')$$

for dominant second-order recombination, and

$$c_p = \frac{k_c c_0}{k} \qquad (5.21')$$

for a dominant first-order recombination.

The expression in Eq. (5.19) must first be modified to account for the fact that on the average only a fraction f of the atoms is available for recombination in process (5). This comes about because each atom spends a part of its time bound to the olefin X , in the form of the radical XBr , following step (2) and before the occurence of step (-2) or step (3), which places it back in circulation. Thus, the fraction f can be expressed as

$$f = \frac{\tau_{Br}}{\tau_{Br} + \tau_{XBr}} \quad , \qquad (5.31)$$

where the τ's are the lifetimes of free bromine and of the radical during the cycle (2), (-2), (3). These can be related in turn to the individual rate constants and reactant concentrations to obtain

$$\frac{1}{\tau_{XBr}} = k_3[Br_2] + k_{-2} \qquad (5.32)$$

and

$$\frac{1}{\tau_{Br}} = k_2[X] \quad . \qquad (5.33)$$

When expressions (5.32) and (5.33) are substituted into Eq. (5.31), the result is

$$f = \frac{k_3[Br_2] + k_{-2}}{k_2[X] + k_3[Br_2] + k_{-2}} \quad . \tag{5.34}$$

As a consequence of this reduction in the available atoms, Eq. (5.14) is modified to the form

$$c = \frac{c_0}{1 + c_0 f^2 k_5 t} \quad , \tag{5.35}$$

and Eq. (5.17) to the form

$$\frac{dc_p}{dt} = \frac{k_c c_0}{1 + c_0 f^2 k_5 t} \quad , \tag{5.36}$$

which contains the explicit dependence upon f and upon k_5. Integrating from time $t = 0$ to t_{max} yields the result

$$c_{p_5} = \frac{k_c}{k_5 f^2} \ln (1 + c_0 f^2 k_5 t_{max}) \quad . \tag{5.37}$$

Equation (5.37) is approximately valid so long as recombination process (5) predominates over process (4), which will be true for concentrations of bromine atoms such that

$$c \geq \frac{k_4}{k_5 f^2} \quad . \tag{5.38}$$

For lower initial concentrations, the entire product yield is given by Eq. (5.21). For higher initial concentrations, there will be a term added to the yield given by Eq. (5.37) to take into account the reaction

which occurs after $t = t_{max}$. Combining the expressions (5.35) and (5.38) for $t = t_{max}$ we find

$$t_{max} = \frac{1}{k_4} - \frac{1}{c_0 f^2 k_5} \quad . \tag{5.39}$$

Inserting this value in Eq. (5.37) yields the result

$$c_{p_5} = \frac{k_c}{k_5 f^2} \ln\left(\frac{c_0 f^2 k_5}{k_4}\right) \quad . \tag{5.40}$$

Combining Eq. (5.38) and Eq. (5.21) we find

$$c_{p_4} = \frac{k_c}{k_5 f^2} \tag{5.41}$$

for the contribution to the total yield occurring after $t = t_{max}$. Hence, the complete expression for the product yield, according to the theory developed here, is

$$c_p = c_{p_5} + c_{p_4} = \frac{k_c}{k_5 f^2}\left[\ln\left(\frac{c_0 f^2 k_5}{k_4}\right) + 1\right] \quad , \tag{5.42}$$

for initial concentrations such that second-order recombination is predominant in the beginning.

In the foregoing treatment we have ignored a number of additional reactions, which could conceivably occur. These include the recombination reactions

(R1) $XBr + Br \rightarrow X + Br_2$, and

(R2) $XBr + XBr \rightarrow 2X + Br_2$.

These reactions compete respectively with the product-forming steps

$$(P1) \qquad XBr + Br \rightarrow XBr_2 \quad , \quad \text{and}$$

$$(P2) \qquad XBr + XBr \rightarrow XBr_2 + X \quad .$$

In addition, reactions (R2) and (P2) compete with the polymerization reaction

$$(P3) \qquad XBr + XBr \rightarrow X_2Br_2 \quad .$$

All the above reactions are very rare in that they involve collisions between two species which are both present only in dilute concentrations. This, however, is also true of the second-order recombination process

$$(5) \qquad Br + Br + M \rightarrow Br_2 + M \quad .$$

On the other hand, for a large molecule such as $C_4Br_2F_8$, the more highly exothermic reaction (P1) would be expected to dominate over (R1). Then, since events of type (P1) are much rarer than the normal product-forming step,

$$(3) \qquad XBr + Br_2 \rightarrow XBr_2 + Br \quad ,$$

we can safely ignore reactions (R1) and (P1).

A similar line of reasoning allows us to ignore the reactions (R2) and (P2). The polymerization reaction results in a different product. This did not appear to any appreciable extent following any of the reactions, as evidenced by the absence of extra components on the gas chromatograms. Furthermore, reaction (P3) would be expected to be sterically hindered to a much greater extent than, for example, reaction (3) or (5).

The rate constants k_4, k_5 and k_c are now evaluated for the conditions of the experiment. The rate constant for wall recombination is determined by the diffusion rate of the atoms to the wall. This in turn can be estimated from the expression

$$k_4 \cong \frac{D}{\ell^2} \quad , \tag{5.43}$$

where D is the diffusion coefficient in $cm^2\text{-}sec^{-1}$, and ℓ is the effective average distance to the cell wall. In the reaction cell used in the experiments, this distance was estimated to be 0.5 cm. Other investigators[37] obtained a diffusion constant of ~ 0.12 $cm^2\text{-}sec^{-1}$ for Br atoms in similar gas mixtures, at a total pressure of an atmosphere. Since the diffusion constant is inversely proportional to pressure, it was estimated to be ~ 0.46 $cm^2\text{-}sec^{-1}$ in the present case. This results in a recombination rate of

$$k_4 \cong 1.83 \text{ sec}^{-1} \quad .$$

The recombination rate constant k_5 is obtained from the experimental flash photolysis data of Givens and Willard,[93] following a procedure similar to that used in Section 5.4.3 for dissociation rates. This yields the value

$$k_5 \cong 3.17 \times 10^8 \text{ l mole}^{-1} \text{ sec}^{-1}$$

for the second-order recombination rate constant.

The effective rate constant for the chain reaction can be obtained from the following considerations. Under steady-state conditions in the low pressure limit, the quantum yield Q was expressed according

to Eq. (4.5a) as

$$Q = \frac{2k_2}{k_4} \cdot \frac{k_3[X]\,[Br_2]}{k_3[Br_2] + k_{-2}} \quad . \qquad (4.5a')$$

The effective rate constant k_c was defined in Eq. (5.16) as

$$k_c = \frac{k_2 k_3[X]\,[Br_2]}{k_3[Br_2] + k_{-2}} \quad . \qquad (5.16')$$

Combining these, we now obtain the expression

$$k_c = \frac{k_4\, Q}{2} \quad , \qquad (5.44)$$

in terms of the steady-state quantum yield and the wall recombination rate constant. Extrapolating from the steady-state experimental results of Table 4.3 gives a value for Q of about one molecule per photon, as indicated in Section 4.4.2. Then, from Eq. (5.44) we calculate

$$k_c \cong 0.91 \text{ sec}^{-1} \quad .$$

Figure 5.1 illustrates graphically the product yield per laser pulse calculated by Eq. (5.42) and Eq. (5.21), using the values obtained for the rate constants under conditions where the experimental yield per pulse was 3.8×10^{-8} mole per liter. The solid curves show the theoretical yield as a function of the initial concentration of Br atoms per pulse, for various assumed values of the parameter f^2. The dashed line represents the experimental yield. On the basis of this diagram and the experimental evidence, it is possible to reach some conclusions regarding the magnitudes of c_0 and of f.

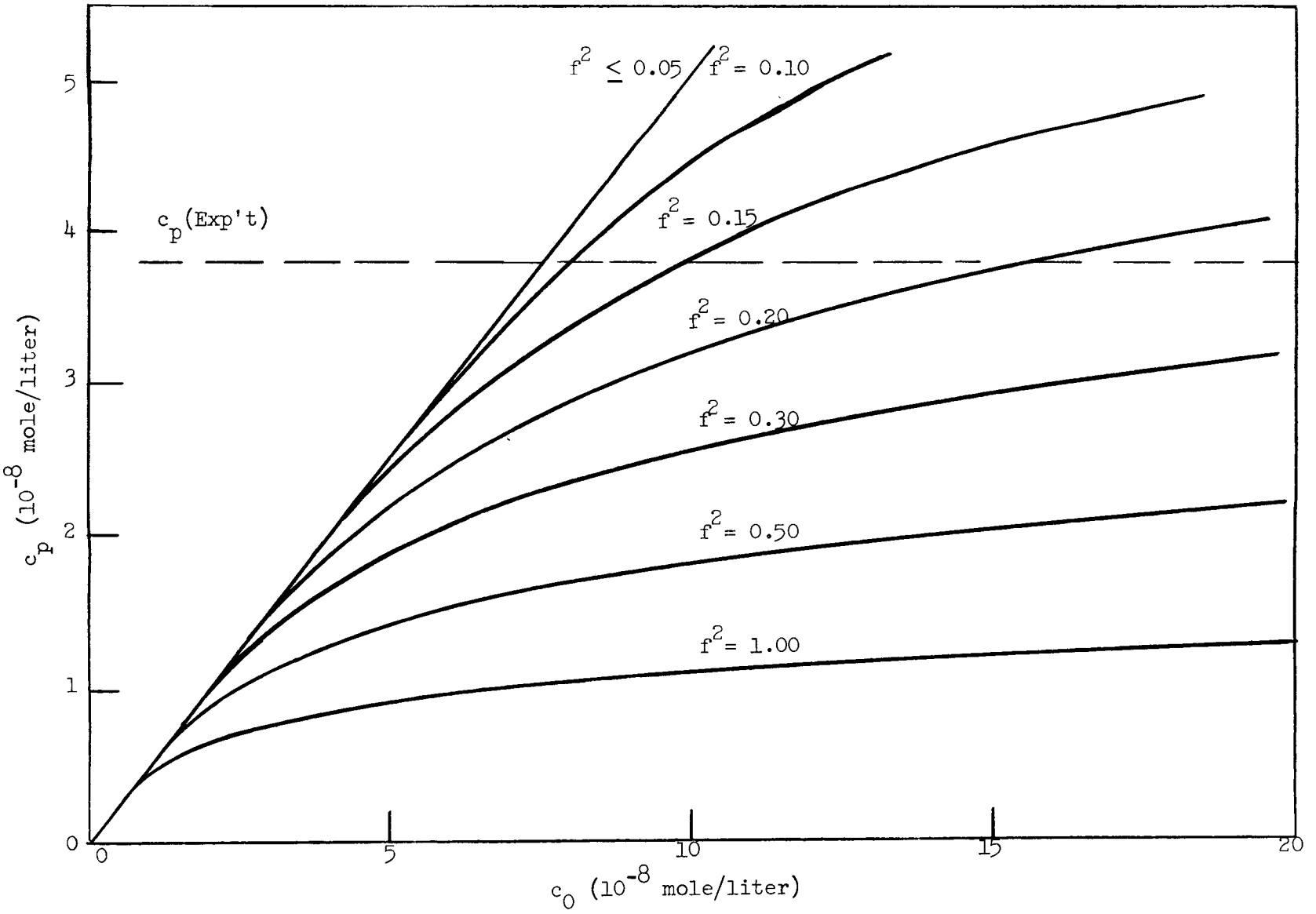

FIG. 5.1--Photochemical yield c_p as a function of initial concentration of Br atoms c_0 per laser pulse, calculated for different values of f^2 in the solid curves. Dashed line shows experimental photochemical yield.

It has been shown in the previous discussion that the processes leading to the dissociation of the bromine molecules into atoms are first-order in the concentration of these molecules. These processes include (a) the absorption of light quanta leading to the formation of excited $^3\Pi_1$ molecules and, (b) the collisional relaxation of these molecules toward equilibrium in which they can readily become dissociated. The important competing processes involving the excited molecules are also first-order. Hence, the initial concentration of atoms, c_0, is directly proportional to the laser energy per pulse. The photochemical yield per pulse was also found to depend almost linearly on the laser pulse energy, as discussed in Section 4.4.1. It therefore follows that the product yield must depend nearly linearly on the initial concentration of atoms per pulse. From Fig. 5.1 it is apparent that this cannot occur unless $f^2 \lesssim 0.1$. This, in turn, restricts c_0 to a range between about 7.5×10^{-8} and 8.5×10^{-8} mole per liter. However, in Section 5.4.3 it was shown that nearly 10^{-5} mole per liter of bromine atoms would be supplied at each pulse if all the excited $^3\Pi_{1,u}$ molecules were to dissociate. The fact that the actual number is less than one percent of this is attributed to very rapid collisional deactivation of the bromine molecules from the $^3\Pi_{1,u}$ electronic state to the $^1\Sigma_g^+$ electronic state. As pointed out in Section 5.4.5, this is the only reasonable process which can be expected to compete with the rapid dissociation process. Since the latter is calculated to occur at a rate of approximately 5×10^7 sec^{-1} under the present experimental conditions, the deactivation process would take place at an average rate of about 5×10^9 sec^{-1}, which is a factor of 5 greater than the gas-kinetic collision frequency. This is not unreasonable, however, because an increase in the effective collision diameter is known to occur in excited molecules.[67,69] Furthermore, the experimental observations of collision broadening in the present investigation (Section 3.4.3), indicated a collision rate greater than that predicted by simple kinetic theory. Finally, similarly large electronic relaxation rates have been found for other molecules.[68,86,97]

The restriction placed upon the value of f by the comparison of theory and experiment implies, according to Eq. (5.34), that the reaction

$$(2) \qquad Br + X \rightarrow XBr$$

is appreciably faster than either its inverse or

$$(3) \qquad XBr + Br_2 \rightarrow XBr_2 + Br \qquad .$$

This is consistent with observations[37,76] that step (2) requires very little if any activation energy for most bromine-olefin reactions. It also implies that process (3) is the rate-determining step in the chain reaction.

5.6 DISCUSSION OF ALTERNATIVE MECHANISMS

In the previous section it was shown that the results of the laser photocatalysis experiments were consistent with the free radical chain reaction mechanism initiated by bromine atoms provided by collisional dissociation of $^3\Pi_{1,u}$ excited bromine molecules. It remained to be established whether or not an alternative mechanism might also be consistent with the experimental results.

A number of the alternatives enumerated in Section 4.1 can clearly be ruled out. It was shown in Section 5.4.4 that if direct molecular addition of excited Br_2 to the fluorocarbon were to compete significantly with collisional dissociation, an isotopic enrichment in the product would be expected. The absence of isotopic enrichment adds to the other evidence already against the molecular addition reaction, making it extremely unlikely. Likewise, ordinary photodissociation of the bromine by absorption of light in an underlying continuum can be rejected as a significant mechanism, because of the sensitive dependence of the reactivity on the individual line absorption spectrum. In particular, the experimental

dependence of the reaction rate on wavelength and on light intensity, illustrated in Fig. 4.4, places an upper limit on the continuous absorption which could occur at 14,400 cm^{-1}. The residual reactivity between absorption lines was no greater than 10% of the reactivity when the laser was tuned to the most prominent line. Even in the former case, the reactivity could easily be attributable to the overlapping wings of adjacent lines. If it were due to a true underlying continuum, however, it would mean that every photon absorbed would produce a pair of dissociated bromine atoms. In contrast to this, we showed in the previous section that, when the excitation occurred in the individual lines, only one molecule on the average was dissociated for every 100 photons absorbed. Thus, continuous absorption is 100 times more efficient for initiating the reaction, but experimentally accounts for no more than 10% as much reactivity as the prominent line. Therefore, continuous absorption, if it occurs at all, is at least 1000 times weaker than the prominent line absorption.

Some simple calculations are sufficient to eliminate as significant reaction mechanisms any heating effects due to conversion of the light energy absorbed in the strong lines. As indicated in Section 4.4.2, this energy was about 0.25×10^{-2} Joule per pulse. When this energy is thermalized among the molecules of the heat bath, it causes a temperature increase given by

$$\Delta T = \frac{\Delta E}{c_v M} ,$$

where ΔE is the energy absorbed per pulse, c_v is the heat capacity per mole, and M is the number of moles of gas in the heat bath. For polyatomic gases, $c_v = 3R$, where R is the gas constant. The 2.5 ml cell at 200 mm pressure contained 2.72×10^{-5} mole. Hence, the temperature increase was about $3.7^{\circ}K$. Convection both inside and outside the cell prevented subsequent pulses from increasing the temperature further.

Calculations using this temperature increase in Eq. (5.26) show that the population of thermally dissociated bromine atoms would nearly double. Even so, this would be only 4×10^{-20} mole/ml , far too small to account for the observed reactivity.

An indirect type of heating mechanism can also be envisioned. With the help of Fig. 3.1 and the Franck-Condon principle, we can see that, if continuous absorption were present at 14,400 cm^{-1} and at a reasonable temperature, it would have to be due to molecules initially in the vibrational states $v'' = 5$ and $v'' = 6$. A temperature increase could then conceivably populate these states sufficiently to enhance the continuous absorption probability. This is actually an indirect example of two-photon absorption, which will be discussed more generally later. The fractional thermal populations of the ground-state vibrational levels can be calculated by means of Eq. (5.22). When this is done, it indicates that a temperature increase of approximately 125°C would be needed to enhance the population, and therefore the continuous absorption, by the observed factor of 10, when the laser is tuned to a strong line. The temperature rise of less than 4°C is, then, clearly not sufficient to produce this effect.

The remaining two-photon absorption processes can be of two types. The first is a single event in which two quanta excite a molecule directly from the ground state. The second type involves absorption of an initial photon which excites the molecule to the $^3\Pi_{1,u}$ state, after which it relaxes to an excited vibrational level of the $^1\Sigma_g^+$ state, where it absorbs a second photon and dissociates. All two photon absorptions produce a yield which is quadratic in the incident light intensity, as opposed to single photon absorption, which results in a linear yield. This behavior alone does not allow us to rule out two photon processes in the present experiments. It is conceivable that the quadratic dependence of the initial Br atom population on light intensity could be offset by logarithmic or square-root dependence of the photochemical yield on the atomic population, so that the overall rate would appear to be linear in the light intensity.

The following considerations, however, make it appear that two-photon processes are not important in the laser photocatalysis of bromine. First, the direct two-photon dissociation must be a resonant process having a real intermediate state, which must be the same individual level of the $^3\Pi_{1,u}$ state which is produced by ordinary one-photon absorption. Otherwise, the photochemical yield would not have its observed dependence on the individual $^3\Pi_{1,u} \leftarrow {}^1\Sigma_g^+$ absorption lines. In such a case, the two-photon absorption probability would be proportional to $|R_{13}|^2$, where

$$R_{13} = \frac{\langle 3|\mu_z|2\rangle\langle 2|\mu_z|1\rangle\, E_0^2}{\omega_0 - \omega_{21} + i/T_2}$$

is the effective two-photon matrix element.[98] For convenience we have labeled the lower, intermediate, and upper states respectively $|1\rangle$, $|2\rangle$, and $|3\rangle$; E_0 and ω_0 are the strength and the frequency of the optical field, ω_{21} is the frequency of the $^3\Pi_{1,u} \leftarrow {}^1\Sigma_g^+$ transition, and T_2 is an effective coherence time; $\langle 3|\mu_z|2\rangle$ and $\langle 2|\mu_z|1\rangle$ are just the ordinary dipole matrix elements between states $|3\rangle$ and $|2\rangle$, and between states $|2\rangle$ and $|1\rangle$, respectively. The values of these dipole matrix elements are determined by the ordinary selection rules for single photon absorption, as outlined in Section 3.2. According to these rules, $\langle 3|\mu_z|2\rangle$ vanishes unless $|3\rangle$ and $|2\rangle$ have opposite symmetry ("g" or "u"). Since $|2\rangle$ has <u>ungerade</u> symmetry, then $|3\rangle$ would be required to have <u>gerade</u> symmetry. The lowest lying states of Br_2 above the $^3\Pi_{1,u}$ state which have the required symmetry are located some 55,000 cm^{-1} above the ground state.[99] This is obviously too high to be reached by the absorption of two photons at 14,400 cm^{-1}. Therefore the direct two-photon process can be rejected.

Absorption of a second photon following relaxation to an upper vibrational level of the $^1\Sigma_g^+$ electronic state is allowed by the electronic selection rules. However, it would have to obey the Franck-Condon principle as well. This restricts the number of vibrational levels in which a molecule could absorb light at 14,400 cm^{-1} and become

dissociated. Again referring to the energy diagram in Fig. 3.1, we find that there are only two groups of these vibrational levels which satisfy the Franck-Condon principle. The first of these, which has been mentioned before, consists of $v'' = 5$ and $v'' = 6$, where there is a marginal possibility for excitation to the $^3\Pi_{1,u}$ potential above the dissociation energy. The second consists of levels $v'' = 8$ to $v'' = 11$, where absorption of light at 14,400 cm^{-1} would lead to dissociation from the repulsive $^1\Pi_u$ state. In either case, however, molecules reaching these vibrational levels remain there only a microsecond or so in the course of the rapid vibrational relaxation toward thermal equilibrium within the ground electronic state. Hence, they are exposed to no more than one percent of the incident laser energy. Under these conditions it is doubtful that any significant number of them become excited to the continuum.

5.7 CONCLUSIONS

In this chapter a detailed comparison of theory and experiment resulted in the elucidation of the mechanism of the photochemical reaction of bromine with selected unsaturated fluorocarbons, and in the determination of the rates of a number of associated dynamic molecular processes. To do this, it was first necessary to express the theory in such a way that it could be conveniently related to the experimental results. Consideration of the possible dynamic processes involving both bromine molecules and bromine atoms then showed that the experimental results were consistent with a chain reaction mechanism. This reaction was initiated by bromine atoms, which were in turn furnished by the rapid collisional dissociation of $^3\Pi_{1,u}$ molecules produced by laser excitation. This occurred even though the laser light was in the absorption region which produced molecules whose energy was some 500 to 800 cm^{-1} below the dissociation energy. Alternative mechanisms were shown to be inconsistent with the observed results.

This was the first study of a photochemical reaction of bromine in which it was demonstrated that excited molecules were formed in the primary process. As such, it provided access to information about dynamic processes which was not formerly available. First, it established that, even under these conditions, molecular addition of bromine to a double bond does not occur to any detectable extent. Second, it provided the first experimental data on collisional electronic energy transfer from the $^3\Pi_{1,u}$ state to the $^1\Sigma_g^+$ state of bromine. This was particularly significant, since the absence of detectable fluorescence from the $^3\Pi_{1,u}$ state would make it extremely difficult to obtain this information in the usual way.[68,86] Also, previous efforts to study this process in bromine using other photochemical techniques were apparently unsuccessful.[100] Third, by means of selective photocatalysis, the present investigation established a new upper limit for the continuous absorption coefficient of bromine at 14,400 cm^{-1}.

VI. EXTENSIONS

The success of the present investigation in demonstrating the use of the monochromatic property of laser light for highly selective excitation of molecules opens the way to numerous similar applications. The purpose of this chapter is to indicate briefly what some of these might be. The principal categories of such future investigations are inorganic and organic photochemistry, molecular energy transfer, and visible and infrared spectroscopy. Attention will be directed only to those applications which involve interaction of laser radiation with individual resonant transitions in materials, and thus demand tunable monochromatic sources, as in the present work. Such sources are not presently available throughout most of the spectrum, but their development is being actively pursued. Reference will be made to some of the more promising advances in this direction in laser technology.

6.1 DIRECT EXTENSIONS OF THE PRESENT WORK

The present work provides a well-established foundation for additional investigations of photochemical reactions and energy transfer in bromine using a tunable ruby laser. Now that the technique has been developed and shown to lead to significant results, it might be worthwhile to repeat the experiments with some modifications designed to increase the accuracy of the numerical results. These modifications would include direct measurement of the absorbed light energy both in laser and conventional photocatalysis in order to obtain a more accurate measurement of the quantum yield. This measurement in the present work was prevented by the geometry of the reaction cell. The resulting uncertainties could affect the numerical results as much as a factor of two or so, which would not, however, alter the general conclusions of the study.

The same basic photochemical reaction could be studied with the substitution of other olefins for the two fluorocarbons used in the present study. In particular, it would now be interesting to observe the laser catalyzed reaction of bromine with an olefin such as ethylene, which produces a very high quantum yield. Also, additional experiments could be performed in which the concentration of the olefin, and perhaps that of a third inert gas, would be varied systematically. This would provide additional details regarding bromine dissociation, recombination, and molecular energy transfer.

The third modification would be the use of a ruby laser which operates continuously, or can be pulsed repetitively with variable intensity and duty factor. Lasers incorporating some of these features have recently become available.[101] Experiments with a laser of this type would allow a comparison between steady-state and pulsed conditions, using monochromatic light in both cases. Differences in the product yield would then be expected under suitable conditions of pressure and geometry, as shown in Section 5.5.

It has been noted that a complete rotational analysis of the $^3\Pi_{1,u} \leftarrow {}^1\Sigma_g^+$ band system of bromine has not yet been performed. If this were done, it would be possible to identify the upper and lower vibrational and rotational energy levels involved in each of the individual line transitions occurring near 14,400 cm^{-1}. This in turn would permit two types of experiments to be done. First, differences in the photochemical quantum yield might be found for excitation to vibrational levels of the $^3\Pi_{1,u}$ state which lie at different energies below the dissociation level. This would provide quantitative data concerning vibrational relaxation within the $^3\Pi_{1,u}$ state. Another type of experiment would consist of monitoring the population of the lower state of the transition during and after the laser pulse by means of a separate light source and a high-resolution monochromater for observing absorption in another transition from the same lower state. This would determine rotational relaxation rates for bromine in the $^1\Sigma_g^+$ state.

With sufficiently sophisticated chemical techniques it might be possible to obtain photochemical isotope separation in bromine by means of selective excitation of an individual isotopic species, as discussed in Section 4.4.5. In view of the very rapid isotopic exchange reaction, it would be necessary to find a suitably fast product-forming reaction to compete with it, not a slow free-radical chain as in the case of fluorocarbons. Such a reaction may be the rapid chain reaction of bromine with ethylene or other unsubstituted olefins, with rapid chain termination by means of wall effects or an inhibitor, which is presently under consideration in this laboratory. Other reactions, such as the exchange $Br_2 + HI \rightarrow HBr + IBr$ have been considered, but calculations showed them to be significantly slower than the isotopic exchange reaction.

It is clear that the foregoing types of experiments, could, in principle, be performed with gases other than bromine, particularly chlorine and iodine, if suitable laser sources were available in their corresponding spectral regions. In these cases, however, care must be taken to allow for known differences in spectral structures and chemical behavior. Other types of photochemical reactions could also be investigated using selective excitation.

6.2 LASER ORGANIC CHEMISTRY

Some of the most interesting potential laser applications belong to the field of organic photochemistry. While laser light has already been used to produce chemical effects in organic materials, in most cases the absorption was nonresonant, and the monochromatic property was not therefore a prime consideration. However, complex organic molecules have many resonant electronic absorptions in the ultraviolet, and vibrational absorptions in the infrared. Many of these resonances are primarily associated with specific bonds within the molecules. Therefore, monochromatic radiation of the proper wavelength should be capable of selectively activating these specific sites in the molecules, potentially influencing the molecules to react at these sites.[42] The recent identification of photochemical activity associated with infrared transitions[27] makes this type of investigation with infrared lasers very

attractive. A theoretical basis for this type of photochemical activation was developed earlier by Duchesne.[102] Examples of specific types of organic photochemical reactions are cis-trans-isomerization, ring closure or ring opening, skeletal rearrangements, and various addition and dissociation processes.[2] Laser organic photochemistry can potentially lead to the efficient synthesis of new materials, as well as to an increased understanding of organic reaction mechanisms. An especially intriguing possibility is the use of monochromatic laser light to effect selective types of changes in the organic molecules found in biological systems, such as genetic cells.

6.3 MOLECULAR ENERGY TRANSFER

In addition to the photochemical observation of molecular energy transfer, as performed in the present investigation and discussed in Section 6.1, other types of molecular energy transfer studies can be facilitated through the use of monochromatic light for selective excitation. One example is the study of cross-relaxation, or the migration of energy among the various normal vibrational modes of polyatomic molecules. This process plays an important role in the activation of specific molecular bonds,[103] which was mentioned in the previous section.

Cross-relaxation, as well as other forms of energy transfer, can be observed through the fluorescence from the energy levels involved in the transfer process. In such studies selective excitation is particularly useful.[104] Heretofore this technique has depended upon the availability of sources whose wavelengths coincide fortuitously with an absorption line of the molecule under observation. This has been true of experiments which utilized strong atomic emission lines for sources,[68,69] as well as a recent study of energy transfer in methane in which the 3.39 μ oscillation of a He-Ne laser was used.[105] This constraint will no longer be imposed, with the development of tunable laser sources.

6.4 LASER ABSORPTION SPECTROSCOPY

The advantages of lasers over conventional light sources for spectroscopy are the same as those for photochemistry. First, the high

monochromaticity can lead to improved resolving power. Second, high peak powers of some pulsed lasers can be used along with certain detection techniques to study very weak absorptions in laboratory gas samples or in the atmosphere. Here also, existing lasers suffer from tuning bandwidth limitations. Previous studies have depended upon near coincidence of a laser frequency with an absorption line of interest. An example is the use of the CO_2 laser to study the spectrum of CO_2 itself.[106] Also, the 3.39 μ line of the He-Ne laser was tuned over a range of ±0.11 cm^{-1} by means of the Zeeman effect in an axial magnetic field, and was used for high resolution absorption measurements in methane and ethane over this limited bandwidth.[107] Also, various xenon and neon laser lines between 3 and 9 μ were Zeeman-tuned over ranges of ±0.1 cm^{-1}, and used to study the fine structure of absorption bands of methane, ethane, propane, carbon tetrachloride, and sulfer hexafluoride.[108] In none of these examples was the tuning bandwidth nearly so great as that achieved with the ruby laser in the present investigation to obtain the absorption spectrum shown in Fig. 3.5. The present techniques therefore permit laser spectroscopic studies over wider frequency bands than in the past. Furthermore, techniques also exist for shifting this frequency band to other spectral regions, as will be discussed in the next section. This, combined with other technological advances, makes future growth of the field of laser spectroscopy very promising.

6.5 TUNABLE LASER SOURCES

The purpose of this section is to enumerate some of the existing techniques for shifting the output frequencies of lasers, and to note a number of recent advances toward the development of broadband tunable laser sources.

Zeeman tuning of gas lasers by the application of magnetic field was mentioned in the previous section. It has been limited to bandwidths of the order of ±0.1 cm^{-1}, fundamentally because higher magnetic fields cause the gain coefficient of the active gas to deteriorate, so that oscillation is eventually quenched. Another technique for frequency shifting does not suffer from this effect, because the active medium

is not affected by the tuning process. This is so-called single-sideband-suppressed-carrier modulation,[109] in which an electro-optic or acousto-optic modulator inside the laser resonator couples light out of the laser which is shifted in frequency from light wave oscillating inside the resonator. This scheme has been used extensively to achieve ± 0.1 cm^{-1} shifts, and can be extended to higher frequencies.

Techniques which can be used to obtain greater shifts in the frequencies of pulsed ruby or neodymium lasers are stimulated Raman scattering,[110] and second and higher order harmonic generation.[111] In the former, frequency shifts of the order of 10^3 cm^{-1} of relatively large amounts of energy have been obtained. In the latter, the frequency of a substantial part of the energy is shifted to a value twice, three times, etc., the original frequency. If the original laser in such an arrangement is thermally tuned, as in the present work, fine tuning also results at the shifted frequency.

Some of the most promising techniques for frequency shifting involve tunable parametric oscillators.[112] These devices produce oscillations at two frequencies whose sum is the incident laser frequency. Phase-matching conditions can be altered by changing the temperature or the orientation of the active material of the device. Such techniques have been used in conjunction with harmonic generation to achieve tuning over bandwidths of 20% in the visible region.[113] Frequency stability and linewidth in these devices remains somewhat of a problem. Recent experiments resulted in the discovery of methods for conveniently testing materials for their usefulness in parametric oscillators.[114] A somewhat related type of tunable oscillator for use with lasers to generate infrared frequencies has been proposed.[115] It is expected that these advances will lead to the increased importance of parametric oscillators as tunable monochromatic sources.

VII. CONCLUSIONS AND SUMMARY

This report has described experiments in which a ruby laser was used as a monochromatic light source for the selective excitation of bromine molecules in the gas phase. The resulting dynamic behavior of the system included relaxation and dissociation of the excited molecules, and the photochemical addition reaction of bromine with selected unsaturated fluorocarbons. The observed dependence of the rate of this reaction on the wavelength and intensity of the light, and on the reactant concentrations, was used to determine the relative rates of the other dynamic processes. To accomplish this, it was first necessary to reformulate the theory of these processes in such a way that it could be related meaningfully to the experimental results.

This was the first photochemical investigation in which the monochromaticity of the laser was specifically exploited. To achieve this it was necessary to apply techniques for frequency tuning and stabilization, as well as mode selection. Preliminary spectroscopic studies of bromine were made to determine the details of its $^3\Pi_{1,u} \leftarrow {}^1\Sigma_g^+$ absorption band system in the 14,400 cm^{-1} region of the ruby laser. No previous photochemical investigation of bromine had been made in this spectral region. Furthermore, the present investigation was the first to demonstrate a photochemical reaction of bromine in which stable excited molecules were formed in the primary process.

The principal objective of this work was to demonstrate the usefulness of the laser as a monochromatic light source for selective photocatalysis. The successful accomplishment of that goal has opened to way to future uses of tunable lasers for selective excitation. At the same time, advances in laser technology make the availability of such sources throughout a considerable part of the spectrum a very promising possibility. Extensions of the present work were suggested in which these sources could be used for photochemical, energy transfer, and spectroscopic studies.

REFERENCES

1. W. A. Noyes, Jr., G. S. Hammond, and J. N. Pitts, Jr., ed., Advances in Photochemistry, Vol. I (Interscience, John Wiley and Sons, New York, 1963).
2. G. S. Hammond and N. J. Turro, Science 142, 1541 (1963).
3. G. Porter, Proc. Roy. Soc. A200, 284 (1950).
4. R. G. W. Norrish, G. Porter, and B. A. Thrush, Proc. Roy. Soc. A216, 165 (1953).
5. H. E. Gunning and O. P. Strausz, "Isotopic Effects and the Mechanism of Energy Transfer in Mercury Photosensitization," in reference 1, pp. 209-274.
6. A. L. Schawlow and C. H. Townes, Phys. Rev. 112, 1940 (1958); also A. L. Schawlow, Scientific American 209, 36 (1963).
7. S. Arrhenius, Z. Physik. Chem. 4, 226 (1889).
8. G. Herzberg, Molecular Spectra and Molecular Structure I. Spectra of Diatomic Molecules, 2nd. Edition (D. van Nostrand, Inc., Toronto, 1950), pp. 472-482.
9. V. N. Kondrat'ev, Chemical Kinetics of Gas Reactions (Pergamon Press, Oxford, 1964) – U. S. A. edition distr. by Addison-Wesley, Palo Alto, pp. 406-466.
10. J. N. Pitts, Jr., F. Wilkinson, and G. S. Hammond, "The 'Vocabulary' of Photochemistry," in reference 1, pp. 1-21.
11. A. L. Schawlow, Bell Laboratories Record 38, 403 (1960).
12. Yoh-Han Pao and P. M. Rentzepis, Appl. Phys. Letters 6, 93 (1965).
13. C. Borde, A. Henry, and L. Henry, Comptes Rendus de l'Academic des Sciences 263B, 619-620 (1966).
14. G. A. Askar'yan, Zhurnal Eksperimental'noi i Teoreticheskoi Fiziki 46, 403 (1964), translated in Soviet Physics (JETP) 19, 273 (1964).
15. L. M. Epstein and K. H. Sun, Nature 211, 5054, 1173-1174 (1966).
16. F. J. McClung and R. W. Hellwarth, Proc. IEEE 51, 46 (1963).

17. M. DiDomenico, Jr., J. E. Geusic, H. M. Morreos, and R. G. Smith, Appl. Phys. Letters 8, 180 (1966); also
D. A. Stetser and A. J. DeMaria, Appl. Phys. Letters 9, 118 (1966).
18. P. A. Schnieper, NEREM Record 1965, Paper TPM-2.
19. R. M. Badger and J. W. Urmston, Proc. Nat. Acad. Sci. 16, 808 (1930).
20. B. H. Billings, W. J. Hitchcock, and M. Zelikoff, J. Chem. Phys. 21, 1762 (1953).
21. S. Mrozowski, Z. Physik 78, 826 (1932).
22. K. Zuber, Helv. Phys. Acta 9, 285 (1936); also Nature 136, 796 (1935).
23. H. Hartley, A. O. Ponder, E. J. Bowen, and T. R. Merton, Phil. Mag. 43, Ser. 6, 430 (1922).
24. W. Kuhn and H. Martin, Naturwiss. 20, 772 (1932).
25. G. Liuti, S. Dondes, and P. Harteck, J. Chem. Phys. 44, 4052 (1966).
26. H. W. Schultz, Internal Memoranda, Carbide and Carbon Chemical Corporation, 1945 and 1947 (received as private communication by A. L. Schawlow).
27. J. D. Baldeschwieler and G. C. Pimentel, J. Chem. Phys. 33, 1008 (1960); also
R. T. Hall and G. C. Pimentel, J. Chem. Phys. 38, 1889 (1963).
28. D. A. Buddenhagen, A. V. Haeff, G. F. Smith, G. Oster, and G. K. Oster, Proc. Nat. Acad. Sciences U. S. 48, 303 (1962).
29. R. M. Wiley, Ann. N. Y. Acad. Sci. 122, 685 (1965).
30. J. F. Verdieck, Presented at 1965 Annual Meeting, American Physical Society, New York (Jan. 27-30, 1965), Paper GG 12.
31. R. A. Olson, paper presented at Symposium on Recent Developments in Research Methods and Instrumentation, National Institute of Health, Bethesda, Maryland (Oct. 7, 1963).
32. G. B. Kistiakowsky and J. C. Sternberg, J. Chem. Phys. 21, 2218 (1953).
33. M. Bodenstein and H. Lütkemeyer, Z. Physik. Chem. 114, 208 (1925).
34. W. Jost, Z. Physik Chem. 134, 92 (1928); B3, 95 (1929).
35. J. W. Urmston and R. M. Badger, J. Amer. Chem. Soc. 56, 343 (1934).
36. A. G. Brown and J. W. T. Spinks, Can. J. Research B15, 113 (1937).
37. K. L. Müller and H. J. Schumacher, Z. Physik Chem. B42, 327 (1939).

38. H. Schmitz, H. J. Schumacher and A. Jäger, Z. Physik Chem. B51, 281 (1942).

39. O. Darbyshire, Proc. Royal Soc. (London) A159, 93 (1937).

40. A. P. Acton, R. G. Aickin, and N. S. Bayliss, J. Chem. Phys. 4, 474 (1936).

41. Handbook of Chemistry and Physics, 44th Edition (Chemical Rubber Publishing Co., Cleveland, 1962), p. 461.

42. H. W. Moos, A. L. Schawlow, and W. B. Tiffany, paper presented at 149th Meeting, American Chemical Soc., Detroit, Mich. (April 4-9, 1965).

43. W. B. Tiffany and A. L. Schawlow, paper presented at the Winter Meeting, American Physical Soc., Stanford, Calif. (Dec. 28-30, 1966), Paper L9.

44. W. G. Brown, Phys. Rev. 38, 1179 (1931); 39, 777 (1932).

45. H. J. Plumley, Phys. Rev. 45, 678 (1934).

46. R. S. Mulliken, J. Chem. Phys. 8, 234 (1940); also Phys. Rev. 57, 500 (1940).

47. A. L. G. Rees, Proc. Royal Soc. (London) 59, 1008 (1947).

48. H. Stammreich, Phys. Rev. 78, 79 (1950).

49. Reference 8, pp. 3-4.

50. B. A. Lengyel, Lasers (John Wiley and Sons, N. Y., 1962) pp. 52-69.

51. I. D. Abella and H. Z. Cummings, J. Appl. Phys. 32, 1177 (1961).

52. B. J. McMurtry, Appl. Optics 2, 767 (1963).

53. V. Evtuhov, Appl. Phys. Letters 6, 141 (1965); also
C. L. Tang, H. Statz, and G. de Mars, J. Appl. Phys. 34, 2289 (1963).

54. A. P. Veduta, A. M. Leontovich, and V. N. Smorchkow, J. Exptl. Phys. (U.S.S.R.) 48, 87-93 (1965), translated in Soviet Physics JETP 21, 59 (July 1965); also
R. L. Townsend, C. M. Stickley, and A. D. Maio, Appl. Phys. Letters 7, 94 (1965).

55. M. Born and E. Wolf, Principles of Optics (Pergamon Press, New York, 1959), p. 322 and p. 328.

56. E. Snitzer, Quantum Electronics III, Proceedings of the Third International Conference, P. Grivet and N. Bloembergen, eds. (Columbia University Press, New York, 1964), pp. 999-1019.

57. D. Röss, Proc. IEEE 52, 196 (1964); also
G. Gehrer and D. Röss, Z. für Naturforschung 20a, 701 (1965).
58. I. H. Malitson, J. Opt. Soc. Am. 52, 1377 (1962).
59. International Critical Tables, Vol. III (McGraw-Hill, New York, 1932), p. 201.
60. J. U. White, J. Opt. Soc. Am. 32, 285 (1942).
61. T. K. McCubbin, Jr., and R. P. Grosso, Appl. Optics 2, 764 (1963).
62. Reference 8 (entire book).
63. Reference 8, pp. 141-145.
64. A. G. C. Mitchell and M. W. Zemansky, Resonance Radiation and Excited Atoms (Cambridge, University Press, 1961).
65. T. L. Cottrell and J. C. McCoubrey, Molecular Energy Transfer in Gases (Butterworths, London, 1961), p. 74.
66. Reference 65, p. 87.
67. E. E. Nikitin and N. D. Sololov, J. Chem. Phys. 31, 1371 (1959).
68. H. P. Broida and T. Carrington, J. Chem. Phys. 38, 136 (1963).
69. J. I. Steinfeld and W. Klemperer, J. Chem. Phys. 42, 3475 (1965).
70. See for example, M. Duquesne, I. Tatischeff, and N. Recouveur, Nuclear Instrum. Methods (Netherlands) 41, 13 (1966), or
J. A. Armstrong, Paper FD2, or G. A. Morton, Paper FD1, 1967 Spring Meeting, Optical Society of America, Columbus, Ohio (April 12-14, 1967).
71. Louis F. Fieser and Mary Fieser, Organic Chemistry, 3rd. Edition (Reinhold Publishing Corp., N. Y., 1956), p. 49ff.
72. H. Steinmetz and R. M. Noyes, J. Am. Chem. Soc. 74, 4141 (1952).
73. P. G. Ashmore, Catalysis and Inhibition of Chemical Reactions (Butterworths, London, 1963), p. 13.
74. S. W. Benson, The Foundations of Chemical Kinetics (McGraw-Hill, New York, 1960) p. 50, p. 53, p. 331.
75. Reference 9, pp. 406-466.
76. E. W. R. Steacie, Atomic and Free Radical Reactions, A. C. S. Monograph No. 125 (Reinhold Publishing Corp., New York, 1954), pp. 56 and 406-409.
77. C. A. McDowell, Nature 175, 860 (1955).
78. Reference 71, pp. 1110-1111.
79. Reference 71, p. 159.

80. J. H. Simons, ed., Fluorine Chemistry, Vol. II (Academic Press, New York, 1954), especially the article by J. H. Simons and T. J. Brice, pp. 334-448.
81. A. M. Lovelace, D. A. Rausch, and W. Postelnek, Aliphatic Fluorine Compounds, A. C. S. Monograph No. 138 (Reinhold Publishing Corp., New York, 1958).
82. K. E. Müller and H. J. Schumacher, Z. Physik. Chem. B35, 285 (1937).
83. For this discussion, see for example, reference 9, pp. 1-8.
84. Reference 8, pp. 124-125.
85. K. F. Herzfeld and T. A. Litovitz, Absorption and Dispersion of Ultrasonic Waves (Academic Press, New York, 1959).
86. A. B. Callear, "Measurement of Energy Transfer in Molecular Collisions," in Appl. Optics, Supplement 2: Chemical Lasers (1965), pp. 145-170.
87. Reference 65, pp. 147-148.
88. See for example, K. E. Shuler, J. Phys. Chem. 61, 849 (1957); and J. Chem. Phys. 31, 1375 (1959).
89. See for example, J. E. Mayer and M. G. Mayer Statistical Mechanics (John Wiley and Sons, New York, 1940), pp. 215-217.
90. Selected Values of Chemical Thermodynamic Properties, Series III (National Bureau of Standards, Washington, D.C., 1954).
91. D. Britton and N. Davidson, J. Chem. Phys. 25, 810 (1956).
92. See for example, reference 65, pp. 184-192, and other references listed therein.
93. W. G. Givens, Jr., and J. E. Willard, J. Amer. Chem. Soc. 81, 4773 (1959).
94. H. B. Palmer and D. F. Hornig, J. Chem. Phys. 26, 98 (1957).
95. D. L. Bunker and N. Davidson, J. Amer. Chem. Soc. 80, 5085, 5090 (1958).
96. R. M. Noyes, J. Amer. Chem. Soc. 88, 4311, 4318 (1966).
97. A. B. Callear and I. W. M. Smith, Trans. Faraday Soc. 59, 1720 (1963).
98. See for example, S. Yatsiv, W. G. Wagner, G. S. Picus, and F. J. McClung, Phys. Rev. Letters 15, 614 (1965), and references listed therein.

99. Reference 8, p. 512.
100. S. Claesson, private communication.
101. See for example, D. Röss, Microwaves 4, 29 (1965); also D. Röss and G. Zeidler, Electronics 39, 115 (1966).
102. J. Duchesne, Bull. Acad. Roy. Belgique, Ser. 5, 38, 197 (1952).
103. See for example, J. N. Butler and G. B. Kistiakowsky, J. Amer. Chem. Soc. 82, 759 (1960).
104. R. C. Millikan, J. Chem. Phys. 43, 1439 (1965).
105. J. T. Yardley and C. B. Moore, J. Chem. Phys. 45, 1066 (1966).
106. See for example, F. Farrena, C. Rossetti, F. Bourbonneux, and P. Barchewitz, Comptes Rendus 263B, 241 (1966).
107. H. J. Gerritsen and M. E. Heller, Appl. Optics, Supplement 2: Chemical Lasers (1965), pp. 73-80.
108. H. Brunet, IEEE J. Quant. Electr. QE-2, 382 (1966).
109. R. Targ, Proc. IEEE 52, 303 (1964); also F. Targ, G. A. Massey, and S. E. Harris, Proc. IEEE 52, 1247 (1964).
110. See for example, G. Eckhardt, IEEE J. Quant. Electr. QE-2, 1 (1966).
111. See for example, P. D. Maker, R. W. Terhune, M. Nisenoff, and C. M. Savage, Phys. Rev. Letters 8, 21 (1962).
112. See for example, J. A. Giordmaine and R. C. Miller, Phys. Rev. Letters 14, 973 (1965).
113. S. A. Akhmanov, V. G. Dmitriev, R. V. Khokhlov, and A. I. Kovrygin, in Physics of Quantum Electronics Conference Proceedings, P. L. Kelley, B. Lax, and P. E. Tannenwald, eds. (McGraw-Hill, New York, 1966), p. 43.
114. S. E. Harris, M. K. Oshman, and R. L. Byer, Phys. Rev. Letters 18, 732 (1967).
115. S. E. Harris, Appl. Phys. Letters 9, 114 (1966).